SYNTHESIS AND REACTIONS OF NEW PYRAZOLE DERIVATIVES

R. Fikry,[a]* N. Ismail,[a] S. Raslan[b] and H. El-Tahawe[b]

Keywords: pyrazoles; pyrazolotriazines; pyrazolotriazoles; pyrazolopyrimidines; pyrazolothiadiazoles

Chemical transformation of 3-amino-5-hydroxy-4-phenylazo-1H-pyrazole (1) provided a series of new pyrazol derivatives such as N-(4-(2-phenyldiazenyl)-2,5-dihydro-3-hydroxy-1H-pyrazol-5-yl)-2 chloroacetamide (**2**) obtained in the reaction of **1** with chloroacetyl chloride. Reaction of 2 with malononitrile and ammonium isothiocyanate gave the corresponding 1-(4-(2-phenyldiazenyl)-5-hydroxy-1H-pyrazol-3-yl)-2-amino-4,5-dihydro-5-oxo-1H-pyrrol-3-carbonitrile (**3**) and 3-(2-phenyldiazenyl)-7-amino-2-hydroxypyrazolo[1,5-a]pyrimidin-5(1H)-one (**4**). Reaction of **1** with P_2S_5 gave the corresponding 3-amino-5-mercapto-4-phenylazo-1H-pyrazole **5**. The reaction of compound 5 with chloroacetic acid, ethyl chloroacetate, tetrahydrofuran, 3-hydroxybenzaldehyde, phenacylbromide and ninhydrine gave the corresponding N-substituted derivatives (**6, 7, 8, 9, 10, 11, 12, 13**), respectively. The reaction of compound **7** with hydrazine hydrate and a consecutive cyclization in the presence of glacial acetic acid and sulfuric acid mixture afforded **12**. 1-(4-(2-Phenyldiazenyl)-5-mercapto-1H-pyrazol-3-yl)-3- phenylthiourea **14** was obtained from reaction of **5** with phenyl isothiocyanate, which was transformed into pyrazolothiadiazole **15** and pyrazolotriazole **16** derivatives with bromine in different solvents. 3-Amino-5-hydrazino-4-phenylazo-1H-pyrazole **17** was obtained from reaction **5** with hydrazine hydrate. Cyclization of compound **17** by reacting it with ethyl acetoacetate, acetylacetone, phthalic anhydride and phenacyl bromide gave the corresponding N-pyrazolylpyrazoles (**18** and **19**), pyrazol-2,3-dihydrophthalazine-1,4-dione (**20**) and pyrazolotriazine (**21**), respectively. Reaction of 17 with sodium nitrite in the presence acetic acid, ethyl pyruvate and carbon disulfide gave the corresponding pyrazolotetrazole (**22**), imidazolopyrazole (**23**) and pyrazolotriazole derivatives (**26**).

* Corresponding Authors
E-Mail: redmof56@yahoo.com
[a] Department of Chemistry, Faculty of Science, Zagazig University, Zagazig, Egypt.
[b] Plant Protection Insititute, (Sharkia branch), Agricultural Research Center, Sharkia, Egypt.

Introduction

Pyrazoles and their substituted derivatives are interesting as potential pharmaceuticals, and intermediates in dye industry. Despite the enormous number of substituted pyrazoles reported in the literature only a limited number of bispyrazole derivatives have so for been reported. Our interest in synthesis and reactivity of the parent compounds arises from promise medicinal chemistry[1-3] and organometallic complex reactivity. The present investigation is in continuation of our previous work on 3-amino-5-hydroxy-4-phenylazo-1H-pyrazole (**1**) and all analysis is agreement with the structure.[4]

Experimental

Melting points were recorded using SMP30 Melting Point Apparatus (Stuart) and are uncorrected. The IR spectra were record on KBr discs using a FTIR 600 series spectrophotometer (JASCO) and ^{1}H NMR spectra (δ ppm) were recorded on a Varian 300 MHZ spectrometer using CDCl3 as solvent.

_N_-(4-(2-Phenyldiazenyl)-2,5-dihydro-3-hydroxy-1_H_-pyrazol-5-yl)-2-chloroacetamide (2).

To a solution of compound **1** (0.21 g, 1 mmol) in dioxane (30 mL), chloroacetyl chloride (0.09 g, 1 mmol) was added drop wise with stirring at room temperature. The reaction mixture was refluxed for 30 min. at 60 °C, the solution was concentrated to a small volume, poured into ice-cold water and recrystallized from ethonal, yield 60 %. M. p.210 °C. IR (KBr): 3425 (O-H), 3335 (N-H), 1700 (C=O) cm^{-1}. 1H-NMR($CDCl_3$): 2.8 (s, 2H, CH_2), 5.0 (s, 1H, NH), 6.8-7.8 (m, 5H, Ar-H), 9.0 (s, 1H, NH), 12.33 (br, 1H, OH). Anal. Calcd. for $C_{11}H_{10}N_5O_2Cl$: C: 47.24 %; H: 3.60 %; N: 25.04 %; Cl: 12.67 %; Found : C: 47.21 %; H: 3.61 %; N: 25.05 %; Cl: 12.68 %.

1-(4-(2-Phenyldiazenyl)-5-hydroxy-1_H_-pyrazol-3-yl)-2-amino-4,5-dihydro-5-oxo-1_H_-pyrrol-3-carbonitrile (3).

To a solution of compound **2** (0.27 g, 1 mmol) in dioxane (30 mL) a catalytic amount of TEA (triethylamine) (0.5 mL), malononitrile (0.06 mL, 1 mmol) was added. The reaction mixture was refluxed for 4 h, cooled, poured onto cold water and neutralized with dilute HCl, the precipitate was collected, filtered off, dried and recrystallized from dioxane. Yield 54 %, M. p. 300 °C. IR (KBr): 3540 (O-H), 3375 (NH_2), 3280 (N-H), 3050 ($CH_{aromatic}$), 2240 (CN), 1690 (C=O) cm^{-1} . ^{1}H-NMR($CDCl_3$): 2.3 (s, 2H, CH_2), 5.2(s, 2H, NH_2), 7.1-8.9 (m, 5H, Ar-H), 9.2(s, 2H, NH), 12.3(br, 1H, OH). Anal. Calcd. for $C_{14}H_{11}N_7O_2$: C: 54.36 %; H: 3.58 %; N: 31.70 %; Found: C:54.34 %; H: 3.59 %; N: 31.71 %.

3-(2-Phenyldiazenyl)-7-amino-2-hydroxy pyrazolo[1,5-_a_] pyrimidin-5(1_H_)-one (4).

To a solution of compound **2** (0.27 g, 1 mmol) in absolute ethanol (30 mL) containing sodium ethoxide (0.01 g, 1 mmol), ammonium isothiocyanate (0.07 g, 1 mmol) was added. The reaction mixture was refluxed for 5 h. The solid product was collected and recrystallized from ethanol. Yield 69 %. M. p.140 °C. IR (KBr): 3550 (O-H), 3443 (NH_2), 3275 (N-H), 3058 ($CH_{aromatic}$), 1680 (C=O) cm^{-1}. ^{1}H-NMR

Eur. Chem. Bull., **2016**, *5(5)*, 157-162 DOI: 10.17628/ecb.2016.5.157-162

($CDCl_3$): 5.8 (s, 2H, NH_2), 6.8-7.8 (m, 6H, Ar-H and pyrimidine-H), 8.9 (s, 1H, NH), 12.0 (br, 1H, OH). Anal. Calcd. for $C_{16}H_{11}N_7O_3$: C: 53.13 %; H: 4.08 %; N: 30.98 %; Found: C: 53.11 %; H: 4.09 %; N: 30.99 %.

3-Amino-5-mercapto-4-phenylazo-1*H*-pyrazole (5)

A solution of compound **1** (0.2 g, 1 mmol) was heated at reflux temperature in dry pyridine (20 mL) containing phosphorus pentasulfide (0.2 g, 1 mmol) for 5 h. The solution was acidified with dil. HCl and the solid precipitate was filtered off, washed several times with water, dried and recrystallized from dimethylformamide. Yield 75 %, M. p. 200 °C. IR (KBr): 3432 (NH_2), 3375 (NH), 2560 (SH) cm^{-1}. ^{1}H-NMR ($CDCl_3$): 6.3 (s, 1H, NH), 6.8-7.6 (m, 5H, Ar-H), 8.5 (s, 2H, NH_2), 13.04 (s, 1H, SH). Anal. Calcd. for $C_9H_9N_5S$: C: 49.29 %; H: 4.14 %; N: 31.49 %; S: 14.62 %; Found: C: 49.28 %; H: 4.15 %; N: 31.48 %; S: 14.63 %.

2-(4-(2-Phenyldiazenyl)-5-mercapto-1*H*-pyrazol-3-ylamino)-acetic acid (6)

A solution of compound **5** (0.21 g, 1 mmol), chloro acetic acid (0.08 g, 1 mmol) and sodium acetate (0.07 g, 1 mmol) was heated at reflux temperature for 3 h in absolute ethanol (20 mL), the precipitate was collected and recrystallized from ethanol. Yield 75 %. M. p. 256 °C. IR (KBr): 3300 (OH), 3260 (NH), 2641 (SH), 1700 (C=O) cm^{-1} ^{1}H-NMR ($CDCl_3$): 2.8(s, 2H, CH_2), 5.8 (s, 1H, NH), 7.0-7.8 (m, 5H, Ar-H), 8.9 (s, 1H, NH), 12.0 (s, 1H, OH), 13.2 (s, 1H, SH). Anal. Calcd. for $C_{11}H_{11}N_5O_2S$: C: 47.64; H: 3.99; N: 25.25; S: 11.56 %; Found: C: 47.263; H: 3.98; N:25.28; S: 11.55 %.

Ethyl 2-(4-(2-phenyldiazenyl)-5-mercapto-1*H*-pyrazol-3-yl)aminoacetate (7)

A solution of compound **5** (0.21 g, 1 mmol), ethyl chloroacetate (0.11 g, 1 mmol) and sodium acetate (0.07 g, 1 mmol) in absolute ethanol (20 mL) were heated at reflux temperature for 3 h. After cooling to room temperature, the precipitate was filtered off, dried and recrystallized from ethanol. Yield 70 %. M. p. 246 °C. IR (KBr): 3480 (NH), 2650 (SH), 1710 (C=O) cm^{-1}. ^{1}H-NMR ($CDCl_3$):1.26(t, 3H, CH_3), 2.8(s, 2H, CH_2), 4.2 (q, 2H, CH_2), 5.8 (s, 1H, NH), 7.0-7.8 (m, 5H, Ar-H), 8.9 (s, 1H, NH), 12.9 (s, 1H, SH). Anal. Calcd. for $C_{13}H_{15}N_5O_2S$: C: 51.13; H:4.95; N: 22.93; S: 10.50 %; Found: C: 51.14; H: 4.94; N:22.91; S: 10.52 %.

2-(4-(2-Phenyldiazenyl) -5-mercapto-1*H*- pyrazol -3ylamino)-acetohydrazide (8)

A solution of compound **7** (0.3 g, 1 mmol) was mixed with a solution containing absolute ethanol (15 mL) and hydrazine hydrate (0.05 g, 1 mmol) and the reaction mixture was heated at reflux temperature for 2 h, left standing overnight at 25 °C, the precipitate formed was filtered off, washed with methanol and light petroleum, dried and recrystallized from diluted acetic acid or water. Yield 70 %. M. p. 100 °C. IR (KBr): 3400 (NH_2), 3381 (NH), ($CH_{aromatic}$), 2850 (CH-aliphatic), 2650 (SH), 1686 (C=O) cm^{-1}. ^{1}H-NMR ($CDCl_3$): 4.4 (s, 2H, NH_2), 7.1-7.8 (m, 5H, Ar-H), 9.6 (s, 1H, NH), 9.8 (s, 1H, NH), 13.3 (s, 1H, SH). Anal. Calcd. for $C_{11}H_{13}N_7OS$: C: 45.35; H: 4.49; N:33.65; S: 11.00 %; Found: C: 45.38; H: 46; N: 33.63; S: 11.02 %.

4-(2-Phenyldiazenyl)-3-(pyrrolidin-1-yl)-1*H*-pyrazol-5-thiol (9).

A solution of compound **5** (0.21 g, 1 mmol) and tetrahydrofuran (0.06 g, 1 mmol) in glacial acetic acid (15 mL) were heated at reflux temperature for 8 h. The solvent was reduced to one third of its volume under reduced pressure and after cooling the precipitate formed was collected and recrystallized from ethanol. Yield 52 %. M. p. 190 °C. IR (KBr): 3450 (NH), 3055 ($CH_{aromatic}$), 2645 (SH) cm^{-1}. ^{1}H NMR ($CDCl_3$): 1.4 (m, 4H, $2CH_2$), 2.9 (m, 4H, $2CH_2$), 5.9 (s, 1H, NH), 7.0-7.8 (m, 5H, Ar-H), 13.2 (s, 1H, SH). Anal. Calcd. for $C_{13}H_7N_5S$: C: 58.85; H: 2.65; N: 26.39; S: 12.08 %; Found: C:58.84; H:2.66; N: 26.38; S: 12.09 %.

3-((-4-(2-Phenyl diazenyl) 5-mercapto-1*H*- pyrazol -3-yl imino) methyl)phenol (10).

A solution of compound **5** (0.21 g, 1 mmol) and 3-hydroxybenzaldhyde (0.12 g, 1 mmol) in absolute ethanol (15 mL) was heated at reflux temperature for 7 h, cooling to room temperature, the precipitate formed was filtered off, dried and recrystallized from ethanol. Yield 80 %. M. p. 244 °C. IR (KBr): 3560 (OH), 3450 (NH), 3060 ($CH_{aromatic}$), 2590 (SH), 1634 (C=N) cm^{-1}. ^{1}H-NMR ($CDCl_3$): 7.0-7.8 (m, 9H, Ar-H), 8.6 (s, 1H, N=CH), 9.8 (s, 1H, NH), 12.0 (S,1H,OH), 13.4 (s,1H,SH). Anal. Calcd. for $C_{16}H_9N_5OS$: C: 60.17; H: 2.84; N: 21.93; S: 10.04 %; Found: C: 60.18; H: 2.85; N: 21.94; S: 10.03 %.

2-(4-(2-Phenyldiazenyl) 3-amino-1*H*- pyrazol -5-yl thio) 1-phenylethanone (11).

A solution of compound **5** (0.21 g, 1 mmol), phenacyl bromide (0.19 g, 1 mmol) and sodium acetate (0.07 g, 1 mmol) were heated at reflux in ethanol (15 mL) for 3 h. The precipitate formed was filtered off, washed with water several times, dried and recrystallized from ethanol. Yield 50 %. M. p. 240 °C. IR (KBr): 3450(NH2), 3325 (NH), 1700 (C=O) cm^{-1}. ^{1}H-NMR ($CDCl_3$): 2.5 (s, 2H, CH_2), 5.8 (s, 1H, NH), 7.0-7.8 (m, 10H, Ar-H), 8.9 (s, 2H, NH_2). Anal. Calcd. for $C_{16}H_{15}N_5OS$: C:59.05; H: 4.65; N: 21.52; S: 9.82 %; Found: C: 59.02; H: 4.68; N: 21.53; S: 9.84 %.

***N*-4,5-Diphenylpyrazolo[3,4-*b*][1,4]thiazine-3,4(1*H*)-diamine (12).**

To a solution of compound **11** (0.3 g, 1 mmol) in a glacial acetic acid:sulphuric acid mixture (5 mL:1 mL) were heated on water bath for 5 h. The reaction mixture was allowed to cool, neutralized by sodium carbonate solution (10 %). The precipitate formed was collected and recrystallized from acetic acid. Yield 55 %. M. p. 300 °C. IR (KBr): 3450 (NH_2), 3380 (NH), 3050 ($CH_{aromatic}$) cm^{-1}. ^{1}H-NMR ($CDCl_3$): 5.8 (s, 1H, NH) , 7.0-7.8 (m, 11H, Ar-H and thiazine-H), 8.9 (s, 1H, NH), 9.2(s, 2H, NH_2). Anal. Calcd. for $C_{17}H_{14}N_5S$: C: 63.73; H: 4.40; N: 21.85; S: 10.00 %; Found : C: 63.72; H: 4.41; N: 21.84; S: 10.01 %.

Eur. Chem. Bull., **2016**, *5(5)*, 157-162 DOI: 10.17628/ecb.2016.5.157-162

2-(4-(2-Phenyldiazenyl)-5-mercapto-1*H*-pyrazol-3-yl imino)-2*H*-indene-1,3-dione (13)

A solution of compound **5** (0.12 g, 1 mmol) and ninhydrine (0.17 g, 1 mmol) in absolute ethanol (25 mL) was stirred for 2 h, then the precipitate formed was collected and recrystallized from ethanol. Yield 80 %. M. p. 130 °C. IR (KBr): 3453 (NH), 3058 ($CH_{aromatic}$), 2590 (SH), 1688, 1628 (2C=O) cm^{-1}. ^{1}H-NMR ($CDCl_3$): 5.8 (s, 1H, NH), 7.0-7.9 (m, 9H, Ar-H), 13.0 (s, 1H, SH). Anal. Calcd. for $C_{18}H_{11}N_5O_2S$: C: 59.82; H: 3.06; N: 19.38; S: 8.87 %. Found: C: 59.81; H: 3.07; N: 19.39; S: 8.86 %.

1-(4-(2-Phenyldiazenyl)-5-mercapto-1*H*-pyrazol-3-yl)-3-phenyl-thiourea (14)

A solution of compound **5** (0.21 g, 1 mmol) and phenylisothiocyanate (0.15 g, 1 mmol) was heated at reflux temperature for 7 h in absolute ethanol (30 mL), the precipitate was collected and recrystallized from ethanol. Yield 57 %. M. p. 100 °C. IR (KBr): 3500 (NH), 3055 ($CH_{aromatic}$), 2600 (SH), 1335 (C=S) cm^{-1}. ^{1}H-NMR ($CDCl_3$): 6.8 (s, 1H, NH), 7.0-7.8 (m, 10H, Ar-H), 9.2 (s, 1H, NH), 9.8 (s, 1H, NH) and 13.0 (s, 1H, SH). Anal. Calcd for $C_{16}H_{14}N_6S_2$: C: 54.21; H: 3.98; N: 23.71; S: 18.09 %. Found: C: 54.23; H: 3.96; N: 23.72; S: 18.08 %.

7-(2-Phenyldiazenyl)-2-(phenylamino)pyrazolo[1,5-*b*][1,2,4]-thiadiazol-1-yl-6-thiol (15)

To a solution of compound **14** (0.12 g, 1 mmol) in pyridine (20 mL), bromine (0.15 g, 1 mmol) in pyridine (5 mL) was added dropwise at room temperature. The reaction mixture were heated under reflux for 1 h. The mixture was cooled, poured into water with stirring, the solid precipitated was collected, filtered off, washed with water, dried and recrystallized from ethanol. Yield 57 %. M. p. 90 °C. IR (KBr): 3450 (NH), 3055 ($CH_{aromatic}$), 2680 (SH)cm^{-1}. ^{1}H-NMR ($CDCl_3$): 5.8 (s, 1H, NH) , 7.0-7.9 (m, 10H, Ar-H), 13.0 (s, 1H, SH).Anal. Calcd for $C_{16}H_{12}N_6S_2$: C: 54.52; H: 3.43; N: 23.85; S: 18.19 %. Found: C: 59.53; H: 3.42; N: 23.86; S: 18.18 %.

3-Phenyl-7-(phenyldiazenyl)-3*H*-pyrazolo[1,5-*b*][1,2,4]triazol-2,6-dithiol (16)

To a solution of compound **14** (0.21 g, 1 mmol) in a glacial acetic acid (20 mL), bromine(0.15 g, 1 mmol) in a glacial acetic acid (5 mL) was added dropwise at room temperature. The reaction mixture were heated under reflux for 1 h, cooled, poured into water with stirring. The solid precipitated was filtered off, washed with water, dried and recrystallized from ethanol. Yield 66 %. M. p. 110 °C. IR (KBr): 3065 (CH-aromatic), 2600, 2590 (2SH) cm^{-1} . ^{1}H-NMR ($CDCl_3$): 7.0-7.9 (m, 10H, 2Ar-H), 12.9(s, 1H, SH), 13.2 (s, 1H, SH). Anal. Calcd. for $C_{10}H_{13}N_6S_2$:C: 42.68; H: 4.65; N: 29.86; S: 22.79 %. Found : C: 42.69; H: 4.64; N: 29.87; S: 22.78 %.

3-Amino-5-hydrazino-4-phenylazo-1*H*-pyrazole (17)

Hydrazine hydrate (0.05 g, 1 mmol) was added to a solution of compound **5** (0.2 g, 1 mmol) in absolute ethanol (15 mL), the reaction mixture was heated under reflux for 6 h or until the evolution of H_2S ceased, the solid precipitated was filtered off, dried and recrystallized from ethyl acetate. Yield 75 %. M. p. 270 °C. IR (KBr): 3438 (NH2), 3382 (N-H), 3055 ($CH_{aromatic}$) cm^{-1}. ^{1}H-NMR ($CDCl_3$): 4.5 (s, 1H, NH), δ4.9 (s, 2H, NH_2), δ5.6 (s, 2H, NH_2), δ6.9-7.3 (m, 5H, Ar-H) and at δ8.4 (s, 1H, NH). Anal. Calcd. For $C_9H_{11}N_7$: C: 49.75; H: 5.10; N: 45.14 %. Found: C: 49.76; H: 5.11; N: 45.12 %.

1-(4-(2-Phenyldiazenyl)-3-amino-1*H*-pyrazol-5-yl)-3-methyl-1*H*-pyrazol-5(4*H*)-one (18)

Ethyl acetoacetate (0.1 g,1 mmol) was added to a solution of compound **17** (0.21 g, 1 mmol) in absolute ethanol (20 mL), the reaction mixture was heated under reflux for 10 h. The solution was concentrated and cooled, the solid precipitated was filtered off, dried and recrystallized from benzene. Yield 65 %. M. p. 250 °C. IR (KBr): 3450 (NH_2), 3395 (NH), 3045 ($CH_{aromatic}$), 1688 (C=O) cm^{-1}. ^{1}H-NMR ($CDCl_3$):2.3 (s, 2H, CH_3), 5.8(s, 2H, CH_2 of pyrazolone), 7.2-8.0 (m, 5H, Ar-H), 8.9(s, 2H, NH_2), 12.5 (s, 1H, NH). Anal. Calcd for $C_{13}H_{11}N_7O$: C: 55.51; H: 3.94; N; 34.85 %. Found: C: 55.50; H: 3.93; N: 34.87 %.

4-(2-Phenyldiazenyl)-5-(3,5-dimethyl-1*H*-pyrazol-1-yl)-1*H*-pyrazol-3-amine (19)

Acetyl acetone (0.1 g, 1 mmol) was added to a solution of compound **17** (0.21 g, 1 mmol) in absolute ethanol (20 mL), the reaction mixture was heated under reflux for 10 h. The mixture was concentrated and cooled, the solid precipitated were collected by filtration, dried and recrystallized from benzene. Yield 77 %. M. p. 210 °C. IR (KBr): 3445 (NH_2), 3390 (NH), 3055 ($CH_{aromatic}$) cm^{-1} . ^{1}H-NMR ($CDCl_3$): 1.5 (s, 6H, $2CH_3$), 6.0 (s, 2H, CH_2 of pyrazolone), 7.0-7.8 (m, 5H, Ar-H), 8.4 (s, 2H, NH_2), 13 (s, 1H, NH). Anal. Calcd for $C_{14}H_{13}N_7$: C: 60.20; H: 4.69; N: 35.11 %. Found: C: 60.22; H: 4.68; N: 35.10 %.

2-(4-(2-Phenyldiazenyl)-3-amino-1*H*-pyrazol-5-yl)-2,3-dihydro-phthalazine-1,4-dione (20)

Phthalic anhydride (0.14 g, 1 mmol) was dissolved in a solution of compound **17** (0.21 g, 1 mmol) in acetic acid (30 mL), the reaction mixture was heated under reflux for 10 h. The mixture was concentrated, cooled, poured onto crushed ice, the solid precipitated was collected by filtration, dried and recrystallized from chloroform. Yield 80 %. M. p. 256 °C. IR (KBr): 3445 (NH_2), 3368 (NH), 3095 ($CH_{aromatic}$), 1670, 1685 (2C=O) cm^{-1} . ^{1}H-NMR ($CDCl_3$):5.8 (s, 1H, NH), 6.2(s, 1H, NH), 7.0-7.8 (m, 9H, Ar-H), 8.9(s, 2H, NH_2). Anal. Calcd. for $C_{17}H_9N_7O_2$: C: 59.47; H: 2.64; N: 28.56 %. Found : C: 59.45; H: 2.65; N: 28.57 % .

Eur. Chem. Bull., **2016**, *5(5)*, 157-162 DOI: 10.17628/ecb.2016.5.157-162

(3-Amino-4-(phenylamino)-4,5-dihydro-1*H*-pyrazolo[4,3-*e*]-[1,2,4]triazin-5-yl)(phenyl)methanone (21)

A solution of compound **17** (0.21 g, 1 mmol) and phenacyl bromide (0.1 g, 1 mmol) in absolute ethanol (30 mL) was refluxed for 5 h, the precipitate formed was filtered off, dried and recrystallized from chloroform. Yield 60 %. M. p. 70 °C. IR (KBr): 3468 (NH_2), 3378 (N-H), 3055 ($CH_{aromatic}$), 1703 (C=O) cm^{-1} . ^1H NMR($CDCl_3$): 5.8(s, H, NH), 7.0-7.9 (m, 10H, 2Ar-H), 8.3(s, 1H, NH), 9.2 (s, 1H, NH_2). Anal. Calcd for $C_{17}H_{15}N_7O$: C: 58.84; H: 4.33; N: 28.06 %. Found : C: 58.82; H: 4.34; N: 28.05 %.

6-((Acetoxy)diazenyl)-7-(phenyldiazenyl)-3*H*-pyrazolo[1,5-*d*]tetrazole (22)

A solution of sodium nitrite (0.13 g, 1 mmol) in water (10 mL) was added to a cold solution of **17** (0.21 g, 1 mmol) in acetic acid (20 mL). After completion of addition, the ice bath was removed and srirring was continued for 1 h. The precipitate was filtered off, dried and recrystallized from ethanol. Yield 58 %. M. p. 130 °C. IR (KBr): 3440 (N-H), 3055 ($CH_{aromatic}$), 2120 (N_2), 1703 (C=O) cm^{-1} . ^1H-NMR ($CDCl_3$): 7.0-7.9 (m, 5H, Ar-H), 13.0(s, 1H, NH). Anal. Calcd for $C_{11}H_{11}N_9O_2$: C: 39.63; H: 3.32; N: 37.81 %. Found: C: 39.60; H: 3.33; N: 37.83 %.

7-(2-Phenyldiazenyl)-6-hydrazinyl-2-methyl-5*H*-imidazo[1,2-*b*]pyrazol-3-ol (23)

A solution of compound **17** (0.21 g, 1 mmol) was refluxed in absolute ethanol (20 mL) containing ethyl pyruvate (0.11 g, 1 mmol) for 5 h. The precipitate formed was filtered off, washed several times with water, dried and recrystallized from dioxane. Yield 55 %. M. p. 180 °C. IR (KBr): 3529 (O-H), 3430 (NH_2), 3358 (N-H), 3030 ($CH_{aromatic}$) cm^{-1} . ^1H-NMR ($CDCl_3$):2.8 (s, 3H, CH_3), 4.8(s, 2H, NH_2), 5.8(s, 1H, NH), 7.0-7.8 (m, 5H, Ar-H), 9.6(s, 1H, NH), 12.1 (s, 1H, OH). Anal. Calcd for $C_{12}H_{13}N_7O$: C: 50.15; H: 4.56; N: 34.12 %. Found: C: 50.16; H: 4.57; N: 34.10 %.

Potassium 5-hydrazinyl-4-(phenyldiazenyl)-1H-pyrazol-3 yl-carbamodithioate (24)

To a warmed ethoxide solution prepared by dissolving potassium hydroxide (0.011 g, 1 mmol) in absolute ethanol (30 mL), compound **17** (0.21 g, 1 mmol) and CS_2 (0.07 g, 1 mmol) were added. The reaction mixture wase heated under reflux for 2 h in a water bath. After cooling, the mixture was poured onto crushed ice, neutralized by diluted acetic acid and the solid precipitated was collected by filtration, dried and recrystallized from ethanol. Yield 60 %. M. p. 240 °C. IR (KBr): 3355 (NH_2), 3250 (N-H), 3055 ($CH_{aromatic}$), 1334 (C=S) cm^{-1} . Anal. Calcd for $C_{10}H_{11}N_7S_2$: C: 40.93; H: 3.77; N: 33.42; S: 21.85 %. Found : C: 40.94; H: 3.76; N: 33.43; S: 21.84 %.

***N*-[5-(hydrazino)4-(phenyldiazenyl)-1*H*-pyrazol-3yl]hydrazine-carbothioamide (25):**

A mixture of compound **24** (0.29 g, 1 mmol) and hydrazine hydrate (0.05 g, 1 mmol) was heated in absolute ethanol (15 mL) under reflux for 10-12 h. The solids precipitated was collected, filtered off, dried and recrystallized from chloroform. Yield 55 %. M. p. 265 °C. IR (KBr): 3375 (NH_2), 3280 (N-H), 3050 ($CH_{aromatic}$), 1335(C=S) cm^{-1} .Anal. Calcd for $C_{10}H_8N_9S$: C: 41.95; H: 2.81; N: 44.03; S: 11.20 %. Found : C: 41.94; H: 2.82; N: 44.02; S: 11.21 %.

4-(5-Hydrazinyl-4-phenyldiazenyl-1*H*-pyrazol-3yl)3-phenyl-1*H*[1,2,4]triazole-5(4*H*)-thione (26)

Benzoylchloride (0.12 g, 1 mmol) was added dropwise to a cold solution of thiosemicarbazide derivative **25** (0.29 g, 1 mmol) in dry pyridine (15 mL), the reaction mixture was heated under reflux for 5 h. The solid precipitated was collected by filtration, washed with water several times, dried and recrystallized from ethanol. Yield 55 %. M. p. 300 °C. IR (KBr): 3540 (O-H), 3375 (NH_2), 3280 (N-H), 3050 ($CH_{aromatic}$), 2240 (CN), 1690 (C=O) cm^{-1}. ^1H-NMR ($CDCl_3$): 5.8 (s ,1H, NH), 4.4(s, 2H, NH_2), 7.0-7.8 (m, 10H, Ar-H), 8.6(s, 1H, NH), 12.0 (s,1H, NH). Anal. Calcd. for $C_{14}H_{11}N_7O_2$: C: 54.36; H: 3.58; N: 31.70 %; Found : C: 54.34; H: 3.59; N: 31 %.

RESULTS AND DISCUSSION

3-Amino-5-hydroxy-4-phenylazo-1H-pyrazole **1** was prepared and was allowed to react with chloroacetyl chloride in dioxane at room temperature with formation of the acylated product, namely *N*-(4-(2-phenyldiazenyl)-2,5-dihydro-3-hydroxy-1*H*-pyrazol-5-yl)-2-chloroacetamide **2**. The IR spectra revealed the presence of (C=O) at 1700 cm^{-1} and the absorption bands characteristic for NH_2 group were disappeared completely. The cyclization of compound **2** with malononitrile or ammonium isothiocyanate in various solvents gave the corresponding pyrazolopyrrol-3-carbonitrile **3** and pyrazolo[1,5-*a*]pyrimidine 4 derivatives (Scheme 1).

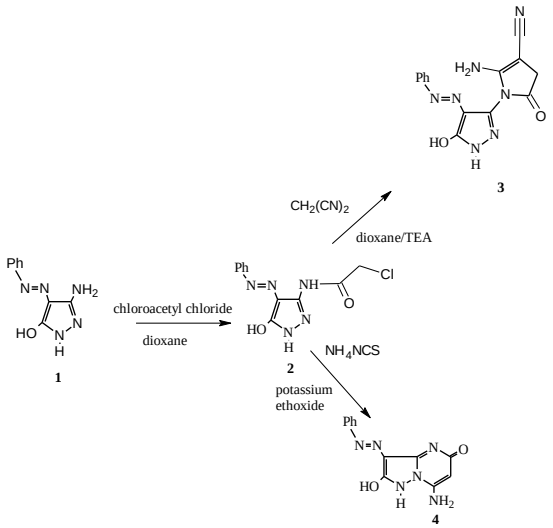

Scheme 1. Synthesis of compounds **1-4**.

IR spectrum of compound **3** unambiguously confirmed the presence of NH_2 group vibrations at 3375 and CN group bands at 2240 cm^{-1}. Treatment of compound **1** with P_2S_5 in dry pyridine gave the corresponding 3-amino-5-mercapto-4-phenylazo-1H-pyrazole (**5).**

 DOI: 10.17628/ecb.2016.5.157-162

Treatment of compound **5** with chloroacetic acid, tetrahydrofuran, 3-hydroxybenzaldhyde, phenacyl bromide and ninhydrine gave the corresponding N-alkylation or condensation products (**6, 7, 9** and **10**, respectively). Reaction of the compound **7** with hydrazine hydrate afforded compound **8**. (Scheme 2). Treatment of compound **5** with phenacyl bromide and ninhydrine gave the corresponding N-alkylation or condensation products **11** and **13**, respectively.

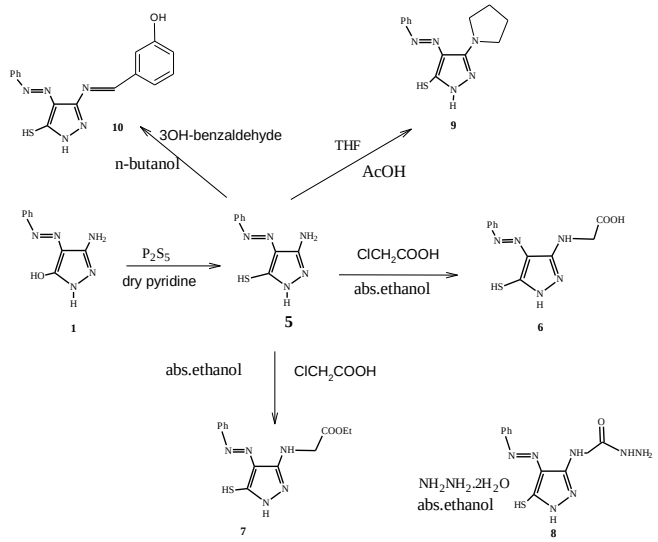

Scheme 2. Synthesis of compounds **5-10.**

In the IR spectrum of compound **13** the bands appear at 1688 and 1682 cm^{-1}, respectively, are characteristic for the C=O groups. The ring closure of compound **11** in the presence of sulphuric acid and acetic acid mixture gave the pyrazolothiazine **12.**

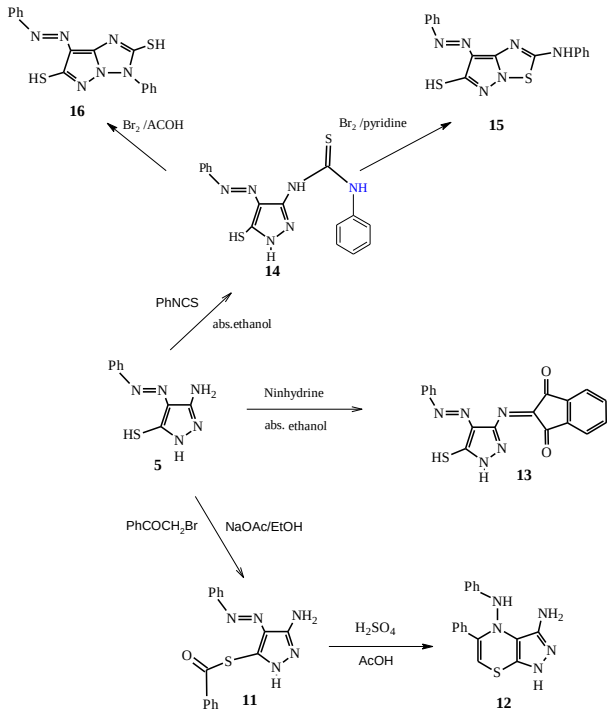

Scheme 3. Synthesis of compounds **11**-**16**.

Reaction of compound **5** with phenyl isothiocyanate gives a pyrazolothiourea derivative (**14**). The compounds pyrazolothiadiazole **15** and pyrazolotriazole **16** were obtained by the reaction of **14** with bromine in different solvent. In the IR spectrum of compound **16** the bands appear at 2600 and 2590 cm^{-1} are characteristic for (SH)groups. (Scheme 3).

3-Amino-5-hydrazino-4-phenylazo-1H-pyrazole **17** was obtained by the reaction of **5** with hydrazine hydrate in the abs. ethanol. Condensation of hydrazinopyrazole **17** with ethyl acetoacetate, acetylacetone, phthalic anhydride and phenacyl bromide in different solvents gave the corresponding N-pyrazolylpyrazole derivatives **18** and **19**, N-alkylated pyrazole **20**, and pyrazolotriazine **21**, respectively (Scheme 4).

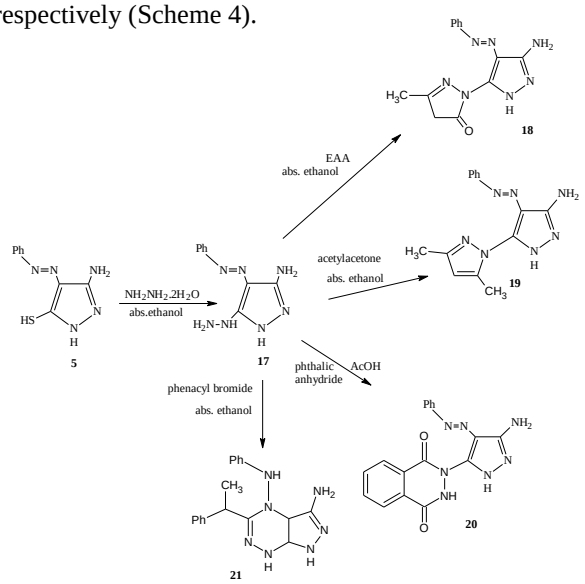

Scheme 4. Synthesis of compounds **17**-**21**.

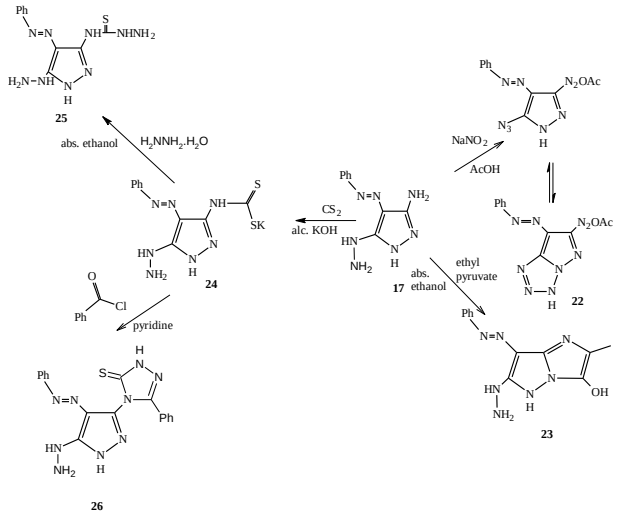

Scheme 5. Synthesis of compounds **22**-**26**.

Diazotization of compound **17** with sodium nitrite and acetic acid led obtain pyrazolo[1,5-*d*]tetrazole derivative **(22).** Cyclization of compound **17** with ethyl pyruvate yielded imidazolo[1,2-*b*]pyrazole **(23).** The structure of compound **23** has assigned on basis of its spectroscopic data.

Eur. Chem. Bull., **2016**, *5(5)*, 157-162 DOI: 10.17628/ecb.2016.5.157-162

The IR revealed the presence of (OH) at 3529 cm-1 moreover, reaction of **17** with carbon disulfide yielded the corresponding pyrazolocarbamodithioate **24**. Hydrazonolysis of compound 17 in the presence hydrazine hydrate afforded pyrazolohydrazinecarbothioamide **25** which underwent further cyclization with benzoylchloride in pyridine afforded pyrazolotriazole **26 (**Scheme 5**).** The structures of all these compounds were elucidated from its spectral and elemental analysis data.

Conclusion

3-Amino-5-hydroxy-4-phenylazo-1H-pyrazole **1** was effectively used as precursor in the preparation of various pyrazole derivatives. N-(4-(2-Phenyldiazenyl)-2,5-dihydro-3-hydroxy-1H-pyrazol-5-yl)-2 chloroacetamide **2** was obtained from reaction of **1** with chloroacetyl chloride, and the further reaction of **2** with malononitrile and ammonium isothiocyanate gave the corresponding 1-(4-(2-phenyldiazenyl)-5-hydroxy-1H-pyrazol-3-yl)-2-amino-4,5-dihydro-5-oxo-1H-pyrrol-3-carbonitrile **3** and 3-(2-phenyldiazenyl)-7-amino-2-hydroxypyrazolo[1,5-*a*]pyrimidin-5(1H)-one **4**.

Thiation of **1** with P_2S_5 gave the corresponding 3-amino-5-mercapto-4-phenylazo-1H-pyrazole **5**. The reaction of compound **5** with chloroacetic acid, ethyl chloroacetate, tetrahydrofuran, 3-hydroxybenzaldehyde, phenacyl bromide and ninhydrine gave the corresponding N-substituted substituted pyrazoles (**6**, **7**, **8**, **9**, **10**, **11**, **12**, **13**), respectively. Hydrazenolysis of **7** in the presence of hydrazine hydrate afforded **8** and cyclization of **11** in the presence glacial acetic acid and sulfuric acid mixture afforded the compound **12**.

The 1-(4-(2-Phenyldiazenyl)-5-mercapto-1H-pyrazol-3-yl)-3-phenylthiourea **14** was obtained from reaction of **5** with phenyl isothiocyanate. Pyrazolothiadiazole **15** and pyrazolotriazole **16** were obtained by the reaction of **14** with bromine in different solvents.

3-Amino-5-hydrazino-4-phenylazo-1H-pyrazole **17** could be obtained from reaction **5** with hydrazine hydrate.

Cyclization of compound **17** by reacting it with ethyl acetoacetate, acetylacetone, phthalic anhydride and phenacyl bromide gave the corresponding N-pyrazolylpyrazole derivatives **18** and **19,** pyrazol-2,3-dihydrophthalazine-1,4-dione **20** and pyrazolotriazine **21**, respectively.

Reaction of **17** with sodium nitrite in the presence acetic acid, ethyl pyruvate and carbon disulfide gave the corresponding pyrazolotetrazole **22**, imidazolopyrazole **23** and pyrazolotriazole derivatives **26**.

References

[1]Elnagd, M. H., Abdalla, S. O., *J. Prakt. Chem*., **1973**, *315*, 1009-1016

[2]Elnagdi,M. H., El Moghayar, M. R. H., Sadek, K. U., *J. Hetercycl. Chem*., **1990**, *48*, 223.

[3]Fikry, R.M., Hataba, M. G., Assy, M. G., *Ind. J. Chem*., 1996, 35, 144-16.

[4]Hardy, . R., *Adv. Heterocycl. Chem*., **1984**, *36*, 343.

[5]Rashad, A. E.; Hegab, M. I.; Abdel-megeid, R. E.; J. A. Micky., *Biorg. Med. Chem.*, **2008**, *16*, 7102-7106

[6]Salih, N A., *Turk. J. Chem*., **2008**, *32*, 229-235.

[7]Seelen, W., Schafe, M., Ernst, A., *Tetrahedron Lett*., **2003**, *44*, 4491-4493.

Received: 24.04.2016.
Accepted: 29.06.2016.

CORROSION RESISTANCE OF MILD STEEL IN SIMULATED CONCRETE PORE SOLUTION IN PRESENCE OF SIMULATED URINE, TARTARIC ACID AND LACTIC ACID

P. Nithya Devi [a], S Rajendran[b]*, J.Sathiyabam[a], M. Pandiarajan[a] , R. Joseph Rathish[c] and S. Santhana Prabha [c]

Keywords: Concrete corrosion, mild steel, urine corrosion, lactic acid, tartaric acid

Corrosion resistance of mild steel in simulated concrete pore solution (SCPS) in presence of simulated urine (SU), tartaric acid and lactic acid has been evaluated by electrochemical studies such as polarization study and AC impedance spectra. These studies lead to the conclusion that, the corrosion resistance of mild steel in various test solutions is as follows. Lactic acid+ SCPS+ urine > tartaric acid+ SCPS+ urine > SCPS > SCPS+ urine > urine. This leads to the conclusion that urination on the concrete structures such as bridges and building should be discouraged. Otherwise, the structure may collapse one day without prior information. However, the inclusion of tartaric acid or better lactic acid during the preparation of concrete admixtures strengthens the structures and should be encouraged

Correspomding author
Fax: +91 451 2424114
E-Mail: susairajendran@gmail.com.
[a] PG and Research Department of Chemistry, G.T.N. Arts College, Dindigul- 624005, India.
E-mail: nithichem7@gmail.com.
[b] Corrosion Research Centre, Department of Chemistry, RVS School of Engineering and Technology, Dindigul-624005, India. E-mail: susairajendran@gmail.com.
[c] PSNACollege of Engineering and Technology, Dindigul, India. Email:rathishjosoph@gmail.com.

Introduction

Reinforced concrete (RC) is a composite material. The reinforcement is usually steel reinforcing bars (rebar) and is usually embedded passively in the concrete before the concrete sets. Concrete is one of the most widely used engineering materials for constructions. Its durability is the major problem affecting the service life of the engineering structures. Corrosion of the steel reinforcement is one of the main reasons causing the premature deterioration of reinforced concrete and leading to a significant economic loss. In order to improve the durability of reinforced concrete, various technologies and methods have been applied. Shrinkage of concrete under restricted conditions leads to cracking in concrete structural members, such as beams, decks, and slabs on grade. One possible method of decreasing and delaying the cracking is to use expansive cement concrete known as shrinkage-compensating concrete (SHCC). Hybrid fiber-reinforced polymer reinforced SHCC structural system shows a good potential for delaying concrete cracking and eliminating steel corrosion.[1]

Durability of RC corroded shear-critical deep beams with near surface mounted carbon fiber-reinforced polymer rods has been examined.[2] Durability is one of the most important aspects of concrete due to its fundamental incidence on the serviceability working conditions of concrete structures. Research on the durability of steel fiber reinforced self-compacting concrete showed that the addition of steel fibers to SCC was very effective in terms of increasing the post-cracking flexural resistance and the energy absorption, and did not affect significantly the self-compacting requisites and the durability indicators of SCC.[3] Similarly, it has been observed that fibres, when provided in sufficient amount to guarantee an adequate toughness to Fibre Reinforced Concrete (FRC), are significantly effective as shear reinforcement.[4] Ji et al.[5] have investigated the effect of degree of pore saturation (PS) in concrete on corrosion current. They showed that the maximum of corrosion current appeared in the water-saturated concrete and it decreased in dried concrete. This due to FeOOH in corrosion layer acting as a depolarizer instead of oxygen.

The corrosion resistance of metals has been tested in simulated concrete pore solution (SCPS), which consists of saturated calcium hydroxide [$Ca(OH)_2$], with the pH ~13.5. Rajendran et al., have investigated corrosion resistance of SS316L in simulated concrete pore solution in presence of trisodium citrate (TSC). The polarization study and AC impedance spectra lead to the conclusion that in presence of TSC, the corrosion resistance of SS 316L simulated concrete pore solution decreases.[6] Pandiarajan et al., have studied the corrosion behaviour of mild steel in simulated concrete pore solution prepared in rain water, well water and sea water.[7] The mechanistic aspects of corrosion inhibition have been studied using polarization study and AC impedance spectra. The scanning electron microscopy study confirms the protection of carbon steel surface by strong adsorption of PVP.[8] Influence of sodium metavanadate on the corrosion resistance of mild steel immersed in simulated concrete pore solution prepared in well water has been investigated by Pandiarajan et al.[9]

Urine is a sterile liquid by-product of the body secreted by the kidneys through a process called urination and excreted through the urethra. Cellular metabolism generates numerous by-products, rich in nitrogen. In some countries, people have the habit of urinating in public places especially on the concrete structures such as bridges and buildings.

This may affect the life time of the bridges and rebars because urine contains corrosive ions such as chlorides.

The present study is undertaken to investigate the corrosion resistance mild steel, in SCPS in the absence and presence of SU, tartaric acid and lactic acid. A saturated solution of calcium hydroxide is used as SCPS.[10] Electrochemical studies such as polarization study and AC impedance spectra have been used to evaluate the corrosion resistance of the mild steel under investigation.

Experimental

Simulated Concrete Pore solution

A saturated calcium hydroxide solution is used in present study, as SCPS solution with the pH-12.5.[10]

Metal specimens

Mild steel specimens (0.0267% S, 0.06% P, 0.4% Mn, 0.1% C and the rest iron) were used in the present study.

Artificial urine

Two solutions A and B are prepared. Just before the experiment they are mixed in 1:1 ratio to create artificial urine.[11] The compositions of A and B are given in Table 1.

Table 1. Constituent of artificial urine.

Solution A		Solution B	
Compounds	Weight g L^{-1}	Compounds	Weight g L^{-1}
$CaCl_2.H_2O$	1.765	$NaH_2PO_4.2H_2O$	2.660
Na_2SO_4	4.862	Na_2HPO_4	0.869
$MgSO_4.7H_2O$	1.462	$C_6H_5Na3O_7.2H_2O$	1.168
NH_4Cl	4.643	NaCl	13.545
KCl	2.130		

Potentiodynamic polarization

Polarization studies were carried out in a CHI–Electrochemical workstation with impedance, Model 660A. The working electrode was mild steel. A saturated calomel electrode (SCE) was the reference electrode and platinum was the counter electrode. From the polarization study, corrosion parameters such as corrosion potential (E_{corr}), corrosion current (I_{corr}) and Tafel slopes (anodic = b_a and cathodic = b_c) were calculated.

AC impedance spectra

The instrument used for polarization study was used to record AC impedance spectra also. The cell setup was also the same. The real part (Z') and imaginary part (Z") of the cell impedance were measured in ohms at various frequencies. Values of the charge transfer resistance (R_t) and the double layer capacitance (C_{dl}) were calculated.

Results and Discussion

Corrosion behavior of mild steel, immersed in SCPS, (saturated calcium hydroxide solution) in presence of SU, tartaric acid, and lactic acid has been investigated by polarization study and AC impedance spectra.

Polarization Study

Polarization study has been used to evaluate the corrosion resistance of metals.[12-14]

When mild steel is immersed in simulated urine (SU), the corrosion potential is -859 mV vs SCE. Linear polarization resistance (LPR) is 4737 ohm cm^2 and the corrosion current (I_{corr}) is 8.349 $x10^{-6}$ A cm^{-2}. When mild steel is immersed in simulated concrete pore solution (SCP), the corrosion potential is -668; mV vs SCE. Linear polarization resistance (LPR) is 10991ohm cm^2 and the corrosion current (I_{corr}) is 5.183$x10^{-6}$ A cm^{-2}. This indicates that the corrosion resistance of mild steel decreases in urine solution. This is due to the presence of corrosive ions present in urine.

When mild steel is immersed in a solution containing simulated urine and SCPS, the corrosion potential is -726 mV vs SCE, linear polarization resistance (LPR) is 9593 ohm cm^2 and the corrosion current (I_{corr}) is 7.680 x 10^{-6} A cm^{-2}. This indicates that the corrosion resistance of mild steel decreases in this solution when compared with the corrosion resistance in SCPS. This is due to the presence of corrosive ions in urine. However, this corrosion resistance is better than that when mild steel is immersed in urine solution only.

When mild steel is immersed in a solution containing simulated urine solution, SCPS and 250 ppm of tartaric acid and 50 ppm of Zn^{2+} ions, the corrosion potential is 740 mV vs SCE. Linear polarization resistance (LPR) is 17075 ohm cm^2 and the corrosion current (I_{corr}) is 3.614 $x10^{-6}$ A cm^{-2}. This indicates that the corrosion resistance of mild steel increases in this solution when compared with the corrosion resistance in SCPS. This is due to the formation of a protective film in presence of tartaric acid. This protective film is more stable. This consists probably of calcium hydroxide, calcium oxide and iron tartrate complex. There is also a probability of anchoring of tartaric acid molecule on the surface film of calcium oxide and calcium hydroxide.

When mild steel is immersed in a solution containing simulated urine solution, SCPS and 250 ppm of lactic acid and 50 ppm of Zn^{2+} ion the corrosion potential is -748; mV vs SCE. Linear polarization resistance (LPR) is17110 ohm cm^2 and the corrosion current (I_{corr}) is 1.860 x 10^{-6} A cm^{-2}. This indicates that the corrosion resistance of mild steel increases in this solution when compared with the corrosion resistance in SCPS and also in presence of a solution containing simulated urine solution, SCPS and 250 ppm of lactic acid. This is due to the formation of a protective film in presence of lactic acid. This protective film is more stable. This consists probably of calcium hydroxide, calcium oxide and iron lactate complex. There is also a probability of anchoring of lactic acid molecule on the surface film of calcium oxide and calcium hydroxide.

 DOI: 10.17628/ecb.2016.5.163-166

Table 2. Corrosion parameters of mild steel immersed in different solutions obtained by polarization study.

System	E_{corr}, mV vs SCE	b_c, mV decade^{-1}	b_a, mV decade^{-1}	*LPR*, ohm cm^2	I_{corr}, A cm^{-2}
SU	-859	144	246	4737	8.349 x 10^{-6}
SCPS	-668	283	243	10991	5.183 x 10^{-6}
SCPS + SU	-726	763	217	9593	7.680 x 10^{-6}
SCPS + SU+ TA 250 ppm + Zn^{2+} 50 ppm	-740	862	169	17075	3.614 x 10^{-6}
SCPS +SU + LA2 50 ppm + Zn^{2+} 50 ppm	-748	134	160	17110	1.860 x 10^{-6}

Table 3. Corrosion parameters of mild steel immersed in different solutions obtained by AC impedance spectra.

System	R_t ohm cm^2	C_{dl} F cm^{-2}	Impedance Log(z/ohm)
SU	47.78	1.067 x 10^{-7}	2.008
SCPS	126.7	4.025 x 10^{-8}	2.417
SCPS + SU	69.1	7.381 x 10^{-8}	2.242
SCPS + SU + TA + Zn^{2+}	134.6	3.788 x10^{-8}	2.187
SCPS + SU + LA + Zn^{2+}	231.3	2.205 x 10^{-8}	2.446

Thus, polarization study (Table 2) leads to the conclusion that, the corrosion resistance of mild steel in various test solutions is as follows.

Lactic acid + SCPS + urine > tartaric acid + SCPS +urine > SCPS +urine > SCPS > urine

AC impedance Spectra

Electrochemical studies such as AC impedance spectra have been used to investigate the corrosion resistance of metals. [15-25]

The results of AC impedance spectral study of mild steel immersed in various test solutions are shown in Table 3. When corrosion rate decreases, due to formation of protective film, the charge transfer resistance value increases and double layer capacitance value decreases the impedance value log (*Z*/ohm) increases and phase angle value increases. Conversely, when corrosion rate increases, R_t value decreases and C_{dl} value increases. Based on these principles and looking at the Table 3, it is inferred that corrosion resistance of mild steel immersed in various test solutions can be arranged in the decreasing order:

Lactic acid+ SCPS+urine > tartaric acid+ SCPS+urine > SCPS > SCPS+urine > urine

Increase in charge transfer resistance and impedance value of mild steel also follows the same sequence. Decrease in double layer capacitance of mild steel follows the same sequence.

These results are in agreement with that derived from polarization study. This leads to the conclusion that urination on the concrete structures such as bridges and building should be discouraged as this induces faster corrosion and may hasten the collapse of the structure. Inclusion of lactic and tartaric acids during the preparation of concrete admixtures is likely to strengthen the structure and increase its life.

Conclusion

Corrosion resistance of mild steel in SCPS in presence of simulated urine, tartaric acid and lactic acid has been evaluated by electrochemical studies such as polarization study and AC impedance spectra. These studies lead to the conclusion that, the corrosion resistance of mild steel in various test solutions is as follows.

Lactic acid + SCPS + urine > tartaric acid + SCPS +urine > SCPS > SCPS + urine > urine.

References

[1]Cao, Q., Ma Z. J., *Constr.Build. Mater*, **2015,** *75*, 450–457

[2]Almassri, B., Kreit, A., Al Mahmoud, F., Francois, R., *Compos.Struct.*, **2015**,123204– 215.

[3]Frazao, C., Camoes, A., Barros, J., Gonçalves, D., *Constr.Build. Mater*,**2015**, 80,55–166.

[4]Conforti, A., Minelli, F., Tinini, A., Plizzari,G.A., *Eng.Struct*, **2015**, *88*,12–21.

[5]Ji, Y-S., Zhan,G., Tan, Z., Hu, Y., Gao, F.,*Constr.Build. Mater*, **2015**, *79*, 214–222.

[6]Rajendran, S., Muthumegala, T.S., Pandiarajan, M., Nithya Devi, P., Krishnaveni, A., Jeyasundari, J., Narayana Samy, B., Hajara Beevi, N., *Zastit. mater.* **2011**, *52*, 85-89.

[7]Pandiarajan.M., Prabhakar, P., Rajendran,S., *Eur.Chem.Bull*, **2012**, *1(7)*,238-240.

[8]Shanthi, T., Rajendran, S., *Res. J. Chem. Sci*, **2013,** *3(9)*, 39-44.

[9]Pandiarajan, M., Rajendran, S., Joseph Rathish, R., Saravanan, R., *J. Chem. Bio.Phy.Sci.Sec.C*. **2014** , *4(1)*, 549-557.

[10]Pandiarajan, M., Prabakaran, P., Rajendran S., *Chem. Sci.Trans*, **2013**, *2*, 605- 613.

[11]Nagalakshmi, R., Rajendran, S., Sathiyabama, J., Pandiarajan, M and Lydia Christy, J., *Eur.Chem. Bull*, **2013**, *2(4)*, 150 -153.

[12]Pandiarajan M, Rajendran S, Sathiya bama, J., Vijaya, N., Shanthy, P., *Chem. Sci. Rev.Lett*, **2014**, *3* , 415-424.

[13]Pandiarajan, M., Rajendran. S., Joseph Rathish, R.,*Res. J. Chem. Sci*, **2014** , *4*, 49-55.

[14]Shanthi, T., Rajendran, S., *J. Chem, Bio. Phy. Scis*, **2013**, *3*, 2550-2556.

[15]Nithya Dvi, P., Sathiya bama, J., Rajendan, S., Joeph rathish, R., Santanaprabha, S., *J.Chem. Pharm. Res.*, **2015**, *7(10S)*, 133-140.

[16]Nagalakshmi, R., Rajendran, S., Sathiyabama, J., *Int. J. Innov. Res. Sci. Eng. Technol*,**2013**, *2*, 420-427

[17]Muthumani. N., Susai Rajendran., Pandiarajan M., Lidia Christ J,,Nagalakshmi, R., *Port. Electrochem. Acta*, **2012**, *30(5)*, 307-315.

[18]Pandiarajan, M., Prabhakar, P., Rajendran, S., *Eur. Chem. Bull*, **2012**, *1(7*), 238.

[19]Nagalakshmi, R., Rajendran, S., Sathiyabama, J., Pandiarajan, M., Lydia Christy, *Eur. Chem.Bull*, **2013**, *2(4)*, 150.

[20]Gowri, S., Sathiyabama, J., Rajendran, S., and Angelin Thangakani, J, *Eur. Chem. Bull*, **2013**, *2(4)*, 214-219.

[21]Nagalakshmi, R., Nagarajan, L. ,Joseph Rathish, R., Santhana Prabha, S., Vijaya, N., Jeyasundari, J., Rajendran, S., *Int. J. Nano. Corr. Sci. Engg*, **2014** , *1* , 39-49.

[22]Nithya Devi, P., Sathiyabama, J., Rajendran, S., Joseph Rathish, R., Santhana Prabha, S, *Int. J. Nano. Corr. Sci. Engg*, **2015**, *2(3)*, 1-13.

Received: 10.05.2016
Accepted: 29.06.2016.

CHEMICAL TRANSFORMATIONS OF 3-AMINO-5-HYDROXY-4-PHENYLAZO-1*H*-PYRAZOLE

R. Fikry,[a]* N. Ismail,[a] S. Raslan,[b] and H. El-Tahawe[b]

Keywords: Pyrazoles, Triazoles, pyrazolopyrimidines.

Reaction of 3-amino-5-hydroxy-4-phenylazo-1H-pyrazole (**1**) with phenacyl bromide, acetic acid anhydride, benzoyl chloride and aromatic aldehydes gave 3-N-alkylated/acylated derivatives (**2**, **4** and **5**) and the corresponding Schiff bases (**6**), respectively. Ring closure for compound **2** in acetic anhydride afforded pyrazolopyrimidine **3**. Reaction of **1** with acetylacetone, ethyl acetoacetate, ethyl cyanoacetate, diethyl malonate and ninhydrine resulted in pyrazolo[1,5-*a*]pyrimidine-5(*H*)-one (**7**, **8**, **9**), pyrazolo[1,5-*a*]pyrimidine-5,7(1*H*,6*H*))-dione **(10)** and pyrazol-3-ylimino-1H-indene-1,3-(2*H*)-dione (**12**) derivatives. Reaction of active methylene group of (phenyldiazenyl)pyrazolo[1,5-*a*]pyrimidin-5,7(1H,6H)-dione (**10)** with phenyldiazonium chloride gave 2-phenylhydrazono derivative (**11**). Moreover, reaction of **1** with $POCl_3$ and P_2S_5 resulted in 5-chloro (**13**) and 5-mercapto (**15**) derivatives, while phthalic anhydride, chloroacetyl chloride, aroyl thiocyanates and ammonium thiocyanate gave the corresponding 3-N-substituted derivatives. Hydrazenolysis of **13** in presence of hydrazine hydrate afforded the 5-hydrazino derivative. The 2-mercapto -7-(phenyladiazenyl)-2,5-dihydropyrazolo[1,5-b]triazole-6-ol (20) and 2-amino -7-(phenyladiazenyl)-2,5-dihydropyrazolo[1,5-*b*][1,2,4]-thiadiazol-6-ol (**21**) were obtained by the reaction of 1-(5-hydroxy)-4-(phenyldiazenyl)-1*H*-pyrtazol-3-yl)thiourea with bromine in different solvents. The structures of newly synthesized compounds have been established by IR, ^{1}H NMR and elemental analysis.

* Corresponding Authors
E-Mail: redmof5@yahoo.com
[a] Department of Chemistry, Faculty of Science, Zagazig Univesity, Zagazig, Egypt
[b] Plant Protection Insititute, (Sharkia branch), Agricultural Research Center, Sharkia-Egypt.

Introduction

Pyrazole ring is a prominent structural motif found in numerous pharmaceutically active compounds, therefore, the synthesis and selective functionalization of pyrazoles are in the focus of organic synthesis. Pyrazoles have been reported to possess antibacterial activity, inhibitor activity against DNA gyrase and topoisomerase IV at their respective ATP-binding sites. Moreover, pyrazole ring containing compounds have received considerable attention owing to their diverse chemotherapeutic potentials including versalite antineoplastic activities, antileukemic, antitumor, antiproliferative agents, GABA receptor antagonists etc. Some pyrazoles act as insecticides, anti-inflamatory and antimicrobial agents.[1-4]

In continuation of our recent work aiming of the synthesis of heterocyclic systems with remarkable biological importance, some new pyrazole derivatives have been prepared and characterized.

Experimental

Melting points were recorded using SMP30 Melting Point Apparatus (Stuart) and are uncorrected. The IR spectra were record on KBr discs using a FTIR 600 Series spectrophotometer (JASCO) and ^{1}H NMR spectra (δ ppm) were recorded on a Varian 300 MHZ spectrometer using $CDCl_3$ as solvent. Elemental analyses were carried out at Micro Analytical Center of Cairo University.

3-Amino-5-hydroxy-4-phenylazo-1*H*-pyrazole (1)

Compound **1** was prepared according to literature procedure and all analysis is agreement with the structure.[2]

2-((4-Phenyldiazenyl)-5-hydroxy-1*H*-pyrazol-3-ylamino)-1-phenylethanone (2)

To a solution of **1** (0.2 g, 1 mmol) in acetic acid (20 mL), phenacyl bromide (0.19 g, 1 mmol) was added and refluxed for 7 h. The soltuon was concentrated and left to cool. The precipitate was filtered off and recrystallized from acetic acid. Yield 75 %, m.p. 200 ^{0}C. Anal. Calcd for $C_{17}H_{15}N_5O_2$ (321.323): C; 63.54; H, 4.70; N, 21.79. Found: C, 63.53; H, 4.72; N, 21.78. IR (KBr) : 3500, 3138, 1680, 1615 cm^{-1} corresponding to OH, NH, C=O, C=N. ^{1}H NMR ($CDCl_3$) δ = 4.2 (s, 2H, CH_2), 7.0-7.5 (m, 10H, Ar-H), 8.2 (s, 1H, NH), 11.0 (s, 1H, NH), 12.0 (s, 1H, OH) .

3-Phenyl-7-(phenyldiazenyl)-5*H*-imidazol[1,2-*b*]pyrazol-6-ol (3)

A solution of compound **2** (0.15 g, 1 mmol) in acetic anhydride (20 mL) was refluxed for 6 h. The solution was cooled and poured into ice. A precipitate was formed, which was crystallized from ethanol. Yield: 66 %, m.p. 300 ^{0}C. Anal. Calcd for $C_{17}H_{13}N_5O$ (303.3): C, 67.32; H, 4.32; N, 23.09. Found: C, 67.34; H, 4.31; N, 23.08. IR (KBr): 3450, 3310, 3010, 1618 cm^{-1} corresponding to OH, NH, $CH_{aromatic}$, C=N. ^{1}H NMR ($CDCl_3$) δ = 7.5-8.0 (m, 11H, Ar-H and H-pyrazole), 8.0 (s, 1H, NH), 8.4 (s, 1H, NH), 12.0 (s, 1H, OH).

***N*-(4-(Phenyldiazenyl)-5-hydroxy-1*H*-pyrazol-3yl)acetamide (4)**

To a solution of compound **1** (0.2 g, 1 mmol) in acetic anhydride (20 mL), pyridine (0.05 mL) was added and the mixture was refluxed for 5 h. The mixture was cooled and poured into ice-cold dilute HCl (5 mL) and stirred till the

 DOI: 10.17628/ecb.2016.5.167-171

crude product begins to precipitate. The precipitate was filtered off and crystallized from ethanol. Yield: 65 %, m.p. 160 ^{0}C . Anal. Calcd for $C_{11}H_{11}N_5O_2$ (245.23): C, 53.87; H, 4.53; N, 28.55.Found: C, 53.89; H, 4.52; N, 28.54. IR (KBr) : 3460, 3300, 3190, 3046, 1710, 1610, 1560 cm^{-1} corresponding to OH, NH, C-$H_{aromatic}$, C=O, C=N, C=C . The ^{1}H NMR ($CDCl_3$) δ = 1.29 (t, 3H, CH_3), 7.4-7.8 (m, 5H, Ar-H), 8.4 (s, 1H, NH), 11.8 (s, 1H, NH), 12.9 (s, 1H, OH).

4-(Phenyldiazenyl)-3-(arylmethyleneamino)-1*H*-pyrazol-5-ol derivatives (5a-d)

An aromatic aldehyde (benzaldehyde, p-chlorobenzaldehyde, p-nitrobenzaldehyde, anisaldehyde) (1 mmol) was added to the solution of compound **1** (0.2 g, 1 mmol) in n-butanol (20 mL), The mixture was refluxed for 5-7 h and then the solvent was removed under reduced pressure. The solid residue was triatureted with n-butanol, residue was filtered off and recrystallized from n-butanol. Compound **5a:** Yield 65%, m.p. 285 °C. Anal. Calcd. for $C_{16}H_{13}N_5O$ (291.298): C, 65.96; H, 4.49; N, 24.05. Found: C,65.95; H, 4.48; N, 24.07. IR (KBr): 3500, 3215, 3190, 3046, 1652, 1610, 1560 cm^{-1} corresponding to OH, NH, C-$H_{aromatic}$, C=N and C=C linkages. ^{1}H NMR ($CDCl_3$) δ = 7.0-7.5 (m, 10H, Ar-H), 8.6 (s, 1H, NH), 8.9 (s, 1H, N=CH), 12.0 (s, 1H, OH).

Compound **5b**: Yield 70 %, m.p. 280 °C. Anal. Calcd. for $C_{16}H_{12}N_5OCl$ (325.743): C, 58.99; H, 3.71; N, 21.50. Found : C,58.98; H,3.73; N,21.49.

Compound **5c**: Yield 63 %, m.p. 287 °C. Anal. Calcd. for $C_{16}H_{12}N_6O_3$ (336.295): C, 57.14; H, 3.59; N, 24.99. Found: C, 57.16; H, 3.58; N, 24.98.

Compound **5d**: Yield 61 %, m.p. 283 °C. Anal Calcd. for $C_{17}H_{15}N_5O_2$ (321.323): C, 63.54; H, 4.70; N, 21.79.Found : C, 63.55; H, 4.71; N, 21.77.

***N*-(4-(phenyldiazenyl)-5-hydroxy-1*H*-pyrazol-3yl)phenyl-carboxamide (6)**

Benzoyl chloride (0.12 g , 1 mmol) and pyridine (0.5 ml) were added to a solution of compound **1** (0.2 g, 1 mmol) without solvent. The mixture was heated for 5 h. After cooling the mixture was poured into ice-cold dilute HCl (5 mL). The precipitate formed was filtered off and recrystallized from ethanol. Yield 50 %, m.p. 190 °C. Anal. Calcd. for $C_{16}H_{13}N_5O_2$ (307.297): C, 62.53; H, 4.26; N, 22.79. Found: C, 62.55; H, 4.25; N, 22.78. IR (KBr) : 3500, 3284, 3168, 3062, 1710, 1596, 1545 cm^{-1} corresponding to OH, NH, C-$H_{aromatic}$, C=O, C=N and C=C linkages. ^{1}H NMR ($CDCl_3$) δ = 7.4-7.8 (m, 10H, Ar-H), 8.4 (s, 1H, NH), 11.8 (s, 1H, NH) and 12.9(s, 1H, OH).

3-(Phenyldiazenyl)-5,7-dimethyl-1,5-dihydropyrazolo[1,5-*a*]pyrimidin-2-one (7)

Acetylacetone (0.1 g, 1 mmol) was added to the solution of compound **1** (0.2 g, 1 mmol) in absolute ethanol (20 mL), the reaction mixture was heated under reflux for 7 h, the solvent was removed under reduced pressure and the solid residue of **7** was collected. Yield 65 %, m.p. 220 °C. Anal. Calcd. for $C_{14}H_{15}N_5O$ (269.294): C, 62.44; H, 5.62; N, 26.00.Found: C, 62.41; H, 5.64; N, 26.01. IR (KBr): 3500, 3284, 3168, 3062, 1710, 1669, 1596, 1545, 1375 cm^{-1} corresponding to OH, NH, C-$H_{aromatic}$, C=O, C=N, C=C, CH_3. ^{1}H NMR ($CDCl_3$) δ 1.8 (s, 3H, CH_3), 2.1 (s, 3H, CH_3), 7.0-7.5 (m, 6H, Ar-H, H-pyrimidine), 8.4 (s, 1H, NH), 11.9 (s, 1H, OH).

3-(Phenyldiazenyl)-2-hydroxy-5-methylpyrazolo[1,5-*a*]pyrimidin-7(1*H*)-one (8)

To a solution of compound **1** (0.2 g, 1 mmol) in acetic acid (20 mL), ethyl acetoacetate (0.11 g, 1 mmol) was added and the reaction mixture was refluxed for 5 h. The solvent was removed under reduced pressure, the precipitate was filtered off and recrystallized from acetic acid. Yield 60 %, m.p. 240 °C . Anal. Calcd. for $C_{13}H_{13}N_5O_2$ (271.267): C, 53.65; H, 4.09; N, 22.75. Found: C, 53.63; H, 4.07; N, 22.70. IR (KBr): 3500, 3460, 3053, 3062, 1720, 1670, 1590 cm^{-1} correspond to OH, NH, C-$H_{aromatic}$, C=O, C=N and C=C linkages. ^{1}H NMR ($CDCl_3$) δ = 1.7 (s, 3H, CH_3), 7.5-8.0 (m, 6H, Ar-H, H-pyrimidine), 8.4 (s, 1H, NH), 11.0 (s, 1H, NH), 12.0 (s, 1H, OH).

7-Amino-3-(phenyldiazenyl)-2-hydroxypyrazolo[1,5-*a*]pyrimidin-5(1*H*)-one (9)

A solution of compound **1** (0.2 g, 1 mmol) and ethyl cyanoacetate was heated at 180 °C in oil bath for 3 h. The mixture was cooled and then washed with ethanol several times. The residue was filtered off and recrystallized from butanol. Yield 75 %, m.p. 180 °C. Anal. Calcd. for $C_{12}H_{12}N_6O_2$(272.256): C, 52.94; H, 4.45; N, 30.86. Found: C, 52.92; H, 4.46; N, 30.87. IR (KBr): 3508, 3406, 3300, 3173, 3010, 1668 cm^{-1} corresponding to OH, NH, NH_2, C-$H_{aromatic}$. ^{1}H NMR ($CDCl_3$) δ = 6.5 (s, 2H, NH_2), 7.0-8.0 (m, 6H, Ar-H, H-pyrimidine), 8.4 (s, 1H, NH), 11.0 (s, 1H, OH), 12.6 (s, 1H, OH).

(Phenyldiazenyl)pyrazolo[1,5-*a*]pyrimidin-5,7(1*H*,6*H*)-dione (10)

Equimolar amounts of compound **1** (0.21 g , 1 mmol) and diethylmalonate (0.16 g, 1 mmol) were dissolved in a solution of sodium ethoxide (0.01 g, 1 mmol) in abs. ethanol (20 mL) and left under reflux for 10 h. The precipitate was formed during cooling was recrystallized from ether. Yield 65 %. M.p. 300 °C . Anal.: Calcd for $C_{12}H_9N_5O_3$ (271.224): C, 53.14; H, 3.35; N, 25.83. Found : C, 53.15; H, 3.33; N, 25.84. IR (KBr): 3300, 3210, 3080, 1710, 1625, 1566 cm^{-1} corresponding to OH, NH, C-$H_{aromatic}$, 2C=O, C=N. ^{1}H NMR ($CDCl_3$) δ = 7.0-7.5 (m, 6H, Ar-H, H-pyrimidine), 8.0 (s, 1H, NH), 8.4 (s, 1H, NH), 12.0 (s, 1H, OH).

2-Hydroxyl-3-(phenyldiazenyl)-6-(2-phenylhydrazono)-6,7–dihydropyrazolo[1,5-*a*]pyrimidin-5,7-(1*H*,6*H*)–dione (11)

An ice–cold mixture of compound **1** (0.26 g, 1 mmol) and sodium acetate (0.07g, 1 mmol) in ethanol (25 mL) was added dropwise with stirring to the solution of the diazonium salt over 10 min, the stirring continued for furthet 30 min. The reaction mixture was left to stand for 2 h at

 DOI: 10.17628/ecb.2016.5.167-171

room temperature, the precipitate formed was collected and recrystallized from ethanol. Yield 84 %, m.p.60 °C. Anal. Calcd. for $C_{18}H_{13}N_7O_3$ (375.33): C, 57.59; H, 3.49; N, 26.12. Found: C, 57.60; H, 3.50; N, 26.00. IR (KBr): 3300, 3200, 3100, 3020, 1710, 1625, 1590 cm^{-1} corresponding to OH, NH, C-$H_{aromatic}$, 2C=O, C=N. ^{1}H NMR ($CDCl_3$) δ = 7.0-7.5 (m, 11H, Ar-H, NH), 8.0 (s, 1H, NH), 8.4 (s, 1H, NH) and 12.0 (s, 1H, OH).

2-(5-Hydroxy-4-(2-phenylhydrazinyl)-1*H*-pyrazol-3ylimino)-1*H*-indene-1,3-(2*H*)-dione (12)

Mixture of compound **1** (0.21 g, 1 mmol) and ninhydrine (0.17g, 1 mmol) in abolute ethanol (25 mL) was stirred for 2 h. The solid product was collected and recrystallized from ethanol. Yield 81 %, m.p. 190 °C. Anal. Calcd. for $C_{18}H_{15}N_5O_4$ (365.331): C, 59.17; H, 4.14; N, 19.17. Found: C, 59.15; H, 4.15; N, 19.18. IR (KBr): 3500, 3400, 3061, 1722, 1591 cm^{-1} corresponding to OH, NH, C-$H_{aromatic}$, C=O, C=N. ^{1}HNMR ($CDCl_3$) δ = 7.0-7.5 (m, 9H, Ar-H), 8.4 (s,1H, NH), 12.0 (s, 1H, OH).

3-Amino-5-chloro-4-phenylazo-1*H*-pyrazole (13)

A solution of compound **1** (0.2 g, 1 mmol) in phosphorus oxychloride (20 mL) was refluxed on a hot plate for 2 h. The reaction mixture was cooled and diluted with ice-cold water. The resulting precipitate was filtered off and recrystallized from chloroform. Yield 66 %, m.p. 170 °C. Anal. Calcd. for $C_9H_8N_5Cl$ (221.642): C, 48.76; H, 3.64; N, 31.59; Cl 1.59. Found: C, 48.75; H, 3.67; N, 31.58; Cl, 1.58. IR (KBr): 3443, 3389, 2857, 1612, 1525 cm^{-1} corresponding to NH_2, NH, C-$H_{aromatic}$, C=N, C=C. ^{1}H NMR ($CDCl_3$) δ = 6.0 (s, 2H, NH_2), 7.0-7.5 (m, 5H, Ar-H), 8.5 (s, 1H, NH).

3-Amino-5-hydrazino-4-phenylazo-1*H*-pyrazole (14)

To a solution of compound **13** (0.21 g, 1 mmol) in ethanol (30 mL), hydrazine hydrate (0.05 g, 1 mmol) was added and the mixture was heated at 90 °C for 6 h. On cooling a precipitate was formed. This precipitate was filtered off and recrystallized from dioxane. Yield 75 %, m.p. 270 °C. Anal. Calcd. for $C_9H_{11}N_7$ (217.227): C, 49.75; H, 5.11; N, 45.14. Found : C, 49.74; H, 5.13; N, 45.13. IR (KBr): 3381, 3197, 3010, 2960, 1634, 1562cm^{-1} corresponding to NH, NH_2, C-$H_{aromatic}$, C=N, C=C. ^{1}H NMR ($CDCl_3$) δ = 4.9 (s, 2H, NH_2), 6.5 (s, 2H, NH_2), 7.0-7.5 (m, 5H, Ar-H), 8.4 (s, 1H, NH), 11.0(s, 1H, NH).

3-Amino-5-mercapto-4-phenylazo-1*H*-pyrazole (15)

The compound **1** (0.2 g, 1 mmol) was heated at reflux temperature in dry pyridine (20 mL) containing phosphorus pentasulfide (0.2 g, 1 mmol) for 5 h. The solution was acidified with dil. HCl, the precipitate formed was filtered off and washed several times with water then recrystallized from DMF. Yield 75 %, m.p. 200 °C. Anal. Calcd. for $C_9H_9N_5S$ (219.262): C, 49.29; H, 4.14; N, 31.49; S, 14.62. Found: C, 49.28; H, 4.15; N, 31.48; S, 14.63. IR (KBr): 3606, 3303, 3177, 1399 cm^{-1} corresponding to NH, NH_2, C-$H_{aromatic}$, C=S. ^{1}H NMR ($CDCl_3$) δ = 6.5 (s, 2H, NH_2), 7.0-7.7 (m, 5H, Ar-H), 8.4 (s, 1H, NH), 13.0 (s, 1H, SH).

2-(5-Hydroxy-4-(phenyldiazenyl)-1*H*-pyrazolo-3yl)isoindoline-1,3-dione (16)

Equimolar amounts of compound **1** (0.21 g , 1 mmol), phthalic anhydride (0.14 g, 1 mmol) and sodium ethoxide (0.01 g, 1 mmol) were dissolved in absolute ethanol (20 mL) and the mixture was refluxed for 10 h. After cooling, the formed precipitate was recrystallized from chloroform. Yield 85 %, m.p. 300 °C. Anal. Calcd for $C_{17}H_{11}N_5O_3$ (333.290): C, 61.25; H, 3.33; N, 21.01. Found: C, 61.24; H, 3.34; N, 21.00. IR (KBr): 3400, 3310, 3080, 1700, 1650, 1560 cm^{-1} corresponding to OH, NH, C-$H_{aromatic}$, 2C=O, C=N. ^{1}H NMR ($CDCl_3$) δ = 7.0-7.5 (m, 9H, Ar-H), 8.3 (s, 1H, NH) , 12.0 (s, 1H, OH).

2-Chloro-*N*-(5-hydroxy-4-(phenyldiazenyl)-1*H*-pyrazol-3yl)-acetamide (17)

To a solution of compound **1** (0.21 g, 1 mmol) in dioxane (30 mL), chloroacetyl chloride (0.09 g, 1 mmol) was added dropwise with stirring at room temperature. The reaction mixture was heated for 30 min at 60 °C, the solution was concentrated to a small volume, poured into ice-cold water and the precipitate formed was recrystallized from ethanol. Yield 60 %, m.p. 210 °C. Anal. Calcd for $C_{11}H_{10}N_5O_2Cl$ (279.676): C, 47.24; H, 3.60; N, 25.04; Cl, 12.67. Found: C, 47.21; H, 3.61; N, 25.05; Cl, 12.68. IR (KBr): 3505, 3410, 1700 cm^{-1} corresponding to OH, NH, C=O. ^{1}H NMR ($CDCl_3$) δ = 2.8 (s, 2H, CH_2), 7.0-7.5 (m, 5H, Ar-H), 8.4 (s, 1H, NH), 11.0 (s, 1H, NH), 12.0 (s, 1H, OH).

***N*-Benzoyl-[5-hydroxy-4-phenylazo-1*H*-pyrazol-3-yl]thiourea (18)**

A mixture of benzoyl chloride (0.12 g, 1 mmol) and ammonium isothiocyanate (0.07 g, 1 mmol) was refluxed in dry acetone (20 mL) for 15 min. Then the compound **1** was added, the mixture was refluxed for 2 h, poured into ice water, the precipitate formed was filtered off, washed with water and recrystallized from ethanol**.** Yield 69 %, m.p. 140 ^{0}C. Anal. Calcd for $C_{17}H_{14}N_6O_2S$ (366.387): C, 55.73; H, 3.85; N, 22.94; S, 8.75. Found: C, 55.74; H, 3.84; N, 22.95; S, 8.74. IR (KBr): 3560, 3440, 3130, 1720, 1383 cm^{-1} corresponding to OH, NH, C-$H_{aromatic}$, C=O, C=S. ^{1}H NMR ($CDCl_3$) δ = 7.0-7.6 (m, 10H, Ar-H), 8.7 (s, 1H, NH), 10.5 (s, 1H, NH), 11.0 (s, 1H, NH), 12.0 (s, 1H, OH).

1-(5-Hydroxy-4-(phenyldiazenyl)-1*H*-pyrazol-3-yl)thiourea (19)

A solution of compound **1** (0.21 g, 1 mmol) in absolute ethanol (30 mL) containing conc. HCl (0.05 mL) and ammonium thiocyanate (0.07 g, 1 mmol) was refluxed for 2 h. The precipitate formed was recrystallized from ethanol. Yield 55 %, m.p. 240 ^{0}C. Anal. Calcd for $C_{10}H_9N_6OS$ (261.278): C, 45.96; H, 3.47; N, 32.16; S, 12.27. Found: C, 45.97; H, 3.48; N, 32.17; S, 12.24. IR (KBr): 3500, 3210, 3100, 3030, 1333 cm^{-1} corresponding to OH, NH, NH_2, C-$H_{aromatic}$, C=S. ^{1}H NMR ($CDCl_3$) δ = 6.8 (s, 2H, NH_2), 7.0-7.7 (m, 5H, Ar-H), 7.9 (s, 1H, NH), 11.0 (s, 1H, NH), 12.0 (s, 1H, OH).

 DOI: 10.17628/ecb.2016.5.167-171

2-Mercapto-7-(phenyldiazenyl)-2,5-dihydropyrazolo[1,5-*b*][1,2,4]triazol-6-ol (20)

To a solution of compound **19** (0.26 g, 1 mmol) in pyridine (20 mL), bromine (0.15g, 1 mmol) in pyridine (5 mL) was added dropwise at room temperature. The mixture was refluxed for 1 h, cooled, poured into water with stirring, the precipitate formed was filtered off, washed with water and recrystallized from ethanol. Yield 65 %, m.p. 140 °C. Anal. Calcd for $C_{10}H_7N_6OS$ (259.262): C, 46.33; H, 2.73; N, 32.42; S, 12.36. Found: C, 46.35; H, 2.71; N, 32.43; S, 12.35. IR (KBr): 3500, 3400, 3180, 3019 cm^{-1} corresponding to OH, NH, NH_2, C-$H_{aromatic}$. ^1H NMR ($CDCl_3$) δ = 7.0-7.5 (m, 5H, Ar-H), 8.4 (s, 1H, NH), 12.0 (s, 1H, OH), 13.9 (s, 1H, SH).

2-Amino-7-(phenyldiazenyl)-2,5-dihydropyrazolo[1,5-*b*][1,2,4]-thiadiazol-6-ol (21)

To a solution of compound **19** (0.26 g, 1 mmol) in glacial acetic acid (20 mL) bromine (0.15 g, 1 mmol) in glacial acetic acid (5 mL) was added dropwise at room temperature. The mixture was refluxed for 1 h, cooled, poured into water with stirring, the precipitate formed was filtered off and recrystallized from ethanol. Yield 66 %, m.p. 120 °C. Anal. Calcd for $C_{10}H_8N_6OS$ (260.27): C, 46.15; H, 3.09; N, 32.29; S, 12.32. Found: C, 46.12; H, 3.08; N, 32.28; S, 12.37. IR (KBr): 3530, 3300, 3160, 3030 cm^{-1} corresponding to OH, NH, NH_2, C-$H_{aromatic}$. ^1H NMR ($CDCl_3$) δ = 6.5 (s, 2H, NH_2), 7.0-7.6 (m, 5H, Ar-H), 8.4 (s, 1H, NH), 12.0 (s, 1H, OH).

RESULTS AND DISCUSSION

Treatment of the compound **1** with phenacyl bromide, acetic anhydride, substituted benzaldehyde and benzoyl chloride in different solvents afforded the corresponding N-alkylated/acylated or condensation products **2**, **4**, **5** and **6**, respectively (Scheme 1).

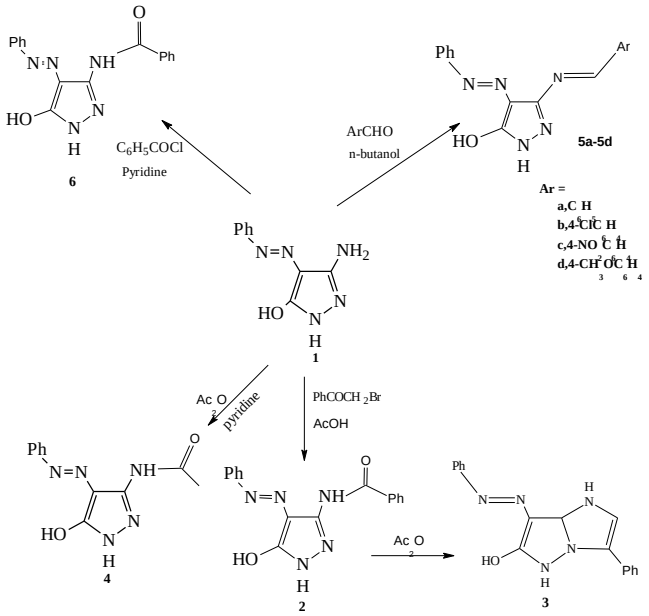

Scheme 1. Synthesis of compounds (**2**) – (**6**).

The ring clousure of compound **2** in acetic anhydride gave the corresponding imidazolopyrazole compound **3.** The IR and NMR spectra of the products confirm that the expected structural blocks were indeed incorporated into the starting molecule. IR spectrum of compound **2** revealed the absorption band at 1680 cm^{-1} for C=O group. Its ^1H NMR showed the presence of signals at δ 8.2 and 4.2 ppm characteristic for NH_2 and CH_2, respectively. IR spectrum of **5** revealed the presence of band at 3215 cm^{-1} for NH, and 1620 cm^{-1}. ^1H NMR showed signals at δ 8.6 ppm for NH. The IR, ^1H NMR and elemental analysis data of compounds **4** and **6** are also in agreement with the structures. IR spectra showed bands at 1710 cm^{-1} for amidic carbonyl groups, while, ^1H NMR of **4** and **6** revealed the presence signals at δ 11.8 ppm for NH_2, in addition to the aromatic proton at δ 7.4-7.8 ppm.

Condensation reaction of **1** with acetylacetone, ethyl cyanoacetate, ethyl acetoacetate or diethylmalonate in different solvent followed by cyclization gave the corresponding pyrazolo[1,5-*a*]pyrimidine derivatives **7**-**10**, respectively (Scheme 2).

However, the reaction of **1** with ninhydrine afforded Schiff' base **11**. The active methylene group in compound **11** reacts with phenyldiazonium chloride affording the hydrazone of pyrazolopyrimidine (**10) (**Scheme 2**).**

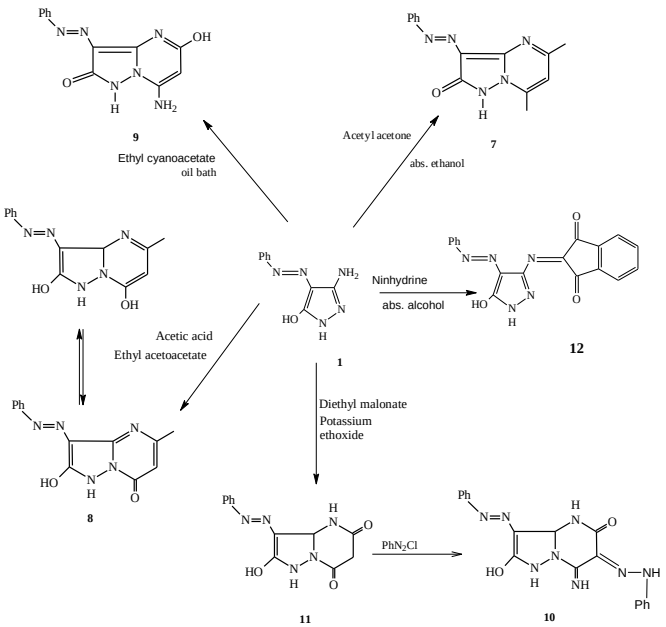

Scheme 2. Synthesis of compounds (**7**) – (**12**).

The structures of compounds **7-12** were assigned by their IR, ^1H NMR and elemental analysis data. IR spectrum of 7 showed absorption band at 1669 cm^{-1} corresponding to CN group and the absorption band for NH_2 is absent. The IR spectrum of **8** revealed the presence of bands at 3460 and 1720 cm^{-1} for NH and C=O groups, respectively, and the bands of NH_2 group are missing. In the IR spectrum of **9,** the bands belong to NH_2 group and C=O amidic group (3300, 3173 and 1668 have appeared. ^1H NMR spectrum of **10** showed the methinyl proton and aromatic protons at δ 7.0-7.5 ppm.

 DOI: 10.17628/ecb.2016.5.167-171

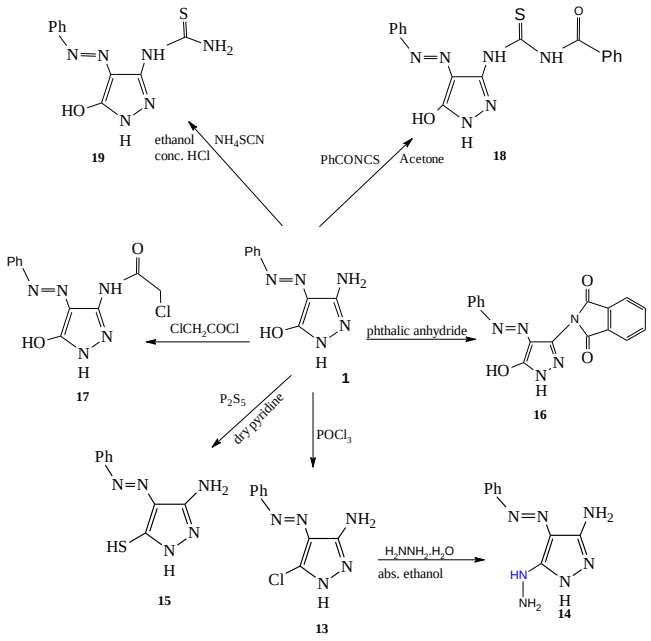

Scheme 3. Synthesis of compounds (**11**) – (**16**).

The reaction of **1** with $POCl_3$ and P_2S_5 resulted the formation of 5-chloro and 5-mercapto, substituted pyrazole compounds, respectively (**13** and **15).** Reaction with Phthalic anhydride resulted in 3-phthalimidoyl derivative (**16**) while that with chloroacetyl chloride resulted in an N-acylated derivative (**17**). Phenyl isothiocyanate and ammonium thiocyanate gave the corresponding thiourea derivatives (**18** and **19)**, respectively (Scheme 3).

Hydrazinolysis of compound **13** with hydrazine hydrate afforded the hydrazinopyrazole derivative **14**. The structure of the products formed in the reactions, given in (Scheme 3), were assigned by IR, ^{1}H NMR and elemental analysis. The IR of compounds **13-19** showed the absence of absorption bands for NH_2 indicating the involving of NH_2 groups in the reactions. In case of compound **16**, the bands appear at 1700 and 1650 cm^{-1}, which are characteristic of the C=O groups.

The ^{1}H NMR and elemental analysis of compounds **13-19** are in agreement with the expected structures.

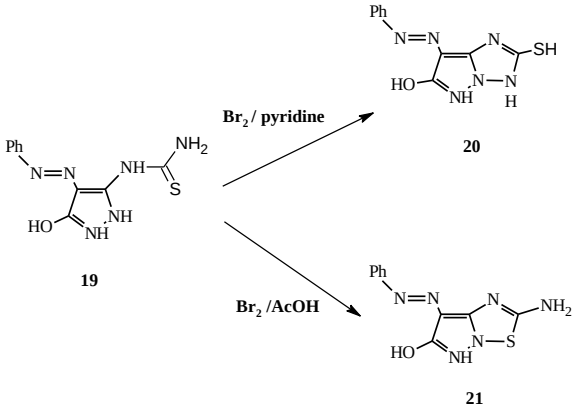

Scheme 4. Synthesis of compounds **20** and **21**.

A pyrazolotriazole **20** and a pyrazolothiadiazole **21** derivative could be obtained in the reaction of **19** with bromine in different solvent. In these reactions the solvent polarity controls the involvement of NH_2 or C=S groups in the cyclization reactions (Scheme 4). The spectral data of **20** an32d **21** confirm the proposed structures.

References

[1]Bondoek, S., Khalifa, W., Fadda, A., *Eur . J. Med. Chem.*, **2011,** *46*, 2555-2561.

[2]Elnagdi, M., Abdalla, S., *J. Prakt . Chem*., **1973,** *315*, 1009 - 1016.

[3]Ouyang, G., Chen, Z., Cai, X., Song, B., Bhadury, P., Yang, S. and Jin, L**.,** *Bioorg. Med. Chem*., **2008,** *16*, 9699 – 9707.

[4]Rashad, A., Hegab, M., Abdel-Megeid, R., Micky, J. and Abdel-Megeid, F**.,** *Bioorg. Med. Chem*., **2008,** *16*, 7102 – 7106.

[5]Yang, B., Yuan, Lu., Chen, C., Cui, J., Cai, M., *Dyes and Pigments*., **2009,** *83*, 144-147.

Received: 24.04.2016.
Accepted: 27.06.2016.

A CSD CRYSTALLOGRAPHIC ANALYSIS OF SOME PREGNANE CLASS OF STEROIDS

Sonia Sharma[a] and Rajni Kant[a]*

Keywords: pregnane, hydrogen bonding, bifurcated hydrogen bond, biological activity, intramolecular interactions, intermolecular interactions, steroids

The structural diversity of steroids as well as their surpassed biological potential qualify them as challenging targets for chemical synthesis and as lead structures for pharmacological research. A total number of thirty-three structures of pregnane derivatives were obtained from the CSD for a comparative analysis of their crystallographic structures, computation of their possible biological activities and molecular packing interaction analysis. Intra and intermolecular interactions of the type X-H…A [X=C,O, N; A=O, N, S, Cl, F] have been analysed for a better understanding of molecular packing in pregnane class of steroids and discussed on the basis of distance-angle scatter plots. Molecular conformations of all the structures have been computed on the basis of the magnitude of torsion angles present in these structures. Results presented in this paper is a part of our ongoing work on the crystallographic aspects of steroidal derivatives of different classes.

*Corresponding Authors
Fax: +91 191 243 2051
E-Mail: rkant.ju@gmail.com
[a] X-ray Crystallography Laboratory, Department of Physics & Electronics, University of Jammu, Jammu Tawi -180 006, India.

Introduction

Steroid hormones play a vital role in a wide variety of essential physiological processes including cell growth, sexual development, maintenance of salt balance and sugar metabolism.[1] Pregnane, a crystalline steroid hydrocarbon, is the parent compound of corticosteroids and progesterone. It is a four-ring structure of which three are six-membered cyclohexane rings and one is a five-membered cyclopentane carbon ring. In addition, it has a side chain of two carbon atoms located at C17 position of the steroid nucleus (Figure 1).

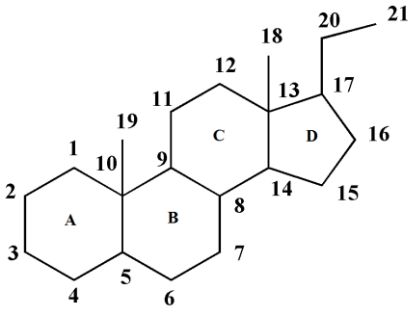

Figure 1. Basic pregnane molecule (C_{21}) with standard atomic numbering scheme.

In the literature on pregnane class of steroids, pregnenolone (3β-hydroxypregn-5-en-20-one) holds a very prominent place and position in the hierarchy of steroid hormones. These are used for addressing various health related issues such as ageing,[2] Alzheimer's disease, depression, mental function,[3,4] fatigue, menopausal symptoms, osteoporosis, Parkinson's disease, rheumatoid arthritis, stress and weight loss,[5] etc. In mammals, like all other steroid hormones, progesterone is essentially the harmone of pregnancy and it is synthesized from pregnenolone. Pregnane and its derivatives have also been reported to possess anti-inflammatory activity, besides anti-asthmatic, cytotoxic, anti-feedant, anti-dyslipidimic and anti-oxidant properties.[6-10] We identified a series of thirty-three pregnane derivatives[11-39] from Cambridge Structure Database (CSD). The chemical structure of each compound and its numbering is presented in Figure 2 while the reference code, chemical name, chemical formula, molecular weight and published reference is presented in Table 1.

Crystallographic comparison

The structures belonging to pregnane series and as obtained from CSD were analyzed for their precise structural parameters which include the crystal class, space group, the number of molecules per asymmetric unit cell, the final R-factor, selected bond distances, bond angles, ring conformations, etc. The information in concise form is presented in Table 2, 3 and 4, respectively. Based on the comparative crystallographic data, the following conclusions can be drawn:

1. The most commonly occurring crystal system is *monoclinic* (57.5%), followed by *orthorhombic* (30.3%), *triclinic* (9.09%) and *trigonal* (3.03%). This observation is in line with the findings of Stout and Jensen.[40]
2. The most frequently occurring space group is $P2_1$ (45.4%), followed by $P2_12_12_1$ (30.3%), C2 (12.1%), P1 (9.09%) and $P3_1$ (3.03%).

 DOI: 10.17628/ecb.2016.5.172-184

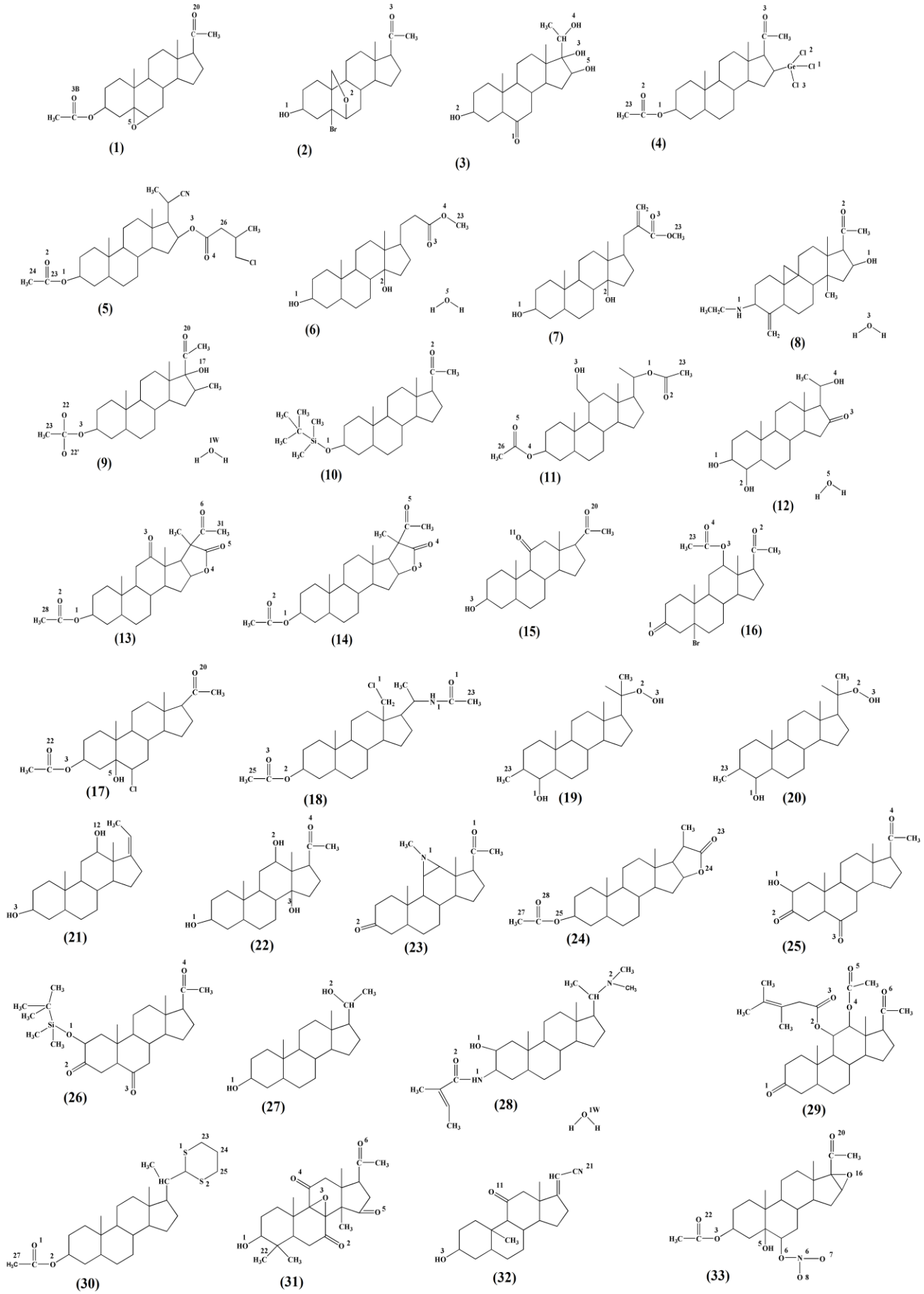

Figure 2. Chemical structure of molecules (**1-33**).

 DOI: 10.17628/ecb.2016.5.172-184

Table 1. CSD code, chemical name/formula, molecular weight and published reference for (M1 - M33)

Mol-ecule	CSD Code	Chemical Name	Chemical formula	MWt. (amu)	Refs.
M-1	BIZPAC	5β,6β-Epoxy-20-oxopregnan-3β-yl acetate	$C_{23}H_{34}O_4$	374.5	[11]
M-2	BOPREO	5α-Bromo-6β,19-oxido-pregnan-3β-ol-20-one	$C_{21}H_{31}BrO_3$	411.0	[12]
M-3	CEQMIU	(-)-(3α,16β,17α,20(S))-3,16,17,20-Tetrahydroxypregnane-6-one	$C_{21}H_{34}O_5$	366.0	[13]
M-4	CIJQOB	β-Acetoxy-16β-trichlorogermyl-5α-pregnan-20-one	$C_{23}H_{35}Cl_3GeO_3$	538.45	[14]
M-5	COYZEW	20(S)-3α-Acetoxy-20-cyano-5β-pregnan-16β-yl (3R)-3-(chloromethyl) butanoate	$C_{29}H_{44}ClNO_4$	506.1	[15]
M-6	CUMYEO	3β,5β,14β,20E)-Methyl 14-hydroxy-pregn-20-ene-21-carboxylate mMonohydrate	$C_{23}H_{36}O_4,H_2O$	394.0	[16]
M-7	CUMYUE	(3β,5β,14β,20E)-Methyl 14-hydroxy-21-methylenepregn-21-carboxylate	$C_{24}H_{38}O_4$	390.0	[16]
M-8	CUZSIZ	3β-(Dimethylamino)-16α-hydroxy-14-methyl-4-methylene-9,19-cyclo-5α-pregnan-20-one monohydrate	$C_{25}H_{39}NO_2,H_2O$	403.59	[17]
M-9	DERHOY	3β-Acetoxy-17α-hydroxy-16α-methylallopregnan-20-one hemihydrate	$C_{24}H_{38}O_4,0.5(H_2O)$	399.55	[18]
M-10	EDIGEE	3β-(t-butyl(dimethyl)silyloxy)-5 α,16α-pregna-20-one	$C2_7H_{48}O_2Si$	432.74	[19]
M-11	FAMYAT	3β,20β-Diacetoxy-11β-hydroxymethyl-5α-pregnane	$C_{26}H_{42}O_5$	434.0	[20]
M-12	GANFUY	3,4,20-Trihydroxypregnan-16-one monohydrate	$C_{21}H_{34}O_4,H_2O$	368.5	[21]
M-13	HOXTEU	7-Acetyl-4α,6α,7-trimethyl-6,8 dioxooctadecahydro-1H naphtho[2',1':4,5]indeno[2,1-β]furan-2-yl acetate	$C_{26}H_{36}O_6$	444.55	[22]
M-14	HOXTIY	7-Acetyl-4α,6α,7-trimethyl-8-oxooctadecahydro-1H-naphtho[2',1':4, 5]indeno[2,1-β]furan-2-yl acetate	$C_{26}H_{38}O_5$	430.56	[22]
M-15	HXPRDO01	(3α-5α)-3-Hydroxypregnane-11,20-dione	$C_{21}H_{32}O_3$	332.47	[23]
M-16	KATXUA	4-Bromo-3,20-dioxopregnan-12-yl acetate	$C_{23}H_{33}BrO_4$	453.4	[24]
M-17	KOFDIT	6β-Chloro-5α-hydroxy-20-oxopregnan-3β-yl acetate	$C_{23}H_{35}ClO_4$	410.96	[25]
M-18	KUTXIH	(20S)-20-Acetamido-18-chloro-5α-pregnan-3β-yl acetate	$C_{25}H_{40}ClNO_3$	438.03	[26]
M-19	LAFCUR	3α,20-Dimethyl-20-hydroperoxy-4β-hydroxy-5β-pregnane	$C_{23}H_{40}O_3$	364.55	[27]
M-20	LAFDAY	4β,20-Dihydroxy-3α,20-dimethyl-5β-pregnane	$C_{23}H_{40}O_2$	348.55	[27]
M-21	LITQUB	(3β,5α,8α,9β,10α,12β,13α,14β,17Z)-pregn-17(20)-ene-3,12-diol	$C_{21}H_{34}O_2$	318.48	[28]
M-22	LOSKAG	3β,12β,14α-Trihydroxypregnan-20-one	$C_{21}H_{34}O_4$	350.48	[29]
M-23	LUVPEX	N-Methyl-11α,12α-aziridino-5β-H-pregnano-3,20-dione	$C_{22}H_{33}NO_2$	343.49	[30]
M-24	OVOQOG	4a,6α,7-Trimethyl-8 oxooctadecahydro-1H naphtho[2',1':4,5]indeno[2,1-β]furan-2-yl acetate	$C_{24}H_{36}O_4$	388.53	[31]
M-25	RAFSAU	2α-hydroxy-5α-pregnane-3,6,20-trione	$C_{21}H_{30}O_4$	346.47	[32]
M-26	RAFSEY	2α-t-butyldimethylsilyloxy-5α-pregnane-3,6,20-trione	$C_{27}H_{44}O_4Si$	460.73	[32]
M-27	ROGNIL	5α-Pregnane-3α,20α-diol	$C_{21}H_{36}O_2$	320.5	[33]
M-28	TUTREG	N-(20-(Dimethylamino)-2-hydroxypregnan-3-yl)-2-methylbut-2-enamide monohydrate	$C_{28}H_{48}N_2O_2,H_2O$	461.69	[34]
M-29	WASCAV	(11α,12β)-12-Acetoxy-11-((3,4-dimethylpent-3-enoyl)oxy)pregnan-3,20-dione	$C_{30}H_{44}O_6$	500.65	[35]
M-30	WETYIE	(20R)-3β-Acetoxy-5α-pregna-20-dithiane	$C_{27}H_{44}O_2S_2$	464.74	[36]
M-31	XOVLUP	8α,9α-Epoxy-4,4,14α-trimethyl-3,7,11,15,20-pentaoxo-5α-pregnane	$C_{24}H_{30}O_6$	414.48	[37]
M-32	YASHOR	3-Hydroxy-11-oxopregn-17-ene-21-nitrile	$C_{21}H_{29}NO_2$	327.45	[38]
M-33	YOTMEA	16α,17α-Epoxy-5α-hydroxy-6β-nitrooxy-20-oxopregnan-3β-yl acetate	$C_{23}H_{33}NO_8$	451.50	[39]

Table 2. Crystal system, space group, *R*-factor, *Z*(*Z*′) for molecules (**1-33**)

Molecule	Crystal system	Space group	R-factor	Z(Z′)
M-1	Orthorhombic	$P2_12_12_1$	0.0414	4
M-2	Orthorhombic	$P2_12_12_1$	0.065	8(2)
M-3	Monoclinic	$P2_1$	0.054	2
M-4	Triclinic	P1	0.0533	2(2)
M-5	Monoclinic	$P2_1$	0.0589	2
M-6	Orthorhombic	$P2_12_12_1$	0.051	4
M-7	Monoclinic	$P2_1$	0.072	2
M-8	Monoclinic	$P2_1$	0.0585	2
M-9	Monoclinic	C2	0.0419	4
M-10	Orthorhombic	$P2_12_12_1$	0.0737	8(2)
M-11	Monoclinic	$P2_1$	0.048	4(2)
M-12	Orthorhombic	$P2_12_12_1$	0.0922	4
M-13	Monoclinic	P21	0.0407	4(2)
M-14	Orthorhombic	$P2_12_12_1$	0.05	4
M-15	Orthorhombic	$P2_12_12_1$	0.0347	4
M-16	Orthorhombic	$P2_12_12_1$	0.0449	4
M-17	Monoclinic	$P2_1$	0.0423	4(2)
M-18	Monoclinic	$P2_1$	0.057	2
M-19	Monoclinic	$P2_1$	0.0446	4(2)
M-20	Trigonal	$P3_1$	0.0474	6(2)
M-21	Monoclinic	$P2_1$	0.0597	4(2)
M-22	Monoclinic	$P2_1$	0.0481	2
M-23	Monoclinic	$P2_1$	0.0472	2
M-24	Monoclinic	C2	0.0456	8(2)
M-25	Monoclinic	$P2_1$	0.0596	2
M-26	Monoclinic	C2	0.053	4
M-27	Monoclinic	$P2_1$	0.044	2
M-28	Orthorhombic	$P2_12_12_1$	0.0549	4
M-29	Monoclinic	C2	0.0389	4
M-30	Monoclinic	$P2_1$	0.0527	4(2)
M-31	Triclinic	P1	0.0481	1
M-32	Orthorhombic	$P2_12_12_1$	0.0343	4
M-33	Triclinic	P1	0.0431	2(2)

3. A careful analysis of the reliability index (R-factor) indicates better precision in the structure determination of these molecules. This parameter ranges between 0.00347 - 0.065 (except for molecule M-7, 10, 12 for which R- factor is relatively high, i.e., 0.072, 0.073 and 0.0922, respectively).

4. The existence of multiple molecules (Z′) phenomenon is quite significant and it exists in molecule M-2, 4, 10, 11, 13, 17, 19-21, 24, 30, 33, respectively.

5. Due to substitution at C3 position of ring A of the steroidal nucleus, there appears a visible change in the bond distances, depending upon whether C2-C3 or C3-C4 is a single or double bond. So, it is of interest to investigate the variation in the C2-C3 (sp^3-sp^3/sp^3-sp^2/sp^2-sp^3) and C3-C4 (sp^3-sp^3/sp^3-sp^2/sp^2-sp^3) bond lengths and C2-C3-C4 (sp^3/sp^2) bond angle in the undertaken structures. The value of the bond C2-C3 (sp^3-sp^3) and C3-C4 (sp^3-sp^3) lies in the range 1.464-1.544Å and 1.485-1.545Å respectively with average value being 1.511Å and 1.516 Å respectively. The bond angle C2-C3(sp^3)-C4 ranges between 108.90°-114.59° having average value 111.38°. However, in structures M-16, 23, 25, 26, 29, 31, both the bond distances C2-C3 and C3-C4 are sp^3-sp^2/sp^2-sp^3 hybridised and lies in the range 1.492-1.528Å and 1.478-1.532Å respectively with average value being 1.508Å and 1.506Å respectively and bond angle (sp^2 hybridised) lies in the range (112.06-116.46°) with average being 114.31°. In M-8, the bond distance C3-C4 is sp^3-sp^2 hybridised having value 1.516 Å.

6. The six- membered rings in all the molecules adopt *chair* conformation with a few exceptions. Like ring B in molecules [M-1] which shows distorted *sofa* conformation and this may be due to the presence of an epoxy group between C5 and C6. Ring B & C in M-8 display *half-chair* conformation, may be due to the presence of a cyclopropane group between C9 and C10; ring A in M-13' &17 show *half-chair* conformation which may be due to the substitution of an acetoxy group at C3; ring A & C in M-23 exhibit *half-chair* conformation due to unusual substitutions at carbon atom C3 and between C11 and C12. Ring B adopts half-chair & ring C distorted *sofa* conformations in M-31which may be due to the presence of an epoxy group between C8 and C9. The relative frequency of various types of conformations occurring in six-membered and five-membered rings in molecules (1-33) are as shown in Figure 3(a, b). The incidence of occurrence of all the six-membered rings in the chair conformation is 93.3%, followed by *half-chair* (5.85%) and distorted *sofa* conformation (1.48%). Similarly, for the five membered rings, the incidence of occurrence of *half-chair* conformation is 44.4%, followed by *envelope* and intermediate between *half-chair* & *envelope* conformations (42.2 & 13.3%), respectively.

 DOI: 10.17628/ecb.2016.5.172-184

Table 3. Selected bond distances (Å) and bond angles (°) for molecules (1-33)

Molecule	Bond distance(Å) [C2-C3]		Bond distance(Å) [C3-C4]		Bond angle(°)	
	sp^3-sp^3	sp^3-sp^2/sp^2-sp^3	sp^3 - sp^3	sp^3 - sp^2/sp^2- sp^3	C3(sp^3)	C3(sp^2)
M-1	1.499		1.512		109.76	
M-2	1.491		1.545		111.51	
M-2'	1.497		1.522		112.9	
M-3	1.519		1.515		111.6	
M-4	1.464		1.531		114.59	
M-4'	1.483		1.504		111.68	
M-5	1.493		1.51		111.41	
M-6	1.499		1.518		110.59	
M-7	1.506		1.524		111.5	
M-8	1.544			1.516	109.22	
M-9	1.498		1.518		111.47	
M-10	1.515		1.519		110.34	
M-10'	1.503		1.51		111.39	
M-11	1.513		1.504		111.16	
M-11'	1.508		1.516		111.12	
M-12	1.518		1.532		110.78	
M-13	1.506		1.515		112.23	
M-13'	1.506		1.509		111.27	
M-14	1.52		1.502		111.61	
M-15	1.527		1.516		111.52	
M-16		1.51		1.515		113.03
M-17	1.511		1.52		112.64	
M-17'	1.52		1.485		113.02	
M-18	1.523		1.521		112.19	
M-19	1.52		1.529		109.86	
M-19'	1.521		1.534		111.25	
M-20	1.521		1.529		108.9	
M-20'	1.511		1.52		109.68	
M-21	1.524		1.509		111.29	
M-21'	1.516		1.518		110.16	
M-22	1.511		1.51		110.52	
M-23		1.498		1.478		112.06
M-24	1.506		1.507		111.22	
M-24'	1.528		1.501		111.49	
M-25		1.528		1.504		116.46
M-26		1.525		1.503		114.52
M-27	1.525		1.506		111.81	
M-28	1.544		1.53		110.11	
M-29		1.496		1.499		114.01
M-30	1.5		1.503		111.33	
M-30'	1.501		1.524		112.4	
M-31		1.492		1.532		115.8
M-32	1.527		1.522		111.1	
M-33	1.508		1.509		111.8	
M-33'	1.503		1.514		112.57	

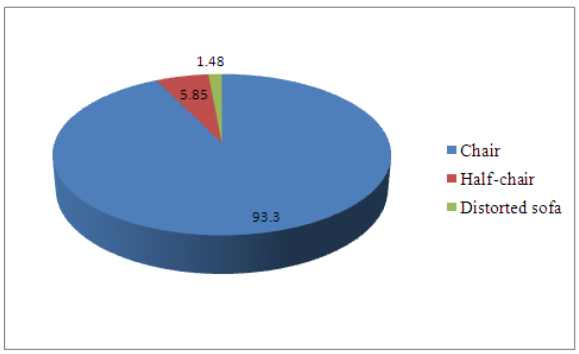

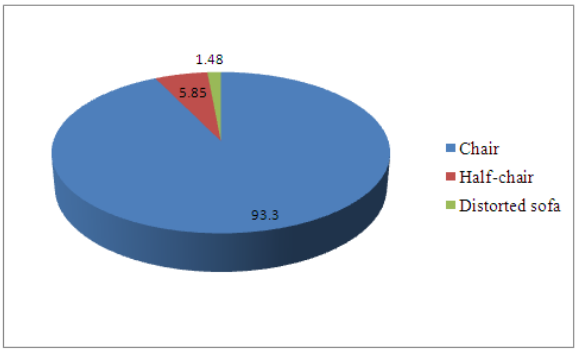

Figure 3. Relative frequency of occurrence (in %) for various types of conformations in (a) six-membered rings A, B and C and (b) five-membered rings D (molecules **1-33**).

Table 4. Computed ring conformations for molecules (1-33)

Molecule	Ring A(conformation)	Ring B(conformation)	Ring C(conformation)	Ring D(conformation)
M-1	Chair	Distorted Sofa	Chair	Half-chair
M-2	Chair	Chair	Chair	Envelope
M-2'	Chair	Chair	Chair	Envelope
M-3	Chair	Chair	Chair	Half-chair
M-4	Chair	Chair	Chair	Half-chair
M-4'	Chair	Chair	Chair	Half-chair
M-5	Chair	Chair	Chair	Half-chair
M-6	Chair	Chair	Chair	Intermediate between envelope and half-chair
M-7	Chair	Chair	Chair	Envelope
M-8	Chair	Half-chair	Half-chair	Half-chair
M-9	Chair	Chair	Chair	Envelope
M-10	Chair	Chair	Chair	Half-chair
M-10'	Chair	Chair	Chair	Half-chair
M-11	Chair	Chair	Chair	Intermediate between envelope and half-chair
M-11'	Chair	Chair	Chair	Envelope
M-12	Chair	Chair	Chair	Envelope
M-13	Chair	Chair	Chair	Half-chair
M-13'	Half-chair	Chair	Chair	Half-chair
M-14	Chair	Chair	Chair	Half-chair
M-15	Chair	Chair	Chair	Envelope
M-16	Chair	Chair	Chair	Half-chair
M-17	Half-chair	Chair	Chair	Envelope
M-17'	Chair	Chair	Chair	Envelope
M-18	Chair	Chair	Chair	Envelope
M-19	Chair	Chair	Chair	Envelope
M-19'	Chair	Chair	Chair	Envelope
M-20	Chair	Chair	Chair	Intermediate between envelope and half-chair
M-20'	Chair	Chair	Chair	Half-chair
M-21	Chair	Chair	Chair	Envelope
M-21'	Chair	Chair	Chair	Intermediate between envelope and half-chair
M-22	Chair	Chair	Chair	Half-chair
M-23	Half-chair	Chair	Half-chair	Half-chair
M-24	Chair	Chair	Chair	Envelope
M-24'	Chair	Chair	Chair	Intermediate between envelope and half-chair
M-25	Chair	Chair	Chair	Half-chair
M-26	Chair	Chair	Chair	Envelope
M-27	Chair	Chair	Chair	Half-chair
M-28	Chair	Chair	Chair	Half-chair
M-29	Chair	Chair	Chair	Half-chair
M-30	Chair	Chair	Chair	Intermediate between envelope and half-chair
M-30'	Chair	Chair	Chair	Half-chair
M-31	Chair	Half-chair	Distorted Sofa	Envelope
M-32	Chair	Chair	Chair	Envelope
M-33	Chair	Chair	Chair	Envelope
M-33'	Chair	Chair	Chair	Envelope

Biological activity predictions

The steroid drug occupies a conspicuous place in the modern therapeutic practice. The broad spectrum of biological activity within the group and the multiplicity of actions displayed by certain individual members make the steroids one of the intriguing classes of biologically active compounds. The biological activity of steroids is related to their chemical structure. PASS (Prediction of Activity spectra for Substances) software[41] emerged as a strong potential tool to predict the biological activity spectrum, is used here to predict the activities of various pregnane related structures. The structural formula of a molecule is presented as a *mol* file to this software and the predictions result in the form of a table containing the list of biological activities. Two values are computed for each activity: P_a -the probability of the compound being active and P_i -the probability of the compound being inactive for a particular activity. Activities with $P_a > P_i$ are retained as possible for a particular compound.

Table 5. Predicted activities (P_a and P_i) for the molecules (1-33)

Mole-cule	Dermatologic $P_a > P_i$	Antieczematic $P_a > P_i$	Antiprurtic $P_a > P_i$	Antiseborrheic $P_a > P_i$	Choleretic $P_a > P_i$	Antisecre-toric, c$P_a > P_i$	Antiinflam-matory, $P_a > P_i$
M-1	0.674 >0.009	0.716 >0.040	0.683 >0.009	0.694 >0.039	0.380 >0.020	0.678 >0.012	0.508 >0.054
M-2	0.637 >0.012	0.668 >0.057	0.689 >0.009	0.373 >0.100	0.292 >0.036	0.244 >0.125	0.589 >0.034
M-3	0.714 >0.007	0.534 >0.119	0.763 >0.005	0.884 >0.005	0.826 >0.003	0.541 >0.024	0.569 >0.039
M-4	0.598 >0.016	0.721 >0.039	0.615 >0.014	0.816 >0.016	0.466 >0.011	0.408 >0.055	-
M-5	0.511 >0.030	0.672 >0.055	0.503 >0.034	0.239 >0.154	-	0.358 >0.071	-
M-6	0.584 >0.018	0.635 >0.071	0.679 >0.009	0.622 >0.051	0.746 >0.003	0.422 >0.051	-
M-7	0.535 >0.025	0.672 >0.056	0.414 >0.055	0.369 >0.101	0.552 >0.007	-	-
M-8	0.442 >0.044	0.736 >0.034	0.345 >0.080	-	-	0.316 >0.084	0.398 >0.097
M-9	0.787 >0.005	0.698 >0.046	0.540 >0.007	0.907 >0.004	0.540 >0.007	0.766 >0.005	0.893 >0.004
M-10	0.704 >0.008	0.512 >0.130	0.333 >0.087	0.316 >0.117	0.232 >0.060	-	-
M-11	0.770 >0.005	0.642 >0.068	0.587 >0.018	0.652 >0.046	0.735 >0.003	0.439 0.045	0.587 >0.035
M-12	0.679 >0.009	0.853 >0.009	0.703 >0.008	0.828 >0.014	0.720 >0.004	0.521 >0.026	0.332 >0.134
M-13	0.627 >0.013	0.642 >0.068	0.747 >0.005	0.709 >0.036	0.648 >0.005	0.473 >0.035	0.615 >0.028
M-14	0.647 >0.011	0.695 >0.047	0.729 >0.006	0.744 >0.029	0.601 >0.005	0.538 >0.024	0.596 >0.033
M-15	0.765 >0.005	0.721 >0.039	0.729 >0.006	0.802 >0.019	0.765 >0.003	0.433 >0.047	0.655 >0.022
M-16	0.668 >0.010	0.530 >0.121	0.469 >0.041	0.805 >0.018	0.278 >0.041	0.370 >0.067	-
M-17	0.639 >0.012	0.688 >0.050	0.669 >0.010	0.641 >0.048	0.225 >0.063	-	0.457 >0.070
M-18	0.619 >0.014	0.510 >0.131	0.385 >0.064	0.339 >0.110	-	0.406 >0.056	-
M-19	0.673 >0.009	0.683 >0.052	0.338 >0.083	0.644 >0.047	0.291 >0.037	0.239 >0.130	-
M-20	0.790 >0.005	0.762 >0.027	0.566 >0.021	0.814 >0.017	0.579 >0.006	0.376 >0.065	0.569 >0.039
M-21	0.676 >0.009	0.735 >0.034	0.688 >0.009	0.832 >0.013	0.697 >0.004	0.585 >0.019	0.472 >0.065
M-22	0.657 >0.011	0.681 >0.052	0.694 >0.008	0.865 >0.008	0.747 >0.003	0.471 >0.036	0.255 >0.206
M-23	0.692 >0.008	0.515 >0.129	0.591 >0.017	0.876 >0.006	0.346 >0.024	0.723 >0.008	-
M-24	0.615 >0.014	0.772 >0.025	0.706 >0.008	0.763 >0.026	0.373 >0.021	0.553 >0.022	0.735 >0.012
M-25	0.757 >0.005	0.627 >0.074	-	0.904 >0.004	0.524 >0.008	0.718 >0.009	0.530 >0.048
M-26	0.796 >0.004	0.542 >0.114	0.365 >0.070	0.567 >0.060	-	-	0.497 >0.058
M-27	0.772 >0.005	0.765 >0.027	0.715 >0.007	0.830 >0.013	0.863 >0.002	0.535 >0.024	0.399 >0.096
M-28	0.552 >0.022	-	0.419 >0.053	0.214 >0.155	-	0.500 >0.137	0.370 >0.112
M-29	0.655 >0.011	0.495 >0.140	0.638 >0.012	0.751 >0.028	0.439 >0.014	0.649 >0.014	0.604 >0.031
M-30	0.795 >0.004	0.667 >0.057	0.693 >0.008	0.745 >0.029	0.501 >0.009	0.594 >0.018	0.496 >0.058
M-31	0.591 >0.017	0.346 >0.242	0.568 >0.021	0.520 >0.069	0.303 >0.033	0.225 >0.144	0.558 >0.041
M-32	0.731 >0.006	0.628 >0.074	0.689 >0.009	0.657 >0.045	0.456 >0.012	0.320 >0.083	0.559 >0.041
M-33	0.621 >0.014	0.363 >0.227	0.754 >0.005	0.270 >0.137	0.211 >0.071	0.394 >0.060	0.884 >0.005

- indicates the absence of a particular type of activity.

The identified molecules of pregnane have been analyzed for the estimation of various activity types viz. *dermatologic, antieczematic, antipruritic, antiseborrheic choleretic, antisecretoric and antiinflammatory.* The computed values of P_a and P_i for the molecules (1-33) are presented in Table 5.

Based on the data as obtained from the simulation studied on biological activity relationship, it is pertinent that all the molecules possess high probability of *dermatologic* activity. Positive *antieczematic* activity has been shown by all the molecules except M-28 and 33.

All molecules show high value of probability for *antprurtic* activity, while in molecules M-8, 10, 18, 19, 25 and 26, this activity is either absent or show low values. The $P_a > P_i$ indicates that all the molecules except [M- 2, 7, 8, 10, 18, 28 and 33] show high value of *antiseborrheic* activity. It appears that all the molecules exhibits high probability of *choleretic* and *antisecretoric* activities except for molecules [M- 1, 2, 5, 8, 16-19, 24-26, 28, 31, 33 and 2, 5, 7, 10, 16, 17, 19, 20, 26 31-33] respectively for which these activities are either absent or have low values. The *anti-inflammatory* activity is prevalent in almost 50% of the identified molecules.

Table 6. Geometry of C-H...O, O-H...O, N-H…O, C-H…Cl, C-H…N, C-H...Br, C-H…F and O-H…N intra and intermolecular interactions

Molecule [Number of donors andacceptors]	**Intramolecular interactions X-H...A**	**H...A(Å) *d***	**X...A(Å) *D***	**X-H...A(°) *θ***
M-9	O17-H17O…O1W	2.188	3.079	170.9
Donors=1				
Acceptors =1				
M-18	C12H12B…Cl1	2.62	3.076	108
Donors=2	C20-H20…Cl1	2.67	3.349	125
Acceptors =2	C20-H20…O1	2.42	2.812	103
M-22	O2-H2…O4	2.01	2.771	158
Donors=1				
Acceptors =1				
	Intermolecular interactions			
M-1	C7-H7B…O3B	2.673	3.631	169.6
Donors=3	C1-H1B…O5	2.535	3.328	139.0
Acceptors =3	C21-H21C…O20	2.599	3.389	139.6
M-2	C21-H26…O3	2.709	3.304	127.6
Donors=4	C2-H20…O2	2.586	3.194	116.3
Acceptors =4	O1'-H43…O1	1.876	2.770	158.7
	O1-H27…O3'	1.714	2.811	145.5
M-3	C1-H10…O1	2.408	3.396	160.9
Donors=6	O2-H21…O1	2.242	2.974	166.7
Acceptors =4	C15-H17…O3	2.281	3.251	152.8
	C2-H7…O4	2.671	3.644	160.2
	O5-H33…O2	2.026	2.887	158.6
	C4-H5…O4	2.710	3.382	125.2
M-4	C23'-H19F…Cl2	2.931	3.811	151.1
Donors=5	C23-H19A…Cl1	2.883	3.723	146.7
Acceptors =4	C4-H4B…Cl3'	2.909	3.686	137.8
	C12-H12A…O2'	2.566	3.485	158.2
	C17-H17A…O2'	2.720	3.638	156.0
M-5	C15-H15B…Cl	2.899	3.803	155.7
Donors=2	C26-H26A…O4	2.676	3.353	127.2
Acceptors =2				
M-6	O5-H37…O3	2.167	2.926	156.9
Donors=4	C23-H32…O1	2.689	3.673	150.3
Acceptors =4	C1-H2…O5	2.716	3.619	156.9
	O5-H38…O1	1.912	2.855	162.7
	O1-H35…O2	2.135	2.845	162.4
M-7	C23-H34…O1	2.529	3.259	127.6
Donors=3	O1-H37…O3	2.164	2.983	157.1
Acceptors =3	C16-H21…O2	2.498	3.543	163.4
M-8	O3-H31…O2	2.169	2.949	159.4
Donors=2	O3-H32…N1	2.049	2.829	158.9
Acceptors =3	O1-H1…O3 (W)	1.979	2.790	170.7
M-9	C23-H23C…O22'	2.651	3.534	153.2
Donors=4	O1W-H1W…O20	2.032	2.845	144.8
Acceptors =3	C2-H2A…O22'	2.699	3.649	166.8
M-10	C8'-H8'…O2	2.538	3.323	136.9
Donors=1				
Acceptors =1				
M-11	C26'-H78…O3	2.626	3.622	156.2
Donors=5	C6-H11…O2'	2.486	3.352	143.5
Acceptors =5	C26-H36…O3'	2.426	3.231	130.3
	C23'-H72…O5	2.714	3.553	153.5
	O3'-H1…O5	1.980	2.906	157.6
	C26'-H79...O5'	2.382	3.480	174.6

M-12	C4-H4A…O1	2.675	3.535	146.8
Donors=4	O1-H1…O5(W)	2.459	3.103	136.4
Acceptors =3	O4-H4…O5(W)	2.039	2.806	154.0
	C4-H4A…O1	2.675	3.535	146.8
	O2-H2…O4	2.183	2.962	158.8
M-13	C28-H28A…O5	2.619	3.420	141.1
Donors=9	C21'-H71B…O2	2.591	3.416	144.1
Acceptors =6	C31'-H81C…O2	2.707	3.463	136.2
	C3'-H53A…O3	2.595	3.432	143.5
	C5'-H55A…O3	2.637	3.481	144.7
	C16-H16A…O2'	2.519	3.331	140.2
	C5-H5A…O3'	2.514	3.360	144.3
	C16'-H66A…O2	2.542	3.429	150.5
	C6-H6A…O5'	2.669	3.596	160.1
M-14	C8-H8A…O2	2.632	2.560	158.0
Donors=3	C14-H14A…O5	2.531	3.466	159.4
Acceptors =3	C16-H16A…O4	2.410	3.217	139.2
M-15	C21-H21B…O3	2.653	3.401	133.3
Donors=3	O3-H3…O11	2.205	2.948	145.6
Acceptors =3	C2-H2A…O20	2.679	3.578	151.1
M-16	C19-H18A…O1	2.635	3.278	123.5
Donors=3	C23-H23A…O4	2.422	3.397	172.9
Acceptors =3	C21-H20C...O2	2.605	3.535	158.5
M-17	C15-H15B…O22	2.466	3.436	177.4
Donors=5	O5-H5A…O20	1.981	2.794	170.9
Acceptors =5	C16-H16A…O5'	2.649	3.617	176.4
	C15'-H15D…O22'	2.322	3.286	172.9
	O5'-H5B…O20'	1.983	2.782	164.7
M-18	C25-H25C…O1	2.683	3.516	143.0
Donors=4	C23-H23C…O3	2.539	3.488	162.8
Acceptors =3	C2-H2C…Cl1	2.882	3.592	129.4
	N1-H1…O1	2.034	2.893	165.3
M-19	O1-H1X…O3	2.087	2.868	164.7
Donors=4	C23-H23C…O2	2.584	3.562	175.3
Acceptors =5	O3-H3X…O1'	1.862	2.740	162.5
	O1'-H1Y…O2'	2.373	3.179	148.6
	O1'-H1Y…O3'	2.023	2.915	170.3
M-20	O16-H1Y…O2	2.104	2.806	152.9
Donors=4	O2-H2X…O2'	1.954	2.818	162.1
Acceptors =4	O2'-H2Y…O1	1.837	2.716	163.2
	O1-H1X…O1'	1.882	2.743	162.2
M-21	O3-H3…O3'	1.943	2.709	170.4
Donors=3	C16'-H16C…O12'	2.435	3.287	143.9
Acceptors =2	C21-H17F…O3'	2.673	3.600	157.8
M-22	C21-H21A…O1	2.610	3.288	127.9
Donors=3	O3-H3…O4	2.187	2.916	149.8
Acceptors =4	C21-H2A…O3	2.658	3.423	136.8
	O1-H1…O2	2.059	2.928	169.7
M-23	C19-H19C…O1	2.628	3.569	166.8
Donors=3	C5-H5A…N1	2.685	3.615	158.5
Acceptors =3	C18-H18C…O2	2.565	3.472	157.7
M-24	C27-H27C…O28'	2.44	3.36	160.22
Donors=1				
Acceptors =1				

M-25	C21-H212…O3	2.707	3.629	158.5
Donors=3	C21-H211…O1	2.678	3.291	121.3
Acceptors =4	C7-H71…O4	2.574	3.525	168.3
	C17-H171…O2	2.633	3.215	118.3
M-26	C1-H11…O3	2.492	3.393	153.8
Donors=2	C9-H91…O3	2.661	3.449	138.0
Acceptors =1				
M-27	O1-H1…O2	1.864	2.698	166.8
Donors=3	C21-H19B…O1	2.561	3.271	130.9
Acceptors =2	O2-H2…O1	1.899	2.741	170.8
M-28	C12-H12B…O2	2.715	3.623	156.2
Donors=4	C21-H21B…O2	2.682	3.588	157.9
Acceptors =3	N1-H1…O1W	2.126	2.972	167.8
	O1W-H1WA…O1	1.892	2.745	153.1
M-29	C4-H4B…O1	2.714	3.539	143.1
Donors=3	C9-H9…O3	2.365	3.321	164.8
Acceptors =3	C21-H30A…O5	2.442	3.345	156.5
M-30	C27'-H27E…O1	2.706	3.659	172.1
Donors=4	C25-H25B…S1	2.848	3.558	130.7
Acceptors =4	C4'-H4'B…O2'	2.695	3.419	131.8
	C23'-H23C…S2'	2.822	2.648	148.0
M-31	C6-H6B…O4	2.655	3.231	118.4
Donors=4	C22-H22A…O4	2.572	3.531	177.1
Acceptors =3	C2-H2A…O5	2.712	3.673	171.1
	C12-H12B…O6	2.488	3.362	149.7
M-32	C15-H15B…O3	2.560	3.327	134.2
Donors=4	C16-H16A…O3	2.687	3.378	127.1
Acceptors =3	C15-H15A…O11	2.465	3.358	149.7
	C7-H7B…O11	2.553	3.329	135.2
	O3-H3…N21	2.204	2.949	147.8
M-33	C15'-H15C…O22	2.614	3.482	149.1
Donors=8	C4-H4A1…O20	2.553	3.242	127.9
Acceptors =5	C5-H5A…O20	2.013	2.822	168.3
	C1'-H1B1…O7	2.616	3.326	130.2
	C1-H1A1…O7'	2.582	3.145	117.2
	C4'-H2B1…O20'	2.550	2.297	133.8
	O5'-H5B…O20'	2.107	2.913	167.6
	C15-H15A…O22	2.529	3.429	154.2

' indicates second crystallographically independent molecule;

Molecular packing interaction analysis

Hydrogen bonds play a very vital role in crystal engineering due to their strength, directionality and flexibility.[41] In almost every crystal structure that contains hydrogen bonding functionalities, the packing cannot be understood without taking into account the hydrogen bonding patterns. The strong hydrogen bond of the type O-H…O and N-H…O remains well documented but the concept of weak hydrogen bonds formed between C-H groups and electronegative atoms has received considerable attention of the community involved in the field of crystal design and engineering. Crystallographers regard these interactions as weak but significant "Directional Intermolecular Forces". It is now very well understood that C-H…O interactions (and other types of weak hydrogen bonds) are important as secondary interactions, and in many instances even play dominant roles in determining crystal packing, molecular conformations and in the stability & activity of biological small and macromolecules.[42-44] A close examination of intra and intermolecular interactions, including the bifurcated hydrogen bond, present in pregnane class of steroids leads us to the existence of intra and intermolecular hydrogen bonds of the type C-H…O, O-H…O, N-H…O, C-H…N, C-H…S, O-H…N, C-H…Cl, C-H…F hydrogen bonds as observed in pregnane are presented in Table 6.

Packing interactions include both the intra and intermolecular hydrogen bonds which are directional interactions with a preference for linear geometry.[45] These interactions can be analyzed in a better way by drawing *d*-θ and *D*-θ scatter plots. The plots include all contacts found in molecule (1-33) with d < 2.84Å and D < 3.81Å at any occurring angle θ. The graphical projection of d(H…A) against θ (X-H…A) and D(X…A) against θ (X–H…A) i.e. *d*-θ and *D*-θ scatter plots have been made for intermolecular hydrogen bonds as presented in Figure 4(a, b).

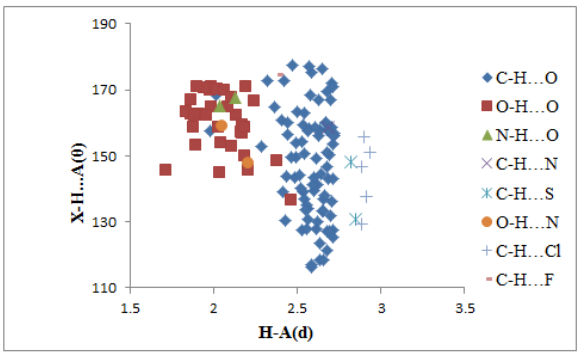

a)

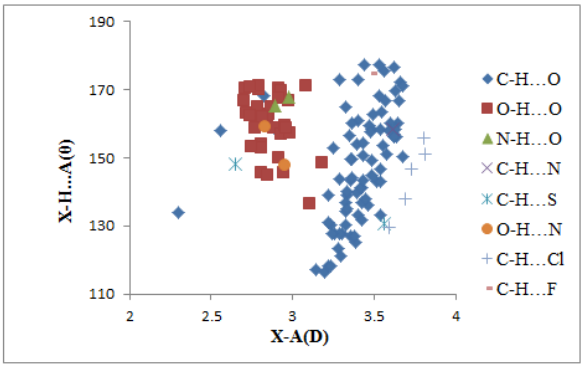

b)

Figure 4. (a) *d*-*θ* scatter plot for intermolecular C-H...O, O-H...O, N-H…O, C-H…N, C-H…S, O-H…N, C-H…Cl and C-H...F. (b) *D*-*θ* scatter plot for intermolecular C-H...O, O-H...O, N-H…O, C-H…N, C-H…S, O-H…N,C-H…Cl and C-H...F.

From *d*-*θ* and *D*-*θ* scatter plots for hydrogen bonds, the following observations have been made:

The scatter spots for C-H…O hydrogen bonds clusters in the range of *d*(H…A) = 2.40-2.75 Å; *D*(X…A) = 3.20-3.70 Å and *θ*(X–H…A) =115-179°.

For the O-H…O type of hydrogen bond, the density of spots is maximum in the *d*(H…A) range of 1.85-2.30 Å, *D*(X…A) range of 2.75-3.1 Å for *θ*(X-H…A) in the range 145-175°.

Almost all the O-H…O contacts belongs to the category of strong H-bonds whereas C-H…O contacts falls in the range of weak interactions.

The relative frequency of occurrence of various types of C-H...O, O-H...O, N-H…O, C-H…N, C-H…S, O-H…N, C-H…Cl and C-H...F intermolecular hydrogen bonds is 64.61, 25.15, 1.53, 0.76, 1.53, 1.53, 3.84 and 0.76%, respectively and it is shown in Figure 5.

Based on the data on hydrogen bonding as presented in Table 6, it is observed that the *d* (H…A) lies between 1.76-2.93Å, *D*(X-A) ranges between 2.29-3.81Å, whereas angular range falls between 116.3-177.4° for all H-bonds. The range for *d* (H…A), *D*(X-A) and angular range *θ*(X–H…A) for C-H…O and O-H…O hydrogen bonds are presented in Table 7 and are compared with the values suggested by Desiraju and Steiner[46] to classify the hydrogen bonds as very strong, strong and weak.

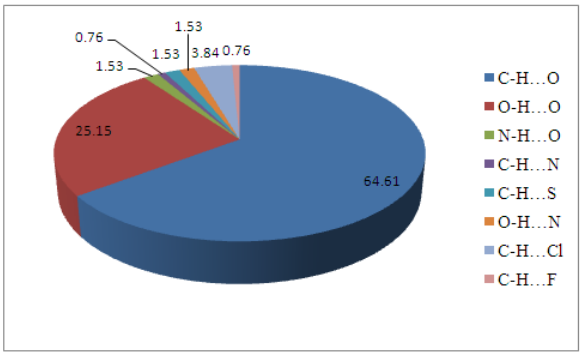

Figure 5. Relative frequency of occurrence (in %) for various types of intermolecular hydrogen bonding.

The overall D(X-A) and d(H…A) range as obtained in case of C-H…O hydrogen bonds comes out to be between 2.56-3.67Å and 1.98-2.72Å respectively, making these interactions fall under the category of "strong to weak" interactions. The angular *θ*(X–H…A) range (116.3-177.4^0) in the present case is tilted more towards the values used to describe weak interactions, hence interactions can be assumed as weak one. However, in case of O-H…O hydrogen bonds, *D*(X-A) and *d*(H…A) range lies between 2.70-3.17Å and 1.71-2.45Å respectively, indicating that the interactions belongs to the category of "strong to weak" inter actions. The angular range (136.4-170.9^0) in case of O-H…O hydrogen bonds lies purely in the range used to describe the interactions as strong one.

The existence of bifurcated hydrogen bonding is the stand out feature of pregnane derivatives. Around 40% of the structures identified for the present work have revealed their existence. In molecule M-1, Oxygen atom O1and O4 act as a bifurcated hydrogen bond acceptor forming intermolecular bonds [C1-H10…O1and O2-H21…O1; C2-H7…O4 and C4-H5…O4] with bifurcated angle of 327.6° and 285.4° respectively. In M-4 (asymmetric unit having two independent molecules), oxygen atom O2' of the acetoxy group acts as bifurcated acceptor forming two hydrogen bonds [C12-H12A…O2' and C17-H17A…O2'] having bifurcated angle of 314.2°. In molecules M-6, oxygen atom O1acts as bifurcated acceptor forming hydrogen bonds [C32-H32…O1 and O5-H38…O1]. In molecule M-12, Oxygen atom O5 of water molecule is involved in bifurcated hydrogen bonding forming bonds [O1-H1…O5 and O4-H4…O5] with a bifurcated angle of 290.4°. In molecule M-13, asymmetric unit is having two independent molecules. Oxygen atom O2 is involved in trifurcated hydrogen bonding forming hydrogen bonds [C21'-H71B…O2, C31'-H81C…O2 and C16'-H66A…O2] and O3 is also acting as bifurcated acceptor in hydrogen bonds C3'-H53A…O3and C5'-H55A…O3 with bifurcated angle of 288.2°. Oxygen atom O1 of M-18 is also acting as bifurcated acceptor with a bifurcated angle of 308.3° in bonds C25-H25C…O1 and N1-H1…O1. Molecule M-19 is having two crystallographically independent molecules in the asymmetric unit. Oxygen atom O1' of second independent molecule is involved in bifurcated hydrogen bonding in which H1Y-atom of O1' is shared between O1'-O2' and O1'-O3' forming two intermolecular H-bonds [O1'-H1Y…O2', O1'-H1…O3'] with bifurcated angle of 318.9°.

Table 7. Geometrical parameters for very strong, strong and weak intermolecular hydrogen bonds

Property	Very strong	Strong	Weak	Present work	
				C-H…O	O-H…O
D(X-A) range (Å)	2.0 -2.5	2.5 - 3.2	3.0 - 4.0	2.56-3.67	2.70-3.17
d(H…A)range (Å)	1.2 -1.5	1.5 - 2.2	2. 0 - 3.0	1.98-2.72	1.71-2.45
θ(X-H…A) range(^{0})	175 - 180	130 -180	90 - 180	116.3-177.4	136.4-170.9

Oxygen atom O3' of molecule M-21 is acting as a bifurcated acceptor in hydrogen bonds O3-H3…O3' and C21-H21A…O3' with bifurcated angle of 328.2°. Oxygen atom O3 of M-26 acts as bifurcated acceptor with bifurcated angle of 291.8° forming [C1-H11…O3 and C9-H91…O3] hydrogen bonds. In M-32, oxygen atoms O4, O3 and O11act as bifurcated acceptors forming hydrogen bonds [C6-H6B…O4 and C22-H22A…O4; C15-H15B…O3 and C16-H16A…O3; C15-H15A…O11and C7-H7B…O11]. Bifurcated bonds are also observed in molecule M-33 where oxygen atoms O22, O20 and O20' are involved in bifurcated hydrogen bonding. A representative view of bifurcated bond having oxygen atom acting as bifurcated acceptor of M-18 is shown in Figure 6.

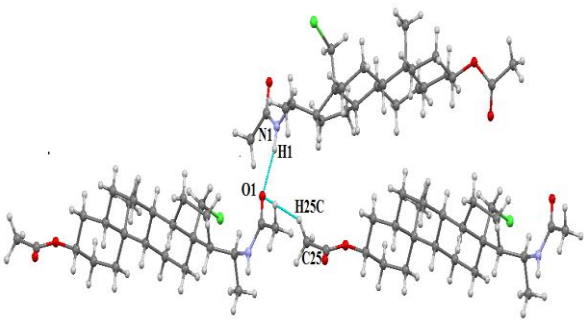

Figure6 Representative view of bifurcated hydrogen bonding in molecule M-18.

Conclusions

The pregnane class of steroids have been analysed in the present work for their crystallographic comparison, biological activity predictions and molecular packing interactions. The molecules in the unit cell are linked by C-H…O/O-H…O/N-H…O interactions and most of these are associated through the acetyl, acetoxy and the hydroxyl group located at different positions of the pregnane derivatives. The biological activity predictions have been made on the basis of a probability scale (P_a and P_i) generated through PASS software. It is depicted that unusual substitution with the basic steroid moiety/nucleus may change the biological activity of the molecule. The nature of the substituent at C3 and C17 positions of the pregnane nucleus makes these molecules very interesting candidates for hydrogen bonding analysis. In most of the cases, the substituent at C3 and C17 positions are primarily responsible for the occurrence of intra and intermolecular hydrogen bonding in pregnanes. Different kind of molecular interactions make up the different crystal structures in the pregnane series. The first and strongest interaction is the O-H...O hydrogen bonds while majority consists of weak C-H…O contacts. We anticipate that the understanding of these interactions in crystal packing will help the chemists /crystallographers to ameliorate a structure to give it desired properties. Hence, the information about the comparative crystallography, biological activity prediction and detailed hydrogen bonding analysis of some pregnane derivatives as presented in the form of a small compendium shall go a log way in understanding the structure and function of steroids.

Acknowledgement

One of the authors, Rajni Kant is thankful to the Indian Council of Medical Research, New Delhi for research funding under project grant no: BIC/12(14)2012.

References

[1]Duax, W. L., Ghosh, D., Pletnev, V., Griffin J. F., *Pure Appl. Chem.*, **1996**, *68*, 1297.

[2]Meldrum, D. R., Davidson, B. J., Tataryn, I. V., Judd, H. L., *Obstet. Gyneccol*, **1981**, *57*, 624.

[3]Flood, J. F., Morley, J. E., Roberts, E., *Proc. Natl. Acad. Sci. USA.*, **1995**, *92*, 10806.

[4]Flood, J. F., Morley, J. E., Roberts, E., Memory- enhancing effects in male mice of pregenolone and steroids metabolically derived from it. *Proc. Natl. Acad. Sci. USA.*, **1992**, *89*, 1567.

[5]Meieran, S. E., Reus, VI., Webster, R., Shafton, R., Wolkowitz, O. M., *Psychoneuroendocrinology*, **2004**, *29*, 486.

[6]Nobile, A., Charney, A.W., Perlman, P. L., Herzog, H. L., Paynee, C. C., Tully, M. E., Jevnik, M. A., Hershberg, E. B., *J. Am. Chem. Soc.*, **1955**, *77*, 4184.

[7]Zhangqing, Y., Khalil, M. A., Hoon, K. D., Lee, H. J., *Tetrahedron Lett.*, **1995**, *36*, 3303.

[8]Shen, Y., Burgoyne, D. L., *J. Org. Chem.*, **2002**, *67*, 3908.

[9]Schun, Y., Cordell, G. A., *J. Nat. Prod.*, **1987**, *50*, 195.

[10]Purushothaman, K. K., Sarada, A., Saraswathi, A., *Can. J. Chem.*, **1987**, *65*, 150.

[11]Pinto, R. M. A., Salvador, J. A. R., Paixao, J. A., *Acta Crystallogr., Sect C. Struct. Commun.*, **2008**, *64*, o279.

[12]Gopalakrishna, E. M., Cooper, A., Norton, D. A., *Acta Crystallogr., Sect. B: Struct. Crystallogr. Cryst. Chem.*, **1969**, *25*, 2473.

[13]Grieco, P. A., Haddad, J., Nunez, M. M. P., Huffman, J. C., *Phytochemistry*, **1999**, *51*, 575.

[14]Pogozhikh, S. A., Ovchinnikov, Y. E., Khrustalev, V. N., Antipin, M. Y., Karpenko, R. G., Kolesnikov, S. P., *Izv. Akad. Nauk SSSR, Ser. Khim.(Russ.) Russ. Chem. Bull.*, **1999**, 116.

[15]Alonso, M. M., Alamo, M. F., Arteaga, M. A. I., *Steroids*, **2009**, *74*, 112.

[16]Rohrer, D. C., Kihara, M., Deffo, T., Rathore, H., Ahmed, K., From, A. H. L., Fullerton, D. S., *J. Am. Chem. Soc.*, **1984**, *106*, 8269.

[17]Parvez, M., Rahman, A., Choudhary, M. I., Parveen, S., Ayatollahi, S. A. M., *Acta Crystallogr., Sect. C: Cryst. Struct. Commun.*, **2000**, *56*, 233.

[18]Bandhoria, P., Gupta, V. K., Gupta, B. D., Varghese, B., *J. Chem. Cryst.*, **2006**, *36*, 427.

[19]Shingate, B. B., Hazra, B. G., Pore,V. S., Gonnade, R. G., Bhadbhade, M. M., *Tetrahedron*, **2007**, *63*, 5622.

[20]Ahmed, F. R., Huber, C. P., *Acta Crystallogr., Sect. C: Cryst. Struct. Commun.*, **1986**, *42*, 1596.

[21]Wang, J. R., Shen, Q., Fang, L., Peng, S. Y., Yang, Y. M., Li, J., Liu, H. L., Guo, Y. W., *Steroids*, **2011**, *76*, 571.

[22]Linares, G. H., Reyes, S. M., Smith, S. M., Ramirez, J. S., Calvario, V. G., Bernes, S., *J.Mex.Chem.Soc.*, **2007**, *51*, 217.

[23]Bandyopadhyaya, A. K., Manion, B. D., Benz, A., Taylor, A., Rath, N. P., Evers, A. S., Zorumski, C. F., Mennerick, S., Covey, D. F., *Bioorg. Med. Chem. Lett.*, **2010**, *20*, 6680.

[24]Geoffroy, P., Ressault, B., Marchioni, E., Miesch, M., *Steroids*, **2011**,*76*, 702.

[25]Pinto, R. M. A., Salvador, J. A. R., Paixao, J. A., Beja, A. M., Silva, M. R., *Acta Crystallogr., Sect. E: Struct. Rep. Online*, **2008**, *64*, o1420.

[26]Benn, M., Vohra, K. N., Parvez, M., *Acta Crystallogr., Sect. E: Struct. Rep. Online*, **2010**, *66*, o933.

[27]Uyanik, C., Hanson, J. R., Nisius, L., Hitchcock, P. B., *J. Chem. Res.*, **2004**,471.

[28]Katona, B. W., Rath, N. P., Anant, S., Stenson, W. F., Covey, D. F., *J. Org. Chem.*, **2007**, *72*, 9298.

[29]Shi, H., Li, Y., *Acta Crystallogr., Sect. E:Struct. Rep. Online*, **2009**, *65*, o1102.

[30]Chenna,P. H. D., Dauban, P., Ghini, A., Baggio, R., Garland, M. T., Burton, G., Dodd, R. H., *Tetrahedron*, **2003**, *59*, 1009.

[31]Linares, M. G. H., Ramirez, J. S., Reyes, S. M., Smith, S. M., Herrera, M. A. F., Bernes, S., *Steroids*, **2010**, *75*, 240.

[32]Marek, A., Klepetarova, B., Elbert, T., *Collect. Czech. Chem. Commun.*, **2011**, *76*, 443.

[33]Olmstea, M. M. and Tahir, H., *Private Communication*, **2008.**

[34]He, K., Du, J., *J. Asian Nat. Prod. Res.*, **2010**, *12*, 233.

[35]Qiu, M. H., Nakamura, N., Min, B. S., Hattori, M., *Chem. Biodiversity*, **2005**, *2*, 866.

[36]Shingate, B. B., Hazra, B. G., Pore, V. S., Gonnade, R. G., Bhadbhade, M. M., *Tetrahedron Lett.*, **2006**, *47*, 9343.

[37]Gonzalz, A. G., Leon, F., Rivera, A., Padron, J. I., Plata, J. G., Zluaga, J. C., Quintana, J., Estevez, F., Bermejo, J., *J. Nat. Prod.*, **2002**,*65*,417.

[38]Stastna, E., Krishnan, K., Manion, B. D., Taylor, A., Rath, N. P., Chen, Z. W., Evers, A. S., Zorumski, C. F., Mennerick, S., Covey, D. F., *J. Med. Chem.*, **2011**, *54*, 3926.

[3]Pinto, R. M. A., Beja, A. M., Salvador, J. A. R., Paixao, J. A., *cta Crystallogr., Sect. E: Struct. Rep. Online*, **2009,** *65*, o1271.

[40]Stout, G. H. and Jensen, L. H., *Crystal Structure Determination*, Macmillan Co., New York, **1968.**

[41]Subramanian, S. and Zaworotko, M. J., *Coord. Chem. Rev.*, **1994**, *137*, 357.[42]Yellin, Z. B. and Leiserovitz, L., *Acta Crystallogr., Sect. B*, **1984**, *40*, 159.

[43]Satonaka, H., Abe, K. and Hirota, M., *Bull. Chem. Soc. Jpn.*, **1988**, *61*, 2031.

[44]Derewenda, Z. S., Derwena, U. and Kobos, P. M., *J. Mol. Biol.*, **1994,** *241***,** 83.

[45] Steiner, T., Angew. Chem., *Int. Ed. Eng.*, **2002**, *41*, 48.

[46]Desiraju, G. R. and Steiner, T., *The Weak Hydrogen Bond in Structural Chemistry and Biology*, OUP,Chichester, **1999**.

Received: 17.06.2016.
Accepted: 08.07.2016.

AN EFFICIENT MICROWAVE-ASSISTED SYNTHESIS OF 2,3-DIHYDROQUINAZOLIN-4(1*H*)-ONES BY A THREE COMPONENT REACTION UNDER CATALYST- AND SOLVENT-FREE CONDITIONS

Arpita Das Gupta[a], Nayim Sepay[a] and Asok K. Mallik[a]*

Keywords: 2,3-Dihydroquinazolin-4(1*H*)-ones, microwave irradiation, catalyst- and solvent-free synthesis, isatoic anhydride, aldehydes, ketones.

An efficient and green synthesis of 2,3-dihydroquinazolin-4(1*H*)-ones by microwave-assisted reaction of isatoic anhydride, ammonium acetate and an aldehyde or a ketone under catalyst- and solvent-free conditions is described.

* Corresponding Authors
E-Mail: mallikak52@yahoo.co.in
[a] Department of Chemistry, Jadavpur University, Kolkata-700 032, India

Introduction

2,3-Dihydroquinazolin-4(1*H*)-ones (**3**) are a class of nitrogen heterocycles that have attracted much attention because of their broad range of pharmacological activities such as antibacterial,[1] antifungal,[2] antimalarial,[3] antitumor,[4] anticancer,[2,5] anti-inflammatory,[6] and anticonvulsant[7] activities. Moreover, they are also used as key intermediates for the synthesis of quinazolin-4(3*H*)-ones.[8-10] Two important routes for synthesis of **3** are the reactions of (i) *o*-aminobenzamide and an aldehyde or a ketone and (ii) isatoic anhydride, an amine or ammonia source and an aldehyde or a ketone. Reactions through both these two routes are known to be carried out by use of different catalysts and solvents.[11-19] The current trend towards development of catalyst-free and solvent-free reaction conditions[20-25] encouraged us to synthesize **3** by the above-said routes by avoiding the use of any catalyst or solvent. Very recently, we have reported a catalyst- and solvent-free synthesis of **3** by the first route.[26] It is evident from the literature that in 2007 Gao *et al.*[27] reported a synthesis of **3** by the second route simply by heating a mixture of the reactants at 70 °C. However, in our hands the reactions were incomplete at 70 °C within the stipulated time (10 min) and hence higher temperature and/or longer time were required to complete the reactions. Owing to the fact that microwave (MW) irradiation has a number of beneficial effects in process chemistry, particularly with respect to reaction time; it has become an attractive tool for synthetic organic chemists. In order to carry out the above-said reaction within a short time, we studied the reaction of isatoic anhydride, ammonium acetate (ammonia source) and an aldehyde or a ketone under the influence of microwave (Scheme 1). The results were very much satisfactory and the remarkable success obtained in this endeavor is presented herein.

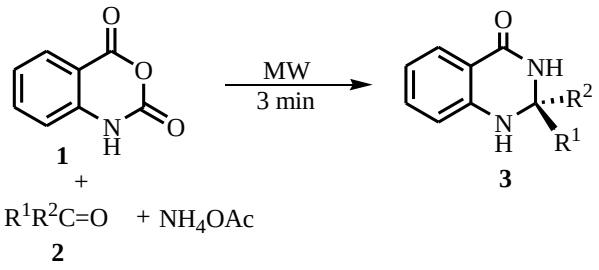

Scheme 1. Microwave-assisted synthesis of 2,3-dihydroquinazolin-4(1*H*)-ones (**3**).

Experimental

Melting points were recorded on a Köfler block. IR spectra were recorded on a Perkin Elmer FT-IR spectrophotometer (Spectrum BX II) in KBr pellets. ^{1}H NMR spectra were recorded in $CDCl_3$ on a Bruker AV-300 (300 MHz) spectrometer. Analytical samples were routinely dried *in vacuo* at room temperature. Microanalytical data were recorded on two Perkin-Elmer 2400 Series II C, H, N analyzers. Mass spectra were measured with a Waters Xevo G2QTof HRMS spectrometer. A mono-mode MW reactor, manufactured by CEM Corporation, USA was used for this study. TLC experiments were performed with silica gel G of SRL Pvt. Ltd make. Petroleum ether had the boiling range of 60-80 °C.

Synthesis of 3 by microwave method

In a typical experiment, an intimate mixture of isatoic anhydride (1 mmol), aldehyde/ketone (1 mmol) and ammonium acetate (2 mmol) was taken in a pyrex beaker (100 mL) and it was subjected to irradiation in the MW reactor at 60 °C (300 W) in an open vessel for 3 min (as monitored by TLC). The reaction mixture was then cooled and crystallized from ethanol, which gave **3** in pure state.

Synthesis of 3 by thermal method

An intimate mixture of isatoic anhydride (1 mmol), aldehyde/ketone (1 mmol) and ammonium acetate (2 mmol) was taken in a round-bottomed flask fitted with an air condenser, and it was heated in an oil bath at 120°C for 10 min. The reaction mixture was then cooled and crystallized from ethanol in order to obtain **3** in pure state.

2,3-Dihydro-2-phenylquinazolin-4(1*H*)-one (3a)

Colorless crystals, yield 92 %, m.p. 217-219 °C (lit.[11] 216-218 °C). IR (KBr): ν/cm^{-1} = 3308, 3188, 3066, 1655, 1610, 1509, 1434. ^{1}H-NMR ($CDCl_3$): δ = 4.39 (br. s, 1H, NH), 5.76 (br. s, 1H, NH), 5.91 (s, 1H, H-2), 6.67 (d, 1H, *J* = 7.9 Hz), 6.91 (t, 1H, *J* = 7.2 Hz), 7.34 (t, 1H, *J* = 7.4 Hz), 7.46 (br. s, 3H), 7.59 (s, 2H), 7.95 (d, 1H, *J* = 7.6 Hz). MS (relative intensity) m/z: 225.2142 (M+1). Anal. Calcd. for $C_{14}H_{12}N_2O$: C, 74.98; H, 5.39; N 12.49. Found: C, 74.72; H, 5.51; N, 12.25.

2,3-Dihydro-2-p-tolylquinazolin-4(1*H*)-one (3b)

Colorless crystals, yield 92 %, m.p. 228-230 °C (lit.[11] 225-227 °C). ^{1}H-NMR ($CDCl_3$): δ = 2.40 (s, 3H, Me), 4.35 (br. s, 1H, NH), 5.72 (br. s, 1H, NH), 5.87 (s, 1H, H-2), 6.66 (d, 1H, *J* = 8.0 Hz), 6.90 (t, 1H, *J* = 7.5 Hz), 7.25 (d, 2H, *J* = 7.9 Hz), 7.33 (t, 1H, *J* = 7.1 Hz), 7.48 (d, 2H, *J* = 7.9 Hz), 7.95 (d, 1H, *J* = 7.1 Hz).

2,3-Dihydro-2-(4-methoxyphenyl)quinazolin-4(1*H*)-one (3c)

Colorless crystals, yield 90 %, m.p. 194-196 °C (lit.[12] 197-198 °C), ^{1}H-NMR ($CDCl_3$): δ = 3.84 (s, 3H, OMe), 4.35 (br. s, 1H, NH), 5.73 (br. s, 1H, NH), 5.85 (s, 1H, H-2), 6.66 (d, 1H, *J* = 7.7 Hz), 6.90 (t, 1H, *J* = 7.5 Hz), 6.95 (d, 2H, *J* = 8.6 Hz), 7.33 (br. t, 1H, *J* = 7.8 Hz), 7.52 (d, 2H, *J* = 8.6 Hz), 7.94 (br. d, 1H, *J* = 7.5 Hz). Anal. Calcd. for $C_{15}H_{14}N_2O_2$: C, 70.85; H, 5.55; N, 11.02. Found: C, 70.70; H, 5.39; N, 10.84.

2-(2-Chlorophenyl)-2,3-dihydroquinazolin-4(1*H*)-one (3d)

Colorless crystals, yield 95 %, m.p. 225-227 °C (lit.[28] 225-226 °C). ^{1}H-NMR ($CDCl_3$): δ = 4.62 (br. s, 1H, NH), 6.03 (br. s, 1H, NH), 6.35 (d, 1H, *J* = 1.6 Hz, H-2), 6.67 (d, 1H, *J* = 8.0 Hz), 6.88 (t, 1H, *J* = 7.5 Hz), 7.30-7.43 (m, 4H), 7.73-7.76 (m, 1H), 7.92 (br. d, 1H, *J* = 7.2 Hz).

2-(4-Chlorophenyl)-2,3-dihydroquinazolin-4(1*H*)-one (3e)

Colorless crystals, yield 95 %, m.p. 206-207 °C (lit.[11] 205-206 °C). ^{1}H-NMR ($CDCl_3$): δ = 4.37 (br. s, 1H, NH), 5.81 (br. s, 1H, NH), 5.89 (s, 1H, H-2), 6.68 (d, 1H, *J* = 8.0 Hz), 6.92 (t, 1H, *J* = 7.5 Hz), 7.35 (t, 1H, *J* = 7.7 Hz), 7.42 (d, 2H, *J* = 8.3 Hz), 7.54 (d, 2H, *J* = 8.3 Hz), 7.94 (d, 1H, *J* = 7.8 Hz)**.** Anal. Calcd. for $C_{14}H_{11}ClN_2O$: C, 65.00; H, 4.29; N, 10.83. Found: C, 65.17; H, 4.17; N 11.02.

2-(4-Bromophenyl)-2,3-dihydroquinazolin-4(1*H*)-one (3f)

Colorless crystals, yield 92 %, m.p. 194-196 °C (lit.[11] 195-197 °C). ^{1}H-NMR ($CDCl_3$): δ = 5.80 (br. s, 1H, NH), 5.89 (s, 1H, H-2), 6.67 (d, 1H, *J* =8.1 Hz), 6.92 (t, 1H, *J* = 7.6 Hz), 7.35 (t, 1H, *J* = 7.6 Hz), 7.48 (d, 2H, *J* = 8.5 Hz), 7.59 (d, 2H, *J* = 8.6 Hz), 7.95 (d, 1H, *J* = 7.5 Hz).

2-(4-(Dimethylamino)phenyl)-2,3-dihydroquinazolin-4(1*H*)-one (3g)

Colorless crystals, yield 93 %, m.p. 208-209 °C (lit.[11] 208-210 °C). ^{1}H-NMR ($CDCl_3$): δ = 2.99 (s, 6H, -NMe_2), 4.33 (br. s, 1H, NH), 5.68 (br. s, 1H, NH), 5.80 (s, 1H, H-2), 6.65 (d, 1H, *J* = 8.0 Hz), 6.73(d, 2H, *J* = 8.6 Hz), 6.88 (t, 1H, *J* = 7.5 Hz), 7.32 (t, 1H, *J* = 7.7 Hz), 7.43 (d, 2H, *J* = 8.6 Hz), 7.94 (d, 1H, *J* = 7.8 Hz).

2-(Benzo[*d*][1,3]dioxol-5-yl)-2,3-dihydroquinazolin-4(1*H*)-one (3h)

Colorless crystals, yield 92 %, m.p. 199-201 °C (lit.[29] 201 °C). ^{1}H-NMR ($CDCl_3$): δ = 4.33 (br. s, 1H, NH), 5.71 (br. s, 1H, NH), 5.82 (s, 1H, H-2), 6.02 (s, 2H, O-CH_2-O), 6.66 (d, 1H, *J* = 8.0 Hz), 6.83 (d, 1H, *J* = 7.9 Hz), 6.90 (t, 1H, *J* = 7.5 Hz), 6.99 (d, 1H, *J* = 7.9 Hz), 7.14 (s, 1H), 7.33 (t, 1H, *J* = 7.5Hz), 7.94 (d, 1H, *J* = 7.4 Hz).

2,3-Dihydro-2-(4-hydroxy-3-methoxyphenyl)quinazolin-4(1*H*)-one (3i)

Colorless crystals, yield 92 %, m.p. 219-220 °C (lit.[30] 220 °C). ^{1}H-NMR ($CDCl_3$): δ = 3.94 (s, 3H, OMe), 4.33 (br. s, 1H, NH), 5.68 (br. s, 1H, NH), 5.77 (s, 1H, H-2/OH), 5.83 (s, 1H, OH/H-2), 6.67 (d, 1H, *J* = 7.8 Hz), 6.88-7.01 (m, 3H), 7.21-7.30 (m, 1H), 7.34 (t, 1H, *J* = 7.8 Hz), 7.95 (d, 1H, *J* = 8.3 Hz).

2,3-Dihydro-2-(thiophen-2-yl)quinazolin-4(1*H*)-one (3j)

Colorless crystals, yield 96 %, m.p. 214-216 °C (lit.[31] 213-215 °C). ^{1}H-NMR ($CDCl_3$): δ = 4.56 (br. s, 1H, NH), 5.97 (br. s, 1H, NH), 6.20 (*s*, 1H, H-2), 6.70 (1H, *d*, *J* = 7.9 Hz), 6.92 (1H, *t*, *J* = 7.4 Hz), 7.02 (1H, *t*, *J* = 4.3 Hz), 7.22 (1H, *br. d*, *J* = 3.3 Hz), 7.35 (1H, *t*, *J* = 7.9 Hz), 7.40(d, 1H, *J* = 5.0 Hz), 7.95 (d, 1H, *J* = 7.7 Hz).

2,3-Dihydro-2-(pyridin-3-yl)quinazolin-4(1*H*)-one (3k)

Colorless crystals, yield 91 %, m.p. 217-218 °C [lit.[32] 219-221 °C]. ^{1}H-NMR ($CDCl_3$): δ = 4.39 (br. s, 1H, NH), 5.86 (br. s, 1H, NH), 5.99 (s, 1H, H-2), 6.70 (d, 1H, *J* = 8.1 Hz), 6.94 (t, 1H, *J* = 7.6 Hz), 7.34-7.44 (m, 2H), 7.96 (br. d, 1H, *J* = 7.8 Hz), 8.03 (br. d, 1H, *J* = 7.8 Hz), 8.71 (br. d, 1H, *J* = 3.5 Hz), 8.78 (br. s 1H).

Compound 3l

Colorless crystals, yield 93 %, m.p. 256-258 °C (lit.[29] 257-260 °C). ^{1}H-NMR ($CDCl_3$): δ = 1.81 (s, 4H, 2 × CH_2), 1.97 (s, 4H, 2 × CH_2), 4.25 (br. s, 1H, NH), 5.89 (br. s, 1H, NH), 6.66 (d, 1H, *J* = 7.9Hz), 6.86 (t, 1H, *J* = 7.6 Hz), 7.31(t, 1H, *J* = 8.0 Hz), 7.90 (d, 1H, *J* = 7.7 Hz).

 DOI: 10.17628/ecb.2016.5.185-188

Compound 3m

Colorless crystals, yield 95 %, m.p. 219-220 °C (lit.[33] 217-219 °C). ^{1}H-NMR ($CDCl_3$): δ = 1.24-1.82 (m, 10H, $5CH_2$), 4.35 (br. s, 1H, NH), 6.27 (s, 1H, NH), 6.64 (d, 1H, *J* = 8.0 Hz), 6.81 (t, 1H, *J* = 7.5 Hz), 7.28 (br. t, 1H, *J* = 7.5 Hz), 7.86 (br. d, 1H, *J* = 7.8 Hz).

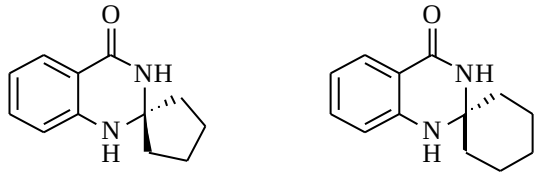

3l **3m**

Figure 1. Structures of compounds **3l** and **3m**.

Results and Discussion

The microwave-assisted reaction being reported involves subjecting of an intimate mixture of isatoic anhydride, ammonium acetate and aldehyde/ketone (1:2:1 mole ratio)

Table1. Optimization of synthesis of **3a** under MW conditions.

Time min	**3**	**5**	**1**	**2**	**3**	**4**	**5**
Temp. °C	45	45	60	60	60	60	60
Yield (%)	0	trace	64	81	92	90	85

directly to microwave irradiation. The time and temperature were first optimized using benzaldehyde (Table 1). The yields of different **3** under the optimized conditions (MW, 3 min, 60 °C) are given in the experimental section with the spectral properties of the individual compounds. The yields of the products were found to be excellent and the reactions were very clean. The crude products of the reactions were pure enough to give analytical samples simply by crystallization from ethanol. This solvent- and catalyst-free methodology is sufficiently mild to tolerate a variety of functionalities. All the synthesized 2,3-dihydroquinazolin-4(1*H*)-ones (**3a-m**) are known in the literature and were identified from their physical and spectral data.[11,12,27-33]

Table 2. Synthesis of **3a** under thermal conditions for 10 min.

Temp. °C	**70**	**80**	**90**	**100**	**110**	**120**	**130**
Unreacted **1** %	30	19	10	5	trace	0	0
Yield %	64	72	80	88	91	92	90

Since in the thermal process reported by Gao *et al.* [27] the reactions were not complete within 10 min at 70 °C, we tried to get an optimized condition using isatoic anhydride, ammonium acetate and benzaldehyde by gradually increasing the reaction temperature for completion of reaction within this time (Table 2). The yields of **3a-m** under the optimized conditions, *i.e.*, at 120 °C and 10 min reaction time, vary between 91 and 96 %.

Conclusions

We have developed a simple microwave-assisted synthesis of 2,3-dihydroquinazolin-4(1*H*)-ones (**3**) without the use of any added catalyst, solvent, surfactant or solid support. The method is very efficient and environmentally benign.

Acknowledgments

Financial assistance from the UGC-CAS and DST-PURSE programs, Department of Chemistry is gratefully acknowledged. The authors also acknowledge the DST-FIST program to the Department of Chemistry, Jadavpur University for providing the NMR spectral data. They are grateful to Professor B. C. Ranu, Department of Organic Chemistry, Indian Association for the Cultivation of Science, Kolkata for extending the facility of using a Scientific Microwave Oven for this study. AD and NS are thankful to the CSIR and UGC, New Delhi for their Research Fellowships.

Conflicts of interest

The authors declare that there is no conflict of interest regarding the publication of this manuscript.

References

[1]Alaimo, R. J., Russell, H. E. J. Med. Chem., **1972**, *15*, 335.

[2]Hour, M.-J., Huang,L.-J., Kuo, S.-C., Xia,Y., Bastow, K., Nakanishi, Y., Hamel, E., Lee, K.-H. J. Med. Chem., **2000**, *43*, 4479.

[3]Takaya,Y., Tasaka, H., Chiba, T., Uwai, K., Tanitsu, M. A., Kim, H. S., Wataya, Y., Miura, M., Takeshita, M., Oshima, Y. *J. Med. Chem.*, **1999**, *42*, 3163.

[4]Xia, Y., Yang, Z., Hour, M., Kuo, S., Xia, P., Bastow, K. F., Nakanishi, Y., Nampoothiri, P., Hackl, T., Hamel E., Lee, K. *Bioorg. Med. Chem. Lett*., **2001**, *11*, 1193.

[5]Jiang, J. B., Hesson, D. P., Dusak, B. A., Dexter, D. L., Kang, G. L., Hamel, E. *J. Med. Chem*., **1990**, *33*, 1721.

[6]El-Sabbagh, O. I., Ibrahim, S. M., Baraka M. M., Kothayer, H. *Arch. Pharm. Chem. Life Sci.*, **2010**, *343*, 274.

[7]Kurogi, Y., Inoue, Y., Tsutsumi, K., Nakamura, S., Nagao, K., Yoshitsugu H., Tsuda, Y. *J. Med. Chem*., **1996**, *39*, 1433.

[8]Hu, B.-Q., Wang, L.-X., Yang, L., Xiang J.-F., Tang, Y.-L. *Eur. J. Org. Chem.*, **2015**, *2015*, 4504.

[9]Hikawa, H., Ino, Y., Suzuki, H., Yokoyama, Y. *J. Org. Chem.*, **2012**, *77*, 7046.

[10]Li, F., Lu L., Ma, J. *Org. Chem. Front.*, **2015**, *2*, 1589.

[11]Safari, J., Gandomi-Ravandi, S. *J. Mol. Cat. A: Chem*., **2014**, *390*, 1.

[12]Labade, V. B., Shinde, P. V., Shingare, M. S. *Tetrahedron Lett*., **2013**, *54*, 5778.

[13]Desroses, M., Scobie M., Helleday, T. *New J. Chem*., **2013**, *37*, 3595.

[14]Wu, X.-F., Oschatz, S., Block, A., Spannenberg, A., Langer, P. *Org. Biomol. Chem*., **2014**, *12*, 1865.

[15]Rahman, M., Ling, I., Abdullah, N., Hashim, R., Hajra, A. *RSC Adv*., **2015**, *5*, 7755.

[16]Mohammadi, A. A., Dabiri, M., Qaraat, H. *Tetrahedron*, **2009**, *65*, 3804.

[17]Niknam, K., Jafarpour, N., Niknam, E. *Chin. Chem. Lett*., **2011**, 22, 69.

[18]Saffar-Teluri, A., Bolouk, S. *Monatsh. Chem.*, **2010**, *141*, 1113.

[19]Salehi, P., Dabiri, M., Baghbanzadeh, M., Bahramnejad, M. *Synth. Commun*., **2006**, *36*, 2287.

[20]Das Gupta, A., Samanta, S., Mondal, R., Mallik, A. K. *Bull. Korean Chem. Soc*., **2012**, 33, 4239.

[21]Galleti, P., Pori, M., Giacomini, D. *Eur. J. Org. Chem*., **2011**, *2011*, 3896.

[22]Panda, S. S., Ibrahim, M. A., Oliferenko, A. A.. Asiri, A. M., Katritzky, A. R. *Green Chem.*, **2013**, *15*, 2709.

[23]Das Gupta, A., Samanta, S., Mondal, R., Mallik, A. K. *Chem. Sci. Trans.*, **2013**, *2*, 524.

[24]Gutierrez, R. U., Correa, H. C., Bautista, R., Vargas, J. L., Jerezano, A.V., Delgado, F., Tamariz, J. *J. Org. Chem.*, **2013**, *78*, 9614.

[25]Chandna, N., Chandak, N., Kumar, P., Kapoor, J. K., Sharma, P. K. *Green Chem*., **2013**, *15*, 2294.

[26]Das Gupta, A., Samanta, S., Mallik, A. K. *Org. Prep. Proced. Int*., **2015**, *47*, 356.

[27]Gao, L., Ji, H., Rong, L., Tang, D., Zha, Y., Shi, Y., Tu, S. *J. Heterocyclic Chem.*, **2011**, *48*, 957.

[28]Yassaghi, G., Davoodnia, A., Allameh, S., Zare-Bidaki, A., Tavakoli-Hoseini, N. *Bull. Korean Chem. Soc*., **2012**, *33*, 2724.

[29]Bharate, S. B., Mupparapu, N., Manda, S., Bharate, J. B., Mudududdla, R., Yadav, R. R., Vishwakarma, R. A. *Arkivoc*, **2012**, *2012*, 308.

[30]Ningdale, V. B., Chaudhary, U. N., Shaikh, K. A. *Arch. Appl. Sci. Res*., **2013**, *5*, 82.

[31]Qiao, R. Z., Xu, B. L., Wang, Y. H. *Chin. Chem. Lett*., **2007**, *18*, 656.

[32]Parish, J. H. A., Gilliom, R. D., Purcell, P. W., Browne, R. K., Spirk, R. F., White, H. D. *J. Med. Chem.*, **1982**, *25*, 98.

[33]Shaabani, A., Maleki, A., Mofakham, H. *Synth. Commun*., **2008**, *38*, 37

Received: 16.06.2016.
Accepted: 08.07.2016.

KINETICS AND MECHANISM OF OXIDATION OF SOME THIOACIDS BY MORPHOLINIUM FLUOROCHROMATE

Ammilal Rao, Trupti Purohit, Preeti Swami, Priyanka Purohit and Pradeep K. Sharma*

Keywords: Halochromates, kinetics, mechanism, oxidation, thioacids, morpholinium fluorochromate.

Oxidation of thioglycolic, thiolactic and thiomalic acids by morpholinium fluorochromate (MFC) in dimethylsulphoxide (DMSO) leads to the formation of disulphide dimers. The reaction is first order in MFC. Michaelis-Menten type of kinetics is observed with respect to the thioacids. Reaction failed to induce the polymerisation of acrylonitrile. The reaction is catalysed by hydrogen ions. The hydrogen ion dependence has the form $k_{obs} = a + b [H^+]$. The oxidation of thiolactic acid has been studied in nineteen different organic solvents. The solvent effect has been analysed by using Kamlet's and Swain's multiparametric equations. A mechanism involving the formation of a thioester and its decomposition in slow step has been proposed.

* Corresponding Authors
E-Mail: drpkvs27@yahoo.com
[a] Department of Chemistry, J.N.V. University, Jodhpur, 342011, India

Introduction

Salts of Cr(VI) have long been used as oxidizing reagents in synthetic organic chemistry. However, these salts are drastic and non-selective oxidants in nature. Further, they are insoluble in most of the organic solvents also. Thus miscibility is a problem. To overcome these limitations, a large number of organic derivatives of Cr(VI) have been prepared and used in synthetic organic syntheses as mild and selective oxidants in non-aqueous solvents.[1] One such compound is morpholinium fluorochromate (MFC).[2] Only a few reports are available in literature regarding oxidation aspects of MFC.[3-4] It is known that the mode of oxidation by Cr(VI) derivatives depends on the nature of the counter-ion attached to the chromium anion. Therefore, in continuation of our earlier work, in the present article, we report the kinetics of the oxidation thioglycolic (TGA), thiolactic (TLA) and thiomalic (TMA) acids by morpholinium fluorochromate in DMSO as solvent. Mechanistic aspects are also discussed.

Experimental

Materials

The thioacids (Fluka) and dithiodiglycolic acid (Evan Chemicals, USA) were commercial products and were used as such. Dithiodimalic and dithiodilactic acids were prepared by the oxidation of the corresponding thiols by ferric alum.[5] The method results in products with nearly 99% purity. The solutions of the thioacids were freshly prepared in DMSO and were standardized by titrating them against a standard solution of iodine.[5,6] MFC was prepared by the reported method[2] and its purity was checked by an iodometric method. The solvents were purified by usual methods.[7] p-Toluenesulphonic acid (TsOH) was used as a source of hydrogen ions.

Stoichiometry

Stoichiometric determinations, as well as the characterization of the products, carried out polarigraphically[8,9] using an automatic (Heyrovsky TP 55A) polarograph. It was found that the cathode wave given by a known sample of disulphide dimer coincided by the wave given by the final product of the oxidation. The reaction exhibited a 1:2 stoichiometry, i.e. 2 moles of the thiol are oxidized per mole of MFC reduced. Further, the reaction mixtures with an excess of MFC were allowed to go to completion and the residual MFC was determined iodometrically. These results also gave a 1:2 stoichiometry (eqn.1). The oxidation state of chromium in completely reduced reaction mixtures, determined by an iodometric method, is 3.95±0.10.

$$2\ RSH + O_2CrFOMH \longrightarrow RS\text{-}SR + H_2O + OCrFOMH \quad (1)$$

MFC undergoes two-electron change. This is in accordance with the earlier observations with structurally similar other halochromates also. It has already been shown that both pyridinium chlorochromate (PCC)[10] and pyridinium fluorochromate (PFC)[11] act as two-electron oxidants and are reduced to chromium (IV) species by determining the oxidation state of chromium by magnetic susceptibility, ESR and IR studies.

Kinetic Measurements

The reactions were carried out under pseudo-first-order conditions by keeping a large excess (× 15 or greater) of the thioacids over MFC. The solvent was DMSO, unless specified otherwise. The reactions were carried out in flasks blackened from the outside to prevent any photochemical reactions and were followed up to ca. 80% conversion by monitoring the decrease in the [MFC] at 352 nm on a spectrophotometer (AIMIL, India, Model MK-II). The MFC showed a λ_{max} of 352 nm. Further, no other species had any noticeable absorbance at this wavelength. The pseudo-first-order rate constants, k_{obs}, were evaluated from the linear least-squares plots of log [MFC] against

time. Duplicate kinetic runs showed that the rate constants are reproducible to within ±3 %. All reactions, other than those to study the effect of [H^+], were performed in the absence of TsOH.

Results and Discussion

Rate-laws

The reactions are of first order with respect to MFC Figure 1 depicts a typical kinetic run. Further, the pseudo-first order rate constant, k_{obs} is independent of the initial concentration of MFC. The reaction rate increases with increase in the concentration of the thioacid but not linearly (Table 1). A plot of $1/k_{obs}$ against 1/[Thioacid] is linear (r > 0.995) with an intercept on the rate-ordinate. Thus, Michaelis-Menten type kinetics are observed with respect to the thioacid. This leads to the postulation of following overall mechanism (2) and (3) and rate law (4).

$$\text{Thioacid} + \text{MFC} \overset{K}{\leftrightarrows} [\text{complex}] \quad (2)$$

$$[\text{Complex}] \xrightarrow{k_2} \text{Products} \quad (3)$$

$$\text{Rate} = k_2 K [\text{TA}] [\text{MFC}] / (1 + K [\text{TA}]) \quad (4)$$

The dependence of reaction rate on the reductant concentration was studied at different temperatures and the values of K and k_2 were evaluated from the double reciprocal plots. The thermodynamic parameters of the complex formation and activation parameters of the decomposition of the complexes were calculated from the values of K and k_2 respectively at different temperatures (Tables 2 and 3).

Table 1. Rate constants for the oxidation of thioacids by MFC at 298 K.

10^3 MFC mol dm^{-3}	[Thioacid] mol dm^{-3}	10^4 k_{obs} s^{-1}		
		TGA	TLA	TMA
1.0	0.10	4.28	21.0	10.0
1.0	0.20	6.68	32.0	15.5
1.0	0.40	9.30	43.5	21.3
1.0	0.60	10.7	49.3	24.4
1.0	0.80	11.6	52.9	26.3
1.0	1.00	12.2	55.3	27.5
1.0	1.50	13.0	58.8	29.5
1.0	3.00	14.1	62.9	31.7
2.0	0.40	9.36	45.9	21.6
4.0	0.40	9.03	44.1	20.7
6.0	0.40	9.18	45.0	22.5
8.0	0.40	9.27	44.7	21.0
1.0	0.20	6.75	33.3	16.2

Test for free radicals

The oxidation of thioacids by MFC, in an atmosphere of nitrogen, failed to induce the polymerization of acrylonitrile. Further, the addition of acrylonitrile had no effect on the rate (Table 1). Thus a one electron oxidation, giving rise to free radicals, is unlikely.

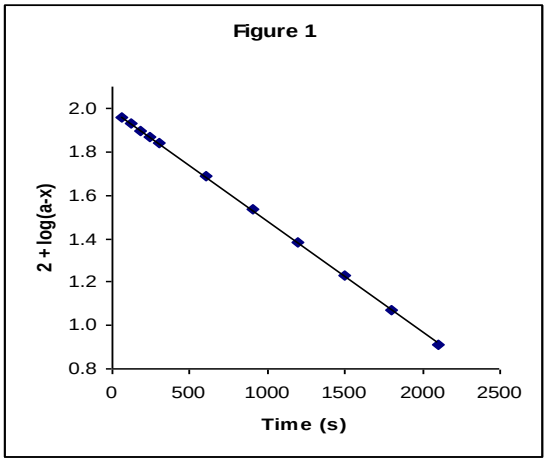

Figure 1. A typical kinetic run.

Effect of acidity

The reaction is catalysed by hydrogen ions (Table 4). The hydrogen- ion dependence has the following form $k_{obs} = a + b [H^+]$. The values of a and b, for TLA, are 20.7±0.13 × 10^{-4} s^{-1} and 37.6±0.21 ×10^{-4} mol^{-1} dm^3 s^{-1} respectively (r^2 = 0.9870). The observed hydrogen-ion dependence suggests that the reaction follows two mechanistic pathways, one is acid-independent and the other is acid-dependent. The acid-catalysis may well be attributed to a protonation of MFC to yield a protonated Cr(VI) species which is a stronger oxidant and electrophile (5).

$$O_2CrFOMH + H^+ \leftrightarrows (HOCrOFOMH)^+ \quad (5)$$

Formation of a protonated Cr(VI) species has earlier been postulated in the reactions of structurally similar halochromates.

Effect of solvents

The oxidation of thiolactic acid was studied in 19 different organic solvents. The choice of solvents was limited due to the solubility of MFC and its reaction with primary and secondary alcohols. There was no reaction with the solvents chosen. The dependence of rate on [Thioacid] and [MFC] were studied in all the solvents. The kinetics were similar in all the solvents. The formation constant of the intermediate complex, K, did not vary much (5.27±0.46) with the solvent but the rate constant, k_2, exhibited much variation in values with different solvents (Table 5).

 DOI: 10.17628/ecb.2016.5.189-192

Table 2. Rate constants for the decomposition of MFC–Thioacids complexes and their activation parameters.

Thioacid	$10^3 k_2$ (dm^{-3} mol^{-1} s^{-1})				$\Delta H^{\#}$	$-\Delta S^{\#}$	$\Delta G^{\#}$
	288 K	298 K	308 K	318 K	kJ mol^{-1}	J mol^{-1}K^{-1}	kJ mol^{-1}
TGA	8.10	15.3	28.8	52.2	44.8±0.3	180± 1	83.3± 0.3
TLA	39.6	67.5	117	189	37.4±0.3	142± 1	79.7± 0.3
TMA	18.9	34.2	60.3	99.0	39.6±0.2	141± 1	81.4± 0.2

Table 3. Formation constants for the decomposition of MFC–thioacids complexes and their thermodynamic parameters.

Thioacid	K dm^3 mol^{-1}				ΔH	$-\Delta S$	ΔG
	288 K	298 K	308 K	318 K	kJ mol-1	J mol-1K-1	kJ mol-1
TGA	4.68	3.88	3.07	2.82	20.2±0.9	49±3	5.78±0.8
TLA	5.31	4.52	3.70	2.88	17.9±0.9	40±3	6.17±0.7
TMA	4.95	4.15	3.33	2.56	19.2±0.9	45±3	5.95±0.7

Table 4. Effect of hydrogen ion concentration on the oxidation of thioacids by MFC

[H$^+$] mol dm^{-3}	0.10	0.20	0.40	0.60	0.80	1.00
TGA	4.95	6.21	7.11	8.28	10.8	11.7
TLA	24.3	28.8	36.9	40.5	52.2	58.5
TMA	11.7	13.5	17.1	19.8	25.2	27.9

[MFC] = 0.001 mol dm^{-3}, [Thioacids] = 1.0 mol dm^{-3}, Temp. = 298 K

The rate constants of the oxidation, k_2, in eighteen solvents (CS_2 was not considered, as the complete range of solvent parameters was not available) were correlated in terms of the linear solvation energy relationship (LESR) of Kamlet and Taft[12] (6).

$$\log k_2 = A_0 + p\pi^* + b\beta + a\alpha \quad (6)$$

Table 5. Effect of solvents on the oxidation of TLA by MFC at 298 K.

Solvents	$10^3 k_{obs}$ s^{-1}	Solvents	$10^3 k_{obs}$ s^{-1}
$CHCl_3$	20.9	Toluene	9.77
$ClCH_2CH_2Cl$	27.5	PhCOMe	36.3
CH_2Cl_2	24.0	THF	14.8
DMSO	67.5	t-BuOH	10.2
Acetone	22.4	1,4-Dioxane	16.2
DMF	41.7	$MeOCH_2CH_2OME$	9.12
Butanone	18.2	CS_2	5.25
Nitrobenzene	33.9	Acetic Acid	4.79
Benzene	12.0	Ethyl Acetate	12.6
Cyclohexane	1.51		

In this equation, π^* represents the solvent polarity, β the hydrogen bond acceptor basicities and α is the hydrogen bond donor acidity. A_0 is the intercept term. It may be mentioned here that out of the 18 solvents, 12 have a value of zero for α. The results of correlation analyses in terms of equation (6), a biparametric equation involving π^* and β, and separately with π^* and β are given below as equations (7) - (10).

$$\log k_2 = -3.71 + 1.34\ (\pm 0.15)\ \pi^* + 0.18\ (\pm 0.13)\ \beta + 0.23\ (\pm 0.12)\ \alpha \quad (7)$$

$R^2 = 0.8850$, $sd = 0.14$, $n = 18$, $\psi = 0.37$

$$\log k_2 = -3.76 + 1.43\ (\pm 0.16)\ \pi^* + 0.10\ (\pm 0.13)\ \beta \quad (8)$$

$R^2 = 0.8560$, $sd = 0.15$, $n = 18$, $\psi = 0.40$

$$\log k_2 = -3.74 + 1.45\ (\pm 0.15)\ \pi^* \quad (9)$$

$r^2 = 0.8502$, $sd = 0.26$, $n = 18$, $\psi = 0.40$

$$\log k_2 = -2.93 + 0.36\ (\pm 0.31)\ \beta \quad (10)$$

$r^2 = 0.0761$, sd = 0.37, $n = 18$, $\psi = 0.99$

Here n is the number of data points and ψ is the Exner's statistical parameter[13].

Kamlet's[12] triparametric equation explains *ca.* 89% of the effect of solvent on the oxidation. However, by Exner's criterion[13] the correlation is not even satisfactory (*cf.* Eqn. 7). The major contribution is of solvent polarity. It alone accounted for *ca.* 85 % of the data. Both β and α play relatively minor roles.

The data on the solvent effect were analysed in terms of Swain's[14] equation (10) of cation- and anion-solvating concept of the solvents also.

$$\log k_2 = aA + bB + C \quad (11)$$

Here A represents the anion-solvating power of the solvent and B the cation-solvating power. C is the intercept term. ($A + B$) is postulated to represent the solvent polarity. The rates in different solvents were analysed in terms of equation (11), separately with A and B and with ($A + B$).

$$\log k_2 = 0.37 + (\pm 0.04)\ A + 1.47\ (\pm 0.03)\ B - 3.88 \quad (12)$$

$R^2 = 0.9939$, $sd = 0.03$, $n = 19$, $\psi = 0.08$

 DOI: 10.17628/ecb.2016.5.189-192

$$\log k_2 = 0.16\ (\pm 0.48)\ A - 3.87 \quad (13)$$

$r^2 = 0.0068$, $sd = 0.39$, $n = 19$, $\psi = 1.02$

$$\log k_2 = 1.44\ (\pm 0.07)\ B - 3.76 \quad (14)$$

$r^2 = 0.9595$, $sd = 0.08$, $n = 19$, $\psi = 0.24$

$$\log k_2 = 1.11 \pm 0.14\ (A + B) - 3.84 \quad (15)$$

$r^2 = 0.7813$, $sd = 0.18$, $n = 19$, $\psi = 0.48$

The rates of oxidation of TLA in different solvents showed an excellent correlation in Swain's equation (cf. Eqn. 12) with the cation-solvating power playing the major role. In fact, the cation-solvation alone account for *ca.* 96% of the data. The correlation with the anion-solvating power was very poor. The solvent polarity, represented by ($A + B$), also accounted for *ca.* 78% of the data. In view of the fact that solvent polarity is able to account for *ca.* 78% of the data, an attempt was made to correlate the rate with the relative permittivity of the solvent. However, a plot of log k_2 against the inverse of the relative permittivity is not linear ($r^2 = 0.5151$, $sd = 0.27$, $\psi = 0.71$).

Mechanism

The lack of any effect of radical scavenger, such as acrylonitrile on the reaction rate and the failure to induce the polymerisation of acrylonitrile, point against the operation of a one-electron oxidation giving-rise to free radicals. The observed solvent effect supports a transition state, which is more polar than the reactant state. The observed Michaelis-Menten type of kinetics with respect to thioacids also leads us to suggest the formation of thioester as an intermediate. It is therefore, proposed that the reaction involves the formation of an ester intermediate and its subsequent decomposition in the slow step (Scheme 1).

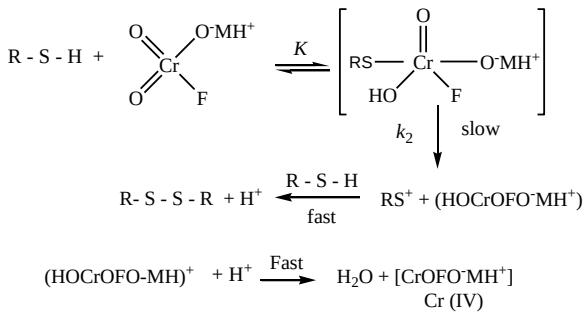

Scheme 1. Mechanism of oxidation of thioacids by MFC.

The formation of a sulphenium cation, in the rate-determining step, is also supported by the observed major role of cation-solvating power of the solvents.

It is of interest to compare here the reaction patterns of the oxidation of thioacids by other halochromates (QFC,[15] QBC[16] and MCC[17]) and MFC.

QFC and MFC represented a Michaelis-Menten type of kinetics with respect to thioacid, whereas the oxidation by QBC and MCC exhibited a second order kinetics, first with respect to each reactant. This may be due to a very low value of the formation constant of the thioester. The solvent effect and [H^+] ion dependence are parallel in all the reactions.

Acknowledgements

Thanks are due to University Grants Commission, New Delhi for financial support in the form of JRF to TP, BSR-Start-up to PP, one time grant to PKS and to Professor Kalyan K. Banerji for constructive help and critical suggestions.

References

[1]Corey, E. J., Suggs, W. J. *Tetrahedron Lett.*, **1975**, 2647; Guziec, F. S., Luzio, F. A. *Synthesis*, **1980,** 691; Bhattacharjee, M. N., Choudhuri , M. K., Dasgupta, H. S., Roy, N., Khathing, D. T., *Synthesis*, **1982**, 588; Balasubramanian, K., Prathiba, V., *Indian J. Chem.*, **1986**, *25B*, 326; Pandurangan, A., Murugesan, V., Palamichamy, P., *J. Indian Chem. Soc.*, **1995**, *72*, 479.

[2]Alangi, S. Z. S., Ghotbabadi, H. S., Baei, M. T., Naderi, S., *Hindawi E-J. Chem.*, **2011**, 8(2), 816.

[3]Vyas, N., Choudhary, A. Sharma, V. *Int. J. Chem.*, **2015**, *4(3)***,** 215.

[4]Alhaji, N. M., Mamani, I., Kayalvizhi, R., ***Chem Sci Trans.***, **2016**, *5(1)*, 258.

[5]Leussing, D .L.and Kolthoff, I. M., *J. Electrochem. Soc.*, **1953**, *100*, 334.

[6] Krammer H. *J. Assoc. Agric. Chem.*, **1952**, *35*, 385.

[7]Perrin, D. D., Armarego, W. L. and Perrin, D. R., *Purification of organic Compounds*, Pergamon Press, Oxford, **1966**.

[8]Kapoor, R .C., Kachhwaha O. P., Sinha, B. P., *J. Phys. Chem.*, **1969**, *73*, 1627.

[9]Kapoor R. C., Kachhwaha, O. P., Sinha, B. P., *Indian J. Chem.*, **1971**, *10*, 499.

[10]Brown, H. C., Rao, G. C., Kulkarni, S. U., *J. Org. Chem.*, **1979**, *44*, 2809.

[11]Bhattacharjee, M. N., Choudhuri, M. K., Purakayastha S. *Tetrahedron*, **1987**, *43*, 5389.

[12]Kamlet, M. J., Abboud, J. L. M., Abraham, M. H., Taft, R. W., *J. Org. Chem.***, 1983**, *48*, 2877.

[13]Exner, O., *Collect. Chem. Czech. Commun.*, **1966**, *31*, 3222.

[14]Swain, C. G., Swain, M. S., Powel, A. L., Alunni, S. *J. Am. Chem. Soc.*, **1983**, *105*, 502.

[15]Khurana, M., Sharma, P. K., Banerji, K. K., *Indian J. Chem.*, **1998**, *37A*, 1011.

[16]Vyas S., Sharma P. K., *Int. J. Chem. Sci.*, **2004**, *2(1)*, 13.

[17]Malani, N., Pohani, S., Baghmar, M., Sharma, P.K., *Indian J. Chem.*, **2008**, *47A*, 1373.

Received: 18.06.2016.
Accepted: 09.07.2016.

SYNTHESIS, SPECTROSCOPIC STUDIES AND BIOLOGICAL PERSPECTIVES OF TRANSITION METAL COMPLEXES OF N/S DONOR SCHIFF BASE

Kiran Singh[a]* and Ritu Thakur[a]

Keywords: Chelate complex,^{1}H-NMR spectra, antimicrobial activity, metal complexes, Schiff base.

Bidentate Schiff base, 4-[(p-dimethylaminobenzylidene)amino]-3-mercapto-6-methyl-1,2,4-triazin-5-one, and its Co(II), Ni(II), Cu(II) and Zn(II) complexes have been prepared and characterized with the aid of various physicochemical techniques like IR, NMR, ESR, elemental, electronic and thermal analysis. The conductance data suggested the non-electrolytic behaviour of the metal complexes. Fluorescence emission study demonstrated that the metal complexes possess more fluorescent intensity as compared to the Schiff base. Stability of the metal complexes has been checked by using Horowitz-Metzger method. The redox property of Cu(II) complexes has been investigated by using cyclic voltammetry. All the newly synthesized compounds have been screened for their *in vitro* antimicrobial activity against six microbial strains and it has been found that some of the tested compounds show good antimicrobial activity as compared to standard drug.

* Corresponding Authors
E-Mail: kiransinghkuk@yahoo.co.in
[a] Department of Chemistry, Kurukshetra University, Kurukshetra 136119, India

Introduction

As Schiff bases have easy preparation, structural variety and varied denticities, they act as most potential group of chelators and have engrossed much attention for many years. In the field of inorganic chemistry, research is further spurred by the formation of chelate complexes of 3d transition metals with Schiff bases containing hard N atom and soft S donor atom.[1] Especially the 2p electrons of N atom of azomethine group and 3p electrons of S atom of thiol group take part in chelation with metal ions. Schiff base bind with metal ion through different types of binding modes.[2-4] Coordination of Schiff base with metal ions remarkably modulates the biological activity of metal complexes such as anticonvulsant,[5] antibacterial,[6] antifungal,[7] anti-HIV[8] and anticancer.[9,10] However, the biological properties of Schiff base depend on the ways in which it combines with metal ion. In many biological processes, metal ions accelerate the activity and efficacy of organic compound. Most of the N containing Schiff base ligand when combine with metal ion show carcinostatic and anti-HIV activities.[11-13] This broad pharmacological usage of Schiff base metal complexes encouraged us to put an effort towards the development of new Schiff base and its complexes with Co(II), Ni(II), Cu(II) and Zn(II) metal ion and further study their biological applications. In the preceding communications[14,15] structural elucidation and biological studies of metal complexes (3d metal ions with substituted 1,2,4-triazine Schiff bases) have been reported. Motivated by above findings, present article concentrate on the synthesis, characterization and antimicrobial studies of Co(II), Ni(II), Cu(II) and Zn(II) complexes derived from Schiff base 4-[(p-dimethylaminobenzylidene)-amino]-3-mercapto-6-methyl-1,2,4-triazin-5-one. Parent ligand and its metal complexes were examined for antimicrobial activity and the comparative account of antimicrobial activity has been discussed.

Experimental

All the chemicals and solvents used in present work were of analytical grade and purchased from Spectro Chem Ltd. IR spectral data of Schiff base and its metal complexes have been recorded in KBr pellets/Nujol mulls on a MB-3000 ABB spectrometer. ^{1}H-NMR of Schiff base and its Zn(II) complexes were examined on a Bruker ACF 300 spectrometer at 300 MHz in $CDCl_3$/DMSO-d_6 using TMS as an internal reference. Thermogravimetric (TG) analysis of the metal complexes were carried out on a Perkin Elmer (Pyris Diamond) instrument at a heating rate of 10 $^{\circ}$C min^{-1} by using alumina powder as reference compound. ESR spectra of the Cu(II) complexes were recorded under the magnetic field of 3000 Gauss at frequency 9.1 GHz by using Varian E-112 ESR spectrometer at SAIF, IIT, Bombay. Magnetic moment measurements were carried out on Vibrating Sample Magnetometer at Institute Instrumentation Centre, IIT, Roorkee. Electronic spectra of the metal complexes were recorded on T 90 (PG Instruments Ltd.) UV/VIS spectrometer in the region of 1100-200 nm by using DMF as solvent. Photoluminescence spectra of the Schiff base and its metal complexes were recorded on SHIMADZU RF-5301 PC spectrophotometer instrument. Electrochemical measurements of Cu(II) complexes were recorded on Ivium Stat Electrochemical Analyzer.

4-Amino-3-mercapto-6-methyl-1,2,4-triazin-5-one (AMMOT) was synthesized according to literature procedure.[16]

To prepare 4-[(p-dimethylaminobenzylidene)-amino]-3-mercapto-6-methyl-1,2,4-triazin-5-one (HL), an ethanolic solution of p-dimethylaminobenzaldehyde (1.034 g, 6.94 mmol) was mixed in ethanolic solution of AMMOT (1 g, 6.94 mmol) and the reaction mixture was refluxed for 8 h. The precipitated product was filtered, washed with ethanol, recrystallized from ethanol and dried under vacuum (Scheme 1), m.p. 232-234 °C. Anal. Calcd. for $C_{13}H_{15}N_5OS$: C, 53.96; H, 5.23; N, 24.20. Found C, 53.85; H, 5.16; N, 24.08.

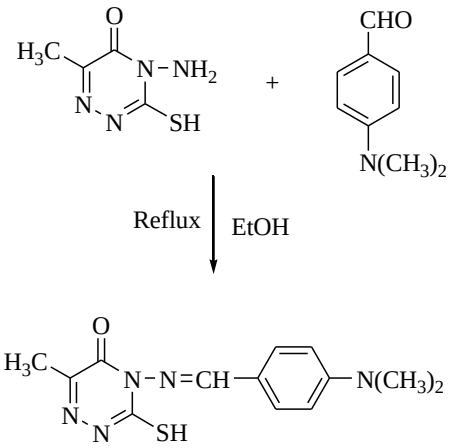

Scheme 1. Synthesis of the Schiff base.

Synthesis of 1:1 metal:ligand complexes

An hot ethanolic solution of Schiff base (0.20 g, 0.69 mmol) was mixed with hot ethanolic solution of acetates of Co(II) (0.172 g, 0.69 mmol), Ni(II) (0.172 g, 0.69 mmol), Cu(II) (0.138 g, 0.69 mmol) or Zn(II) (0.152 g, 0.69 mmol). The solid product formed was filtered, washed successively with warm water, aqueous ethanol, and acetone and then dried.

Co(L)OAc.3H_2O: Anal. Calcd. for $C_{15}H_{23}CoN_5O_5S$: C, 40.54; H, 5.22; N, 15.76; Co, 13.26. Found: C, 40.44; H, 5.18; N, 15.70; Co, 13.19.

Ni(L)OAc.3H_2O: Anal. Calcd. for $C_{15}H_{23}N_5NiO_5S$: C, 40.56; H, 5.22; N, 15.77; Ni, 13.22. Found: C, 40.50; H, 5.15; N, 15.70; Ni, 13.12.

Cu(L)OAc.H_2O: Anal. Calcd. for $C_{15}H_{19}CuN_5O_4S$. C, 42.00; H, 4.46; N, 16.33; Cu, 14.81. Found: C, 41.91; H, 4.37; N, 16.24; Cu, 14.79.

Zn(L)OAc.3H_2O: Anal. Calcd. for $C_{15}H_{23}N_5O_5SZn$: C, 39.96; H, 5.14; N, 15.53; Zn, 14.50. Found: C, 39.90; H, 5.10; N, 15.39; Zn, 14.44.

Synthesis of 1:2 metal:ligand complexes

Hot ethanolic solution of ligand (0.40 g, 1.38 mmol) was mixed with a hot ethanolic solution of acetates of Co(II) (0.172 g, 0.69 mmol), Ni(II) (0.172 g, 0.69 mmol), Cu(II) (0.138 g, 0.69 mmol) and Zn(II) (0.152 g, 0.69 mmol). The product formed immediately was filtered off, washed successively with warm water, aqueous ethanol, and acetone and then dried in desiccator.

$Co(L)_2.2H_2O$: Anal. Calcd. for $C_{26}H_{32}CoN_{10}O_4S_2$: C, 46.49; H, 4.80; N, 20.85; Co, 8.77. Found: C, 46.40; H, 4.75; N, 20.70; Co, 8.71.

$Ni(L)_2.2H_2O$: Anal. Calcd. for $C_{26}H_{32}N_{10}NiO_4S_2$: C, 46.51; H, 4.80; N, 20.86; Ni, 8.74. Found: C, 46.46; H, 4.77; N, 20.73; Ni, 8.69.

$Cu(L)_2$: Anal. Calcd. for $C_{26}H_{28}CuN_{10}O_2S_2$: C, 48.78; H, 4.41; N, 21.88; Cu, 9.93. Found: C, 48.70; H, 4.34; N, 21.78; Cu, 9.87.

$Zn(L)_2.2H_2O$: Anal. Calcd. for $C_{26}H_{32}N_{10}O_4S_2Zn$. C, 46.05; H, 4.76; N, 20.66; Zn, 9.64. Found: C, 45.92; H, 4.70; N, 20.61; Zn, 9.57.

Antimicrobial assay

The Schiff base and its metal complexes were individually tested against a penal of microorganisms viz., *Staphylococcus aureus* MTCC 96, *Bacillus subtilis* MTCC 121, *Pseudomonas aeruginosa* MTCC 741 and *Escherichia coli* MTCC 1652 (bacterial strains) and *Candida albicans* MTCC 227 and *Saccharomyces cerevisiae* MTCC 170 (fungal strain). All the bacterial cultures were procured from Microbial Type Culture Collection (MTCC), IMTECH, Chandigarh.

For *In vitro* antimicrobial activity, the Schiff base and its metal complexes were assayed through Agar well diffusion method.[17] All the microbial culture were adjusted to 0.5 McFarland standard, which is visually comparable to a microbial suspension of approximately $1.5x10^8$ cfu mL^{-1}. 20 mL of Muller Hinton agar medium was poured into each Petri plate and the plates were swabbed with 100 µL inocula of the test microorganisms and kept for 15 min for adsorption. Using sterile cork borer of 8 mm diameter, wells were bored into the seeded agar plates and these were loaded with 100 µL volume with concentration 4.0 mg mL-1 of each compound reconstituted in DMSO. All the plates were incubated at 37 °C for 24 h. Antimicrobial activity of each compound was evaluated by measuring the zone of growth inhibition against the test organisms with zone reader (HiAntibiotic zone scale). DMSO was used as a negative control whereas Ciprofloxacin was used as positive control. This each treatment was repeated thrice for each organism.

Minimum inhibitory concentration (MIC)

MIC is the lowest concentration of an antimicrobial compound that will inhibit the visible growth of a microorganism after overnight incubation. MIC of the Schiff base and its metal complexes was tested against bacterial strains through a modified agar well-diffusion method.[17]

Results and discussion

All the newly synthesized compounds are coloured, stable in air, non-hygroscopic in nature, soluble in DMF and DMSO. All the metal complexes were non-electrolytic in nature which indicated their stability toward dissociation in DMF solution.

Table 1. IR Frequencies of Schiff base and the metal complexes.

Compound	υ (N=CH)	υ (C-S)	υ (S-H)	υ ($OCOCH_3$)	υ (H_2O/OH)	υ (M-S)	υ (M-N)
HL	1589	-	2854	-	-	-	-
Co(L)(OAc).3H_2O	1574	818	-	1740	3425	328	450
Co$(L)_2$.2H_2O	1582	818	-	-	3550	305	480
Ni(L)(OAc).3H_2O	1574	818	-	1744	3433	333	492
Ni$(L)_2$.2H_2O	1582	756	-	-	3433	360	460
Cu(L)(OAc).H_2O	1582	810	-	1744	3487	352	530
Cu$(L)_2$	1582	810	-	-	-	347	508
Zn(L)(OAc).3H_2O	1574	810	-	1744	3580	343	522
Zn$(L)_2$.2H_2O	1582	810	-	-	3495	370	474

IR spectra

The comparative IR frequencies of HL and all the metal complexes have been recorded in the region 4000-700 cm^{-1} and the important bands are listed in table 1. IR frequencies reveal the binding mode of HL with metal ions. In HL, a characteristic band observed at 1589 cm^{-1} due to υ (-CH=N-) stretching vibration which underwent to lower frequency (1574-1582 cm^{-1}) in the spectra of metal complexes, corroborating the coordination through azomethine nitrogen atom.[18,19] It is further supported by a new band (in far IR) which appeared in the region 450- 530 cm^{-1} ascribed to υ (M-N) stretch. Another characteristic band appeared at 2854 cm^{-1} due to υ (-SH) stretching vibration in the ligand, which is not observed in the spectra of the metal complexes shows the deprotonation of thiol group and complexation through S atom of thiol group. The deprotonation was further supported by a new stretching vibration (in far IR) observed in the region of 305-370 cm^{-1} due to υ (M-S).

In metal complexes, stretching vibration appeared in the region 3425-3580 cm^{-1} which can be assigned to υ (-OH) stretch. A characteristic band was observed at 1697 cm^{-1} in Schiff base as well as in the metal complexes due to υ (C=O) stretch which concluded the non-participation of keto group in chelation. IR spectra of 1:1 metal complexes exhibited a band in the region 1740-1744 cm^{-1} due to υ (-$OCOCH_3$) stretch. Furthermore, the absorption band ~1612 cm^{-1} and ~1435 cm^{-1} corresponding to the asymmetric and symmetric stretch of acetate group being an indication of monodentate coordination of acetate ion.[20,21]

^{1}H-NMR spectra

The chemical shift value of different types of protons of Schiff base and its Zn(II) complexes have been recorded in DMSO-d_6 solvent using TMS as internal standard. Schiff base displays two characteristics peaks at δ = 8.20 and 10.21 ppm due to imine proton (-CH=N-) and proton of thiol group (-SH) respectively. In Zn(II) complexes, the signal due to imine proton is deshielded and observed at δ 8.87 ppm which indicates the linkage through imine N atom. Signal due to thiol proton of Schiff base is absent in the complexes indicating the deprotonation and subsequent participation in complexation.[22,23] In addition, the spectrum of 1:1 Zn(II) complex shows singlet at δ + 2.40 ppm due to 3H of –$OCOCH_3$ group.

Electronic absorption spectra and magnetic moment measurements

The electronic absorption spectra of 10^{-3} M solutions of 1:1 and 1:2 metal complexes have been recorded in DMF at room temperature. The electronic absorption spectra of 1:1 and 1:2 Co(II) complexes exhibit two bands in the region 10500-11476 cm^{-1} and 20254-20841 cm^{-1} attributable to $^4T_{1g}$ (F) → $^4T_{2g}$ (F) (υ_1) and $^4T_{1g}$ (F) → $^4T_{1g}$ (P) (υ_3) transitions respectively. These two transitions support the octahedral geometry of Co(II) complexes. Band-Fitting equation has been used to calculate the ligand field parameters (Table 2) like D_q, B, β, β % .The values of D_q were found in the range 1160-1270 cm^{-1} which again confirms the octahedral geometry for Co(II) complexes. Racah interelectronic repulsion parameter (B) was found to be less than free ion value, which clearly indicates the orbital overlap and delocalization of d-electrons. The values of β were less than unity, supporting the partial covalent character of M-L bond. The magnetic moment values for Co(II) complexes were found in the range 4.4-4.8 BM, which in the expected range (4.3-5.0 BM) of octahedral complexes[24] and clearly indicates the presence of three unpaired electrons.

The electronic absorption spectra of 1:1 and 1:2 Ni(II) complexes exhibit three absorption bands in the region 9687-10698 cm^{-1}, 16918-17655 cm^{-1} and 24487-24721 cm^{-1} assigned to $^3A_{2g}$ (F) → $^3T_{2g}$ (F) (υ_1), $^3A_{2g}$ (F) → $^3T_{1g}$ (F) (υ_2) and $^3A_{2g}$ (F) → $^3T_{1g}$ (P) (υ_3) transitions respectively. The ligand field parameters like D_q, B, β, β % have also been calculated for Ni(II) complexes. The values of D_q were found to be 960-1070 cm^{-1} which supports an octahedral geometry. The values of B were less than free ion value, which shows the orbital overlap and delocalization of d-electrons. The values of β were less than unity signifying the partial covalent nature of metal-ligand bond. The observed magnetic moment values for Ni(II) are in the range of 3.3-3.5 BM, which is in good agreement with the reported range of octahedral complexes[24,25] and indicates the presence of two unpaired electron.

The electronic absorption spectra of 1:1 and 1:2 Cu(II) complexes exhibit one absorption band in the region 18610-19781 cm^{-1} attributed to $^2B_{1g}$ → $^2A_{1g}$ transition, which is indicative of square planar geometry of copper complexes. Square planar geometry is further confirmed by the observed magnetic moment value (1.9-2.0 BM), which is in the expected range of square planar complexes[24] and indicates the paramagnetic nature of Cu(II) complexes.

Table 2. Some electronic spectral data of metal complexes.

Compounds	D_q cm^{-1}	B cm^{-1}	υ_2 / υ_1	B	β %
Co(L)(OAc).3H$_2$O	1169.3	729.8	1.09	0.751	24.9
Co(L)$_2$.2H$_2$O	1269.4	705.5	2.10	0.726	27.4
Ni(L)(OAc).3H$_2$O	968.7	822.9	1.74	0.790	21.0
Ni(L)$_2$.2H$_2$O	1069.8	685.5	1.65	0.658	34.2

Fluorescence spectra

Fluorescent spectra of Schiff base and its 1:2 metal complexes have been recorded in 10^{-3} M solution in DMF at EX wavelength of 265 nm. Fluorescent data helps us to investigate the changes in fluorescent property of Schiff base when it binds with metal ion.[26] The emission spectra are presented in Figure 1.

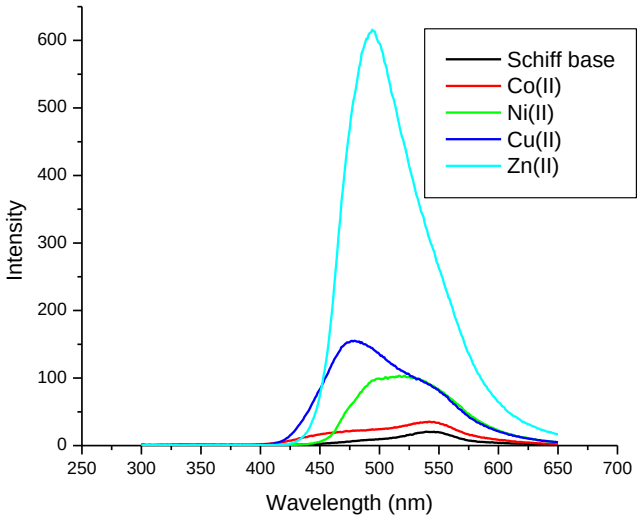

Figure 1. Photoluminescence spectra of Schiff base and its 1:2 metal complexes

The emission wavelengths were observed at 542 nm, 521 nm, 479 nm, and 494 nm for Co(II), Ni(II), Cu(II) and Zn(II) complexes respectively. A weak emission band was observed at 539 nm for Schiff base. Metal complexes show highest fluorescent intensity as PET process is blocked due to engagement of lone pair of electrons of ligand with metal ion. Among all the complexes, Zn(II) complex shows highest fluorescent intensity. On the other hand, coordination between ligand and metal ion reduces the loss of energy via radiation less thermal vibrations.[27] Thus, enhancement in fluorescent intensity was observed and it is evident that fluorescence emission intensity of ligand increase upon coordination and order of their fluorescent intensity are Zn(II) > Cu(II) > Ni(II) > Co(II) > Schiff base.

Electron Spin Resonance spectra

The powder ESR spectra of Cu(L)(OAc).H$_2$O and Cu(L)$_2$ have been recorded which resolved the parallel and perpendicular features of *g*-factor. The ESR parameters, calculated for Cu(L)(OAc).H$_2$O, are $g_\parallel$= 2.12, $g_\perp$= 2.06, g_{av} = 2.08, *G* = 2.04) and for Cu(L)$_2$ are ($g_\parallel$ = 2.14, $g_\perp$= 2.07, g_{av} = 2.09, *G* = 2.03). This g value is the characteristics of axial symmetry and trends $g_\parallel > g_\perp > g_e$ (2.0023) indicates that electron is most likely to be in the $d_{x^2-y^2}$ orbital.[28] In addition, the exchange interaction parameter is calculated by Hathaway expression (eqn. 1).

$$G = \frac{g\parallel - 2.0023}{g\perp - 2.0023} \qquad (1)$$

The *G* value is found to be less than 4.0 indicating considerable exchange interaction in Cu(II) complexes.[29,30] Furthermore, the observed g value was less than 2.3 which suggests the partial covalent nature of metal-ligand bond.[28] Thus, these ESR parameters support the square planar geometry of the Cu(II) complexes.[31]

Thermogravimetric Analysis

The thermal analysis of 1:2 complexes of Co(II), Ni(II), Cu(II) and Zn(II) metal ion have been studied in temperature range of 50-700 °C under air atmosphere by using α-Al_2O_3 as reference. TG curves are presented Figure 2. The mass loss were obtained from this TG curve is compared with the calculated values. This TG data is further supported by DTA curves.

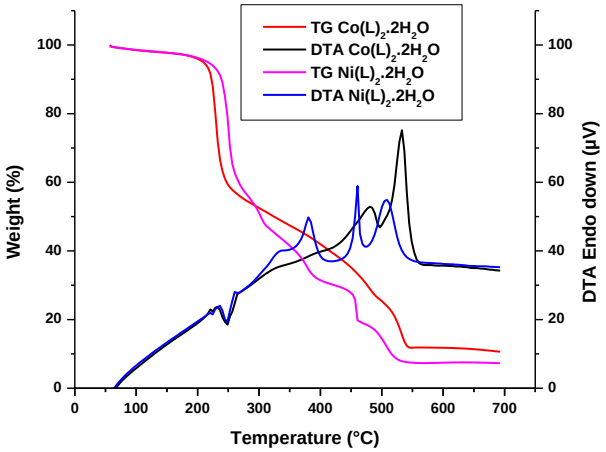

Figure 2a. TG and DTA plot of CoL$_2$.2H$_2$O and NiL$_2$.2H$_2$O

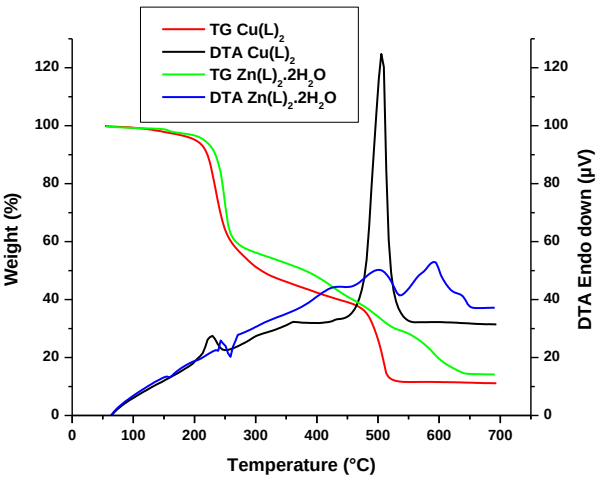

Figure 2b. TG and DTA plot of CuL$_2$ and ZnL$_2$.2H$_2$O

 DOI: 10.17628/ecb.2016.5.193-201

The TG curve of $Co(L)_2.2H_2O$ shows decomposition in three successive steps. First decomposition step from 95-220°C, results in mass loss 5.00 % (Calcd. 5.36 %) associated with the removal of coordinated water molecules. Second step shows decomposition within temperature range 221-310 °C due to loss of organic moiety with estimated mass loss of 43.10 % (Calcd. 43.82 %). Third decomposition step (311-520°C) involved mass loss 41.45 % (Calcd. 42.03 %) confined to the removal of triazine ring. The final weight of the residue corresponds to CoO.

TG degradation of $Ni(L)_2.2H_2O$ also occurred in three steps. First decomposition step attributed to the loss of coordinated water molecules in the temperature range 110-220 °C with mass loss 5.05 % (Calcd. 5.36 %). Second decomposition step (221-285 °C) reasonably accounted for the mass loss 43.15% (Calcd. 43.83 %) confined to the loss of organic moiety. Third decomposition step has been observed from 286-500 °C assigned to the removal of triazine ring with mass loss 42.00 % (Calcd. 42.04 %) leaving behind the NiO as residue.

In case of $Cu(L)_2$, degradation took place in two major steps. First degradation step has been observed from 120-290 °C results in mass loss 45.09 % (Calcd. 45.97 %) associated with removal of organic moiety. Second degradation step (291-495 °C) indicates the removal of triazine ring with mass loss 44.01 % (Calcd. 44.09 %) leaving CuO as residue.

The TG curve of $Zn(L)_2.2H_2O$ shows three step degradation. First degradation step was observed from temperature range 100-220 °C with mass loss 5.21 % (Calcd. 5.31 %) attributed to the removal of two water molecules. Second step (221-280 °C) exhibited mass loss 43.12 % (Calcd. 43.38 %) indicates the loss of organic moiety. Third decomposition involved mass loss 41.29 % (Calcd. 41.61 %) corresponds to the release of triazine ring in the temperature range from 281-550 °C. The remaining residue was estimated as ZnO.

Table 3. Calculated Activation Energies (kJ mol^{-1}) for Individual Stages in degradation of metal complexes.

Compounds	E_1^* (r^2)	E_2^* (r^2)	E_3^* (r^2)
$Co(L)_2.2H_2O$	5.87 (0.94)	1.94 (0.95)	1.85 (0.98)
$Ni(L)_2.2H_2O$	6.89 (0.96)	23.9 (0.91)	2.66 (0.97)
$Cu(L)_2$	16.2 (0.92)	1.15 (0.94)	-
$Zn(L)_2.2H_2O$	9.94 (0.97)	22.7 (0.91)	1.75 (0.98)

*1,2 and 3 stands for first, second and third stage, r^2 stands for regression coefficient; Heating rate = 10 °C min^{-1}.

Kinetic Calculations

Horowitz-Metzger method[32] is used for non-isothermal degradation of $Co(L)_2.2H_2O$, $Ni(L)_2.2H_2O$, $Cu(L)_2.2H_2O$ and $Zn(L)_2.2H_2O$.

Table 4. Biological activity of Schiff base and its Metal Complexes.

Compound	**Diameter of growth of inhibition zone in mm[a]**					
	B. subtilis	***S. aureus***	***E.coli***	***P. aeruginosa***	***C. albicans***	***S. cerevisiae***
HL	17	14	13	14	10	16
$Co(L)(OAc).3H_2O$	12	14	12	16	21	14
$Co(L)_2.2H_2O$	14	15	10	17	19	19
$Ni(L)(OAc).3H_2O$	15	17	15	18	18	15
$Ni(L)_2.2H_2O$	14	15	16	18	16	16
$Cu(L)(OAc).H_2O$	14	14	14	12	12	12
$Cu(L)_2$	18	16	14	18	18	15
$Zn(L)(OAc).3H_2O$	18	15	22	18	18	19
$Zn(L)_2.2H_2O$	17	20	20	20	19	19
Ciprofloxacin	24.0	26.6	25.0	22	-	-
Amphotericin-B	-	-	-	-	16.6	19.3

[a]Values, including diameter of the well (8 mm), are means of three replicates.

Table 5. MIC (μg mL^{-1}) of the synthesized compounds.

Compounds	***B. subtilis***	***S. aureus***	***E. coli***	***P. aeruginosa***	***C. albicans***	***S. cerevisiae***
HL	50	-	-	-	-	50
$Co(L)(OAc).3H_2O$	-	-	-	50	25	-
$Co(L)_2.2H_2O$	-	-	-	50	25	25
$Ni(L)(OAc).3H_2O$	-	50	-	50	50	-
$Ni(L)_2.2H_2O$	-	-	50	50	50	50
$Cu(L)(OAc).H_2O$	-	-	-	-	-	-
$Cu(L)_2$	50	50	-	50	50	-
$Zn(L)(OAc).3H_2O$	50	-	25	50	50	25
$Zn(L)_2.2H_2O$	50	25	25	25	50	25
Ciprofloxacin	6.25	6.25	6.25	12.5	-	-
Amphotericin-B	-	-	-	-	12.5	12.5

The kinetic parameters like α (degree of conversion), T_s (temperature at which 1/(1- α) = 1/exp = 0.368), θ, E (calculated from the slope of the graph between ln ln [1/1-α] and θ) and ln ln[1/1- α] can be calculated by using the eqn. 2, where *R* is Universal Gas Constant.

$$\ln \ln [1/1-\alpha] = E\theta/RT_s^2 \quad (2)$$

The following stability order of the complexes $Cu(L)_2$ > $Zn(L)_2.2H_2O$ > $Ni(L)_2.2H_2O$ > $Co(L)_2.2H_2O$ has been suggested by Horowitz-Metzger method and their activation energy values are presented in Table 3 and Figure 3.

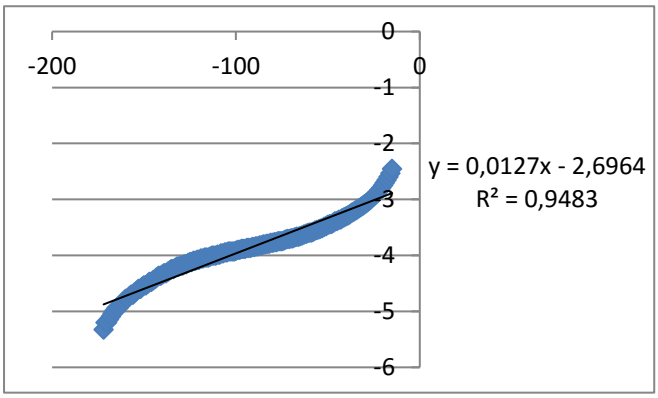

Figure 3a. Horowitz-Metzger plot of ln ln[1/1-α] against θ for first stage decomposition of $Co(L)_2.2H_2O$

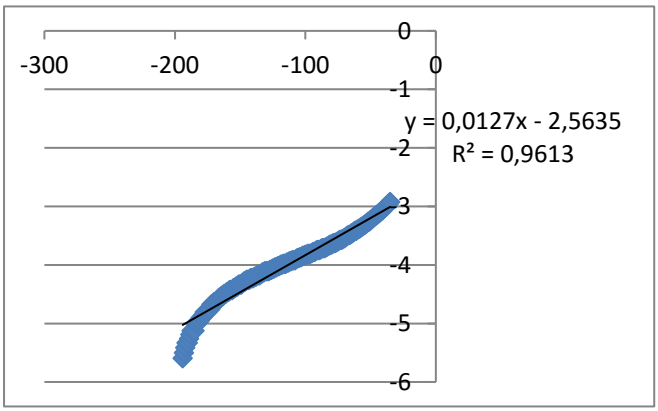

Figure 3b. Horowitz-Metzger plot of ln ln[1/1-α] against θ for first stage decomposition of $Ni(L)_2.2H_2O$

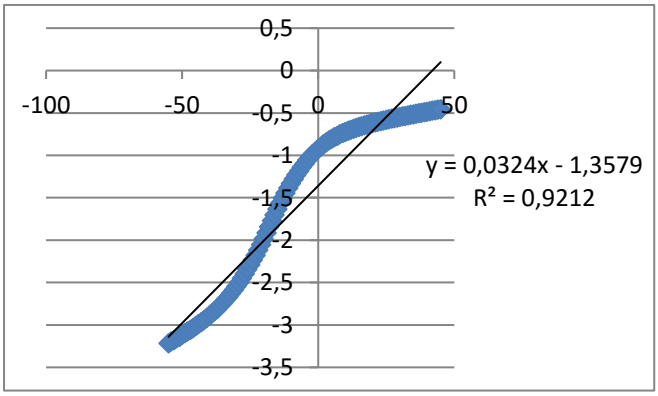

Figure 3c. Horowitz-Metzger plot of ln ln[1/1-α] against θ for first stage decomposition of $Cu(L)_2$

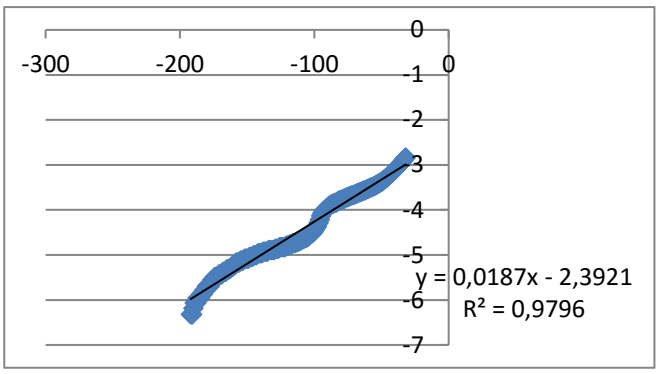

Figure 3d. Horowitz-Metzger plot of ln ln[1/1-α] against θ for first stage decomposition of $Zn(L)_2.2H_2O$

Electrochemical Studies

Cyclic Voltammogram of copper complexes have been recorded in DMF with a scan rate of 0.5 to -1.3 V by using $n Bu_4N^+ClO_4^-$ (TBAP) as supporting electrolyte (Figure 4). $Cu(L)(OAc).H_2O$ and $Cu(L)_2$ show reduction peaks in forward sweep at E_{Pc} = - 0.1 V and E_{Pc} = - 0.99 V assigned to $Cu^{2+/+}$ couple and oxidation peaks at E_{Pa} = - 0.65 V and E_{Pa} = - 0.60 V assigned to $Cu^{+/2+}$ couple.

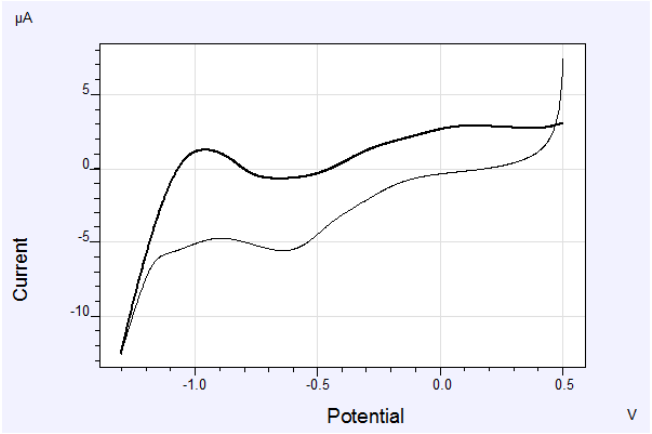

Figure 4. Cyclic Voltammogram of $Cu(L)_2$

For $Cu(L)(OAc).H_2O$ and $Cu(L)_2$ half wave potentials ($E_{1/2}$) were found to be 0.375 V and 0.795 V respectively, indicating a one-electron transfer. The peak to peak separation value (ΔE_P = 0.55 V and 0.39) between cathodic and anodic potential is high. Above data deduced that redox couples are related to quasi reversible one electron transfer process.[33,34]

Antimicrobial activity

Schiff base and its respective metal chelates were screened for antimicrobial activity against four bacterial strains and two fungal strains by using agar well diffusion method.[35] All the data of antimicrobial evaluation are summarized in Table 4 and Figure 5.

For gram positive bacteria inhibition zone were observed in the range 12-20 mm, 10-22 mm for gram negative bacteria and 10-21 mm for yeast. $Cu(L)_2$ and $Zn(L)(OAc).3H_2O$ exhibit maximum inhibition zone of 18 mm against *B. subtilis* while $Zn(L)_2.2H_2O$ exhibit maximum inhibition zone of 20 mm towards *S. Aureus* and *P. aeruginosa*. $Zn(L)(OAc).3H_2O$ showed significant activity (18-22 mm) against *E. coli*, *C. albicans* and *S. cerevisiae*. $Co(L)(OAc).3H_2O$ shows the highest activity (21 mm) against *C. albicans*. Beside this, $Co(L)_2.2H_2O$ and $Zn(L)_2.2H_2O$ exhibit good activity (19 mm) towards *C. albicans* and *S. cerevisiae* respectively.

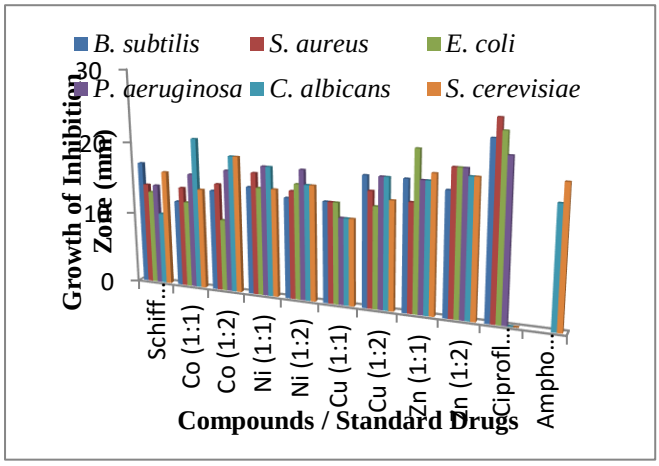

Figure 5. Antibacterial activities of synthesized compounds

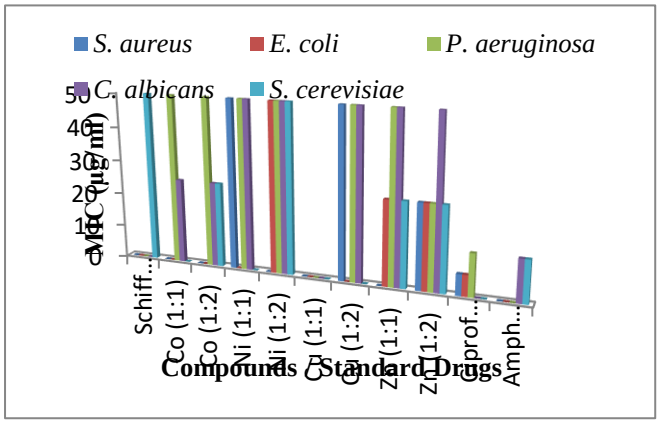

Figure 6. Comparison of MIC of Schiff base and its metal complexes with standard drugs

Against most of the strains, Zn(II) complexes showed the highest activity and follow the order *C. albicans* ≈ *S. cerevisiae* > *P. Aeruginosa* > *E. coli.* The data showed that metal complexes show better biological activity as compared to Schiff base.[36,37] It is explained by

Overtone's concept[38] of cell permeability and Tweedy's Chelation theory.[39] According to the Overtone's concept of cell permeability, the lipid membrane surrounding the cell favors the passage of only lipid-soluble material; therefore, liposolubility is an important factor which controls the antimicrobial activity. On chelation, polarity of the metal ion is reduced to a greater extent due to the overlapping of the ligand orbital and partial sharing of the positive charge of the metal ion with donor groups. Moreover, delocalization of the π-electrons over the whole chelate ring is increased and the lipophilicity of the complex is enhanced.[39,40] The increased lipophilicity enhances the penetration of the complexes into the lipid membranes and blocks the metal binding sites in the enzymes of microorganisms.

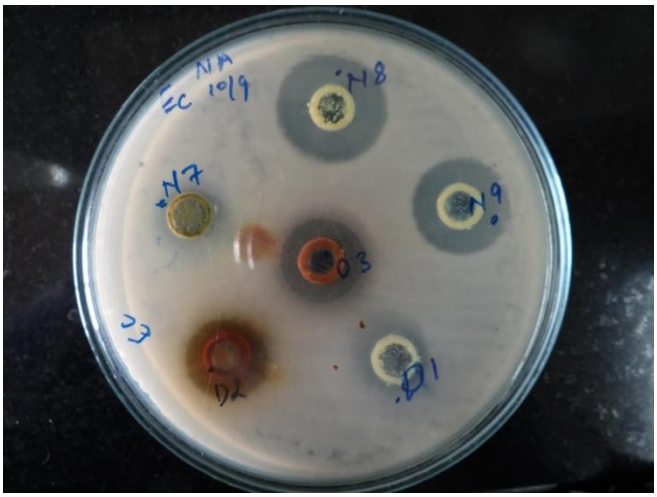

Figure 7a. Inhibition zone of Zn^{II} complexes (N8 and N9) against bacteria *E. coli*

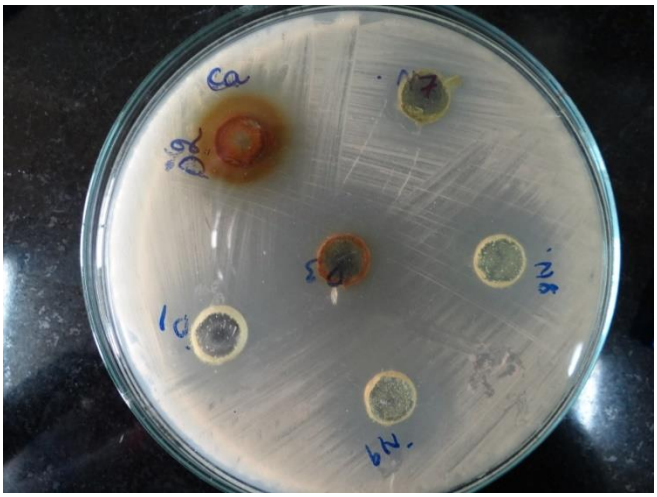

Figure 8b Inhibition zone of Zn^{II} complexes (N8 and N9) against fungi *C. albicans*

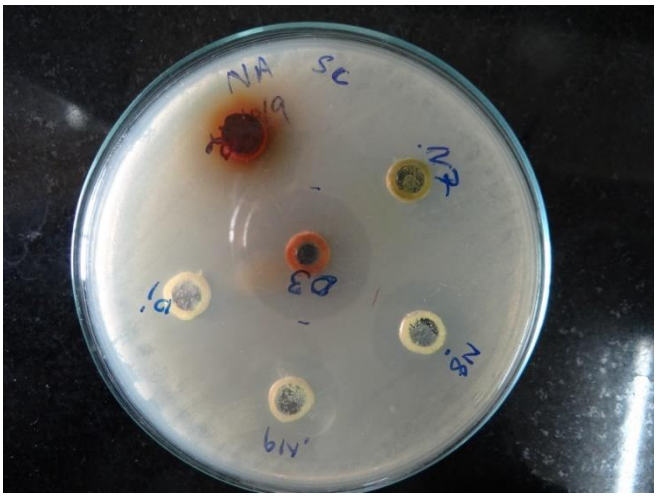

Figure 8c Inhibition zone of Zn^{II} complexes (N8 and N9) against fungi *S. cerevisiae*

MIC value of the tested compound was found to be in the range of 25-50 μg mL^{-1} and presented in Table 5 and Figure 6. The Zn(II) complexes exhibit better antibacterial and antifungal activities against *C. albicans*, *S. cerevisiae*, *P. Aeruginosa* and *E. coli*, (Figure 7) than the others..

The obtained data reveals that Co(II), Ni(II) and Zn(II) complexes exhibited octahedral geometry while Cu(II) complexes exhibit square planar geometry. The proposed structures are presented on Figure 8.

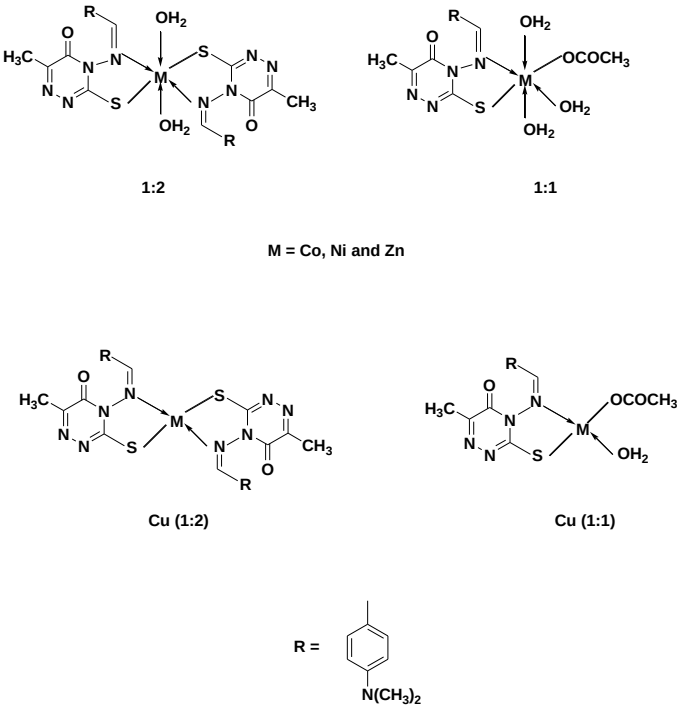

Figure 7. Proposed structures of Schiff base metal complexes.

Conclusions

Various physicochemical techniques have been used to characterize the Schiff base as well as metal complexes. IR spectra reveal that Schiff base act as bidentate ligand as they are coordinated with metal centre via N and S atoms. TG and kinetic studies have been used to determine the thermal stability of the complexes. Presence of lattice water molecules are calculated by TG. The Co(II), Ni(II) and Zn(II) complexes exhibit octahedral geometry while Cu(II) complexes exhibit square planar geometry. Biological experiments indicated that the metal complexes exhibit higher biological activity as compared to noncoordinated Schiff base. The Zn(II) complexes exhibit the best antibacterial and antifungal activities against *C. albicans*, *S. cerevisiae*, *P. Aeruginosa* and *E. coli* among the studied complexes.

Acknowledgments

The authors are grateful to the Chairman, Department of Chemistry for providing necessary research facilities. One of the authors (Ritu) expresses heartfelt thanks to UGC, New Delhi for providing financial assistance (SRF). In addition thanks are extending to the Head of SAIF-PU, IIT Bombay, IIT Roorkee and Jamia Hamdard, New Delhi for carrying out different analysis.

References

[1]Krishnan,B., Vijayanthimala, R., *J. Chem. Biol. Phyd. Sci*, **2015**, *5*, 1139.

[2]Ejidike, I. P., Ajibade, P. A., *Molecules*, **2015**, *20*, 9788.

[3]Mahalakshmi, N., Rajavel, R., *Arabian J. Chem*., **2014**, *7*, 509.

[4]Nagesh, G. Y., Mahadev, U. D., Mruthyunjayaswamy, B. H. M., *Int., J. Pharm. Sci. Rev. Res*., **2015**, *31*, 190.

[5]Sridhar, S. K., Pandeya, S. N., Stsbles, J. P., Ramesh, A., *Eur. J. Pharm. Sci*., **2002**, *16*, 129.

[6]Prakash, A., Singh, B. K., Bhojak, N., Adhikari, D., *Spectrochim. Acta, Part A*,**2010**, *76*, 356.

[7]Bharti, S. K., Nath, G., Tilak, R., Singh, S. K., *Eur. J. Med. Chem*., **2010**, *45*, 651.

[8]Al-masoudi, N. A., Aziz, N. M., Mohammed, A. T., *Phosphorus, Sulphur Silicon Relat. Elem*., **2009**, *184*, 2891.

[9]Creaven, B. S., Devereux, M., Foltyn, A., McClean, S., Rosair, G., Thangella, V. R., Walsh, W., *Polyhedron*, **2010**, *29*, 813.

[10]Shakir, M., Azam, M., Ullah, M. F., Hadi, S. M., *J. Photochem. Photobiol*, **2011**, *104*, 449.

[11]Chohan, Z. H., Kausar, S., *Met. Based Drugs*, **2000**, *7*, 17.

[12]Chohan, Z. H., Jaffery, M. F., Supuran, C. T., *Met. Based Drugs*, **2001**, *8*, 95.

[13]Racane, L., Kulenovic, V. T., Jakic, L. F., Boykin, D. W., Zamola, G. K. ,*Heterocycles*, **2001**, *55*, 2085.

[14]Abou-Hussein, A. A., Linert, W. ,*Spectrochim. Acta, Part A*, **2015**, *141*, 223.

[15]Naik, K. H. K., Ashok, B., Naik, N., Mulla, J. A. S., Prakasha, A., *Spectrochim. Acta, Part A*, **2015**, *141*, 88.

[16]Singh, K., Kumar, Y., Puri, P., Sharma, C., Aneja, K. R., *Int. J. Inorg. Chem*., **2012** doi: 10.1155/2012/873272.

[17]Aneja, K. R., Sharma, C., *Judishapur J. Microbiol*., **2011**, *4*, 175.

[18]Shanker, K., Rohini, R., Kumar, K. S., Reddy, P. M., Ho, Y. P., Ravinder, V., *J. Indian Chem. Soc*., **2009**, *86*, 153.

[19]Keypour, H., Shayesteh, M., Golbedaghi, R., Blackman, A. G., Cameron, S. A., *Transition Met. Chem*., **2013**, *38*, 611.

[20]Atkins, A. J., Black, D., Finn, R. L., Marin-Becerra, A., Blake, A. J., Ruiz-Ramirej, L., Li, W-S., Schroder, M., *Dalton Trans*., **2003**, *9*, 1730.

[21]Singh, A. K., Pandey, O. P., Sengupta, S. K., *Spectrochim. Acta, Part A*, **2012**, *85*, 1.

[22]Singh, K., Raparia, S., Surain, P., *Med. Chem. Res*., **2014**, doi: 10.1007/s00044-014-1298-0.

[23]Singh, K., Kumar, Y., Puri, P., Sharma, C., Aneja, K. R., *Arabian J. Chem*., **2013** doi: 10.1016/j.arabjc.2012.12.038.

[24]Kumar, D., Syamal, A., Jaipal, Gupta, P. K., *J. Indian Chem. Soc*., **2007**, *84*, 217.

[25]Kumar, D., Chadda, S., Sharma, J., Surain, P., *Bioinorg. Chem. Appl*., **2013**, doi: 10.1155/2013/981764.

[26]Shanmugakala, R., Tharmaraj, P., Sheela, C. D., Chidambaranathan, N., *Med. Chem. Res*., **2014**, *23*, 329.

[27]Das, D., Chand, B. G., Sarker, K. K., Dinda, J., Sinha, C., *Polyhedron*, **2006**, *25*, 2333.

[28]Kivelson, D., Neiman, R., *J. Chem. Phys*., **1961**, *35*, 149.

[29]Bagihalli, G. B., Avaji, P. G., Patil, S. A., Badami, P. S., *Eur. J. Med. Chem*., **2008**, *43*, 2639.

[30]Hathaway, B. J., Billing, D. E., *Coord. Chem. Rev*., **1970**, *5*, 143.

[31]Boraey, H. A. E., Rahman, R. M. A., Atia, E. M., Hilmy, H., *Central Eur. J. Chem*., **2010**, *8*, 820.

[32]Singh, K., Ritu,Vikas K., *J. Chem. Biol. Phys. Sci*., **2015**, *5*, 2691.

[33]Hazra, M., Dolai, T., Pandey, A., Dey, S. K., Patra, A., *J. Saudi Chem. Soc*., **2014**, doi: 10.1016/j.jscs.2014.02.009.

[34]Wu, H., Kou, F., Jia, F., Liu, B., Yuan, J., Bai, Y., *Bioinorg. Chem. Appl*., **2011**, doi: 10.1155/2011/105431.

[35]Okeke, M. I., Iroegbu, C. U., Eze, E. N., Okoli, A. S., Esimone, C. O., *J. Ethnopharmacol*., **2001**, *78*, 119.

[36]Singh, K., Kumar, Y., Puri, P., Kumar, M., Sharma, C.,*Eur. J. Med. Chem*., **2012**, 52, 313.

[37]Patil, S. A., Unki, S. N., Kulkarni, A. D., Naik, V. H., Badami, P. S., *Spectrochim. Acta, Part A*, **2011**, *79*, 1128.

[38]Anjaneyula, Y., Rao, R. P., *Synth. React. Inorg. Met. Org. Chem*., **1986**, *16*, 257.

[39]Dharamraj, N., Viswanathamurthi, P., Natarajan, K., *Transition Met. Chem*., **2001**, *26*, 105.

[40]Raman, N., Kulandaisamy, A., Jeyasubramanian, K., *Polish J. Chem*., **2002**, *76*, 1085.

Received: 05.06.2016
Accepted: 26.07.2016.

DIFFERENTIAL IMPACT OF MULTI-WALLED CARBON NANOTUBES ON GERMINATION AND SEEDLING DEVELOPMENT OF *GLYCINE MAX*, *PHASEOLUS VULGARIS* AND *ZEA MAYS*

Olga Zaytseva[a]* and Günter Neumann[a]

Keywords germination, seedling growth, carbon nanotubes, soybean, common bean, maize.

This study is designed to investigate the effects of carbon nanomaterials (multi-walled carbon nanotubes, MWCNTs) under controlled conditions on three different plant species. The study covers the effects of MWCNT dosage, treatment duration, and the plant-developmental stage, including imbibition, germination and seedling development. Germination experiments are conducted under standardized laboratory conditions based on the protocols of the International Seed Testing Association with aqueous MWCNT suspensions at a dosage of 0, 100 and 1000 mg L^{-1} applied as seed treatments during 36 h after sowing prior to radicle emergence, using soybean (*Glycine max* (L.) Merr. cv. BR-16 Conquista), common bean (*Phaseolus vulgaris* L. cv. Bohnen maxi) and maize (*Zea mays* L. cv. Surprise) as test plants. The seed treatment with MWCNTs reduced the speed of water uptake particularly by soybean seeds. This is associated with an increased germination percentage and reduced development of abnormal seedlings, while mean germination time is unchanged. However, during later seedling development, negative effects on root growth, particularly affecting fine root development are recorded for all investigated plant species. In soybean, this effect is first detected at 8 days after sowing and requires a minimum MWCNT seed exposure of 36 h. Inhibition of root growth is associated with reduced metabolic activity of the root tissue as indicated by tetrazolium vitality staining. The nitrate uptake was lower in MWCNT-treated plants, which is mainly attributed to the smaller root system. The results demonstrate that even under standardized experimental conditions, excluding environmental factors and effects induced by carbon nanomaterials, plant responses to MWCNT exposure exhibit differences, depending on plant species but also on the physiological status and the developmental stage of individual plants.

* Corresponding Authors
E-Mail: olga.zaytseva@uni-hohenheim.de
[a] Institute of Crop Science (340h), Faculty of Agriculture, University of Hohenheim, Stuttgart, 70593, Germany

Introduction

Carbon nanotubes (CNTs) are nanostructured carbon allotropes of cylindrical shape, possessing outstanding physical and chemical properties. Multi-walled carbon nanotubes (MWCNTs) are the most important class of carbon nanomaterials with the highest production volumes and numerous technical applications. In the recent past, potential applications have been extended to agriculture with first patents as germination stimulants, plant growth promoters, fertilizers and fertilizer synergists, as well as delivery systems for agrochemicals, antifungal and antimicrobial agents. However, the published literature reflects a high heterogeneity of plant responses to MWCNT treatments, including both, positive and negative effects in some plant species and the complete absence of responses in others.[1-10] The subject matter is reviewed by O. Zaytseva and G. Neumann.[11]

Positive effects of MWCNTs added to agar media at concentrations of 10−40 mg L^{-1} on seed germination and seedling growth of tomato (*Solanum lycopersicum* L.) are reported by Khodakovskaya et al.[1] and Morla et al.[2] Later, Lahiani et al.[3] reported accelerated germination of barley (*Hordeum vulgare* L.), maize (*Zea mays* L.) and soybean (*Glycine max* (L.) Merr.) seeds in a Murashige and Skoog medium amended with 50−200 mg L^{-1} MWCNTs. Srivastava and Rao[4] reported that germination of wheat (*Triticum aestivum* L.), maize and peanut (*Arachis hypogaea* L.) was enhanced by application of 50 mg L^{-1} MWCNTs. The reports listed above suggested that MWCNT application increased the seed water content by perforation of the seed coat. Additionally, Lahiani et al.[3] reported increased expression of aquaporin-related genes, playing a role in water uptake, related with germination, root elongation and plant growth. Positive effects of MWCNTs on seed germination have been also related to the presence of metal catalyst impurities in the applied MWCNT materials.[12]

Similarly, during later seedling development and early growth, positive effects of MWCNTs on root and shoot elongation have been reported for a range of plant species, such as tomato, wheat, soybean, maize, mustard (*Brassica juncea* L.), and black lentil (*Vigna mungo* (L.) Hepper), even in cases when the plant roots had direct contact with the MWCNTs. The expression of effects was concentration-dependent with beneficial effects at lower levels of MWCNT application and inhibition at higher concentrations. Induction of oxidative stress associated with formation of reactive oxygen species (ROS), membrane damage, electrolyte leakage, mitochondrial dysfunctions and DNA aberrations are characterized as determinants of MWCNT toxicity during seedling development and early growth of red spinach (*Amaranthus tricolor* L.), rice (*Oryza sativa* L.), lettuce (*Lactuca sativa* L.) and cucumber (*Cucumis sativus* L.), and small seeds being more sensitive than large seeds. By contrast, Lin and Xing[5] did not find any

effect of MWCNTs when applied in concentrations of 1000−2000 mg L^{-1} on seed germination and root elongation of five plant species (radish (*Raphanus sativus* L.), rape (*Brassica napus* L.), ryegrass (*Lolium perenne* L.), lettuce, maize and cucumber. Similarly, Stampoulis et al.[6] reported no effects on germination of zucchini (*Cucurbita pepo* L.), and Miralles et. al.[12] observed no effects of MWCNTs on alfalfa (*Medicago sativa* L.) and wheat.

Various reasons such as genotypic differences, plant developmental stage, experimental setups, type, dosage, formulation and agglomeration have been discussed to explain the heterogeneity of plant responses to MWCNT treatments. In view of the highly variable effects of MWCNT on plant performance, reported in the literature, a systematic analysis of factors determining the effects of MWCNTs such as MWCNT dosage, duration of exposure to MWCNT treatments, plant-developmental stage including imbibition, germination and seedling development on selected plant species are studied. Soybean, common bean (*Phaseolus vulgaris* L.) and maize are selected as representative crops. Apart from plant growth responses, MWCNT effects are evaluated using assays for physiological activity of the test plants (nutrient uptake, vitality staining).

Experimental

MWCNTs and preparation of MWCNT suspensions

Multi-walled carbon nanotubes (MWCNTs) (NanoTechCenter Ltd., Tambov, Russia), produced by chemical vapor deposition (purity > 98%) with a minimum length of 2 µm, external diameter of 20−70 nm and internal diameter of 5−10 nm were used for the experiments. The selected concentrations for MWCNT application (100 and 1000 mg L^{-1}) were in the range reported in various other studies.[1-9] Working suspensions of MWCNTs were prepared directly in deionized (DI) water and dispersed by ultrasonification (SONOREX SUPER RK 510 H; 35 KHz, Bandelin Electronic, Berlin, Germany) for 30 min.

Test plants

Three plant species: soybean (*Glycine max* (L.) Merr. cv. BR-16 Conquista), common bean (*Phaseolus vulgaris* L. cv. Bohnen maxi) and maize (*Zea mays* L. cv. Surprise) were selected. Seeds were stored in darkness at 4 °C and brought to room temperature one day before use.

Impact of MWCNTs on seed water uptake

Hydration of seeds by imbibition is an important factor triggering the start of seed germination and seed hydration has been influenced by MWCNT treatments in various earlier reports.[1,3] Therefore, the effects of MWCNTs on seed water uptake were investigated during the first twelve hours of imbibition. A germination test was performed in Petri dishes (control: DI water; treatments: 100 and 1000 mg L^{-1} MWCNTs) for studying the kinetics of water uptake by seeds. An additional control without MWCNT was included with seeds imbibing more slowly between four layers of moist filter paper: one sheet of filter paper (58×58 cm, MN710, Macherey und Nagel, Düren, Germany) was folded lengthwise two times to obtain a 4-layer paper strip, which was soaked with 60 ml of DI water according to its maximum water holding capacity. Ten seeds were placed along the upper edge of the paper strip, which is subsequently folded, forming a paper roll with the seeds inside. The paper rolls were placed in upright position into a plastic germination box (30×20×10 cm) and kept under the same growth conditions as the seeds in Petri dishes. Water uptake was recorded by determining weights of the seeds from the Petri dishes and from the filter paper rolls at 1 h intervals during 12 h.

Impact of MWCNTs on the seed germination

The influence of MWCNTs on germination of the three plant species was estimated in standardized filter paper germination tests according to the ISTA rules[13]. For treatments, suspensions of MWCNTs in DI water were applied in concentrations 100 mg L^{-1} and 1000 mg L^{-1}; deionized (DI) water was used as a control. Five mL of un-precipitated MWCNT suspensions or DI water were evenly distributed in plastic Petri dishes (diameter 96 mm, Greiner, Nürtingen, Germany) with 3 layers of filter paper (Blue ribbon MN 640d, Macherey und Nagel, Düren, Germany) on the bottom. Thereafter, ten seeds per Petri dish were distributed equidistantly into the MWCNT suspensions or DI water. Thus, the concentrations of MWCNTs in working suspensions (100 mg L^{-1} and 1000 mg L^{-1}) translated into an actual MWCNT dosage of 50 and 500 µg $seed^{-1}$. Petri dishes were covered with lids and placed into an incubator (BD 115, Binder, Tuttlingen, Germany). Depending on the plant species, temperature during the germination test as well as test duration were maintained according to the ISTA rules[13] and presented in Table 1. During the germination tests, the number of germinated seeds was counted every 12 h and final germination percentage was determined on the day specified in Table 1. Seeds are considered to be germinated when the radicle length reaches 2 mm.[14] Two indices were calculated to describe the results of the germination tests: germination percentage (*GP*)[15] and mean germination time (*MGT*). [15]

Table 1. Conditions maintained during the germination test.

Plant species	Temp., °C	First count, day	Final count, day
Maize	25	4	7
Soybean	25	5	8
Common bean	25	5	9

Impact of MWCNT seed treatment on seedling development

The germination test showed that radicles started to emerge after 36 h of seed imbibition. Therefore, the seed treatment with MWCNTs in the succeeding experiments was limited to 36 h to avoid direct interactions of MWCNTs with the emerging radicles. After 36 h of seed treatment in Petri dishes, seeds were transferred to filter paper rolls in germination boxes as described above.

The lids of the germination boxes were opened and the boxes placed into a climate chamber with a 14 h light period at an average temperature of 23 °C with regular additions of 25 ml DI water per filter roll to compensate for evaporation. No nutrients were supplied to the seedlings because cotyledons can provide organic and mineral nutrients to young seedlings for up to ten days after emergence.[16,17] At 10 DAS, the number of abnormal seedlings were counted as defined in ISTA rules.[13] In brief, seedlings are classified as abnormal if there are significant damages or deformations of essential structures (cotyledons, hypocotyl, primary leaves and primary roots), which can prevent normal plant development. Subsequently, shoot length of normal seedlings was recorded and the seedlings were harvested for biomass and root length determination. For root morphology analysis, fresh root samples, stored in 30% (v/v) ethanol, were carefully separated on transparent Perspex trays and subsequently digitalised with an Epson Expression 10000Xl scanner (Epson, USA). Root analysis was performed using the WinRHIZO software (Regent Instruments, Quebec, Canada).

Nitrate uptake by seedlings

A short (24 h) hydroponic experiment was performed to investigate the effect of short-term (36 h) MWCNT seed treatment on nutrient uptake by seedlings developed from the treated seeds. Soybean and common bean seeds were treated for 36 h in Petri dishes with 1000 mg L^{-1} MWCNTs or DI water (control). Thereafter, seeds were transferred to filter paper rolls were moistened with DI water and were grown until 10 DAS as described above. Thereafter, three representative seedlings per replicate were transferred for 24 h into beakers containing 100 mL of nutrient solution (chemical composition of the nutrient solution is in Appendix A). To estimate the amount of nitrate (NO_3^-) absorbed by the seedlings, the volume of the nutrient solutions as well as the nitrate (NO_3^-) concentration in the beakers were measured before and after the incubation pweriod. The NO_3^- concentration was determined by using nitrate-sensitive test strips (Merck KGaA, Darmstadt, Germany) and the color intensity on the strips was quantified colorimetrically (Hermann Wolf GmbH&Co.KG, Wuppertal, Germany).

After 24 h of seedlings exposure to nutrient solution, two of three seedlings were harvested for biomass and root length determination and one seedling per replicate was stained with 2, 3, 5-triphenyltetrazolium chloride (TTC) as a measure of the metabolic activity of the root tissue.

TTC reduction assay

Vitality staining of root tissues was performed with roots of soybean and common bean seedlings, developed from seeds treated for 36 h with 0 or 1000 mg L^{-1} MWCNTs, which were grown in filter paper rolls until 10 DAS and subsequently incubated for 24 h in nutrient solution as described above. Prior to TTC staining the roots were rinsed with DI water and then placed into 50 mL of TTC solution (0.08% TTC in 0.05 M sodium phosphate buffer, pH 7.4) for 24 h in the dark.[18] In metabolically active cells, TTC is reduced by dehydrogenases, forming red-colored insoluble triphenylformazan (TF). The color intensity reflects the degree of metabolic activity in the stained tissues. After an incubation time of 24 h, the TTC solution was discarded, roots were rinsed three times with DI water, cut into segments of 1 cm and immersed into 10 mL of 95% (v/v) ethanol for 24 h at 4 °C for extraction of TF. Thereafter, the ethanol extract was filtered (Blue ribbon MN 640d, Macherey und Nagel, Düren, Germany) and the absorbance of the filtrate was measured spectrophotometrically at a wavelength of 485 nm (U-3300, Hitachi Ltd. Tokyo, Japan). Reduction of TTC is calculated as absorption of TF produced per root [Abs485 $seedling^{-1}$] and per unit root dry weight [Abs485 gDW^{-1}].

Statistical analysis

All experiments were performed in a completely randomized design. Statistical analysis was conducted with SigmaPlot 11.0 software using the Student t-test for comparison of two treatments and one-way ANOVA for comparison of multiple treatments. The level of significance is determined at a P value ≤ 0.05. All results in tables and graphs are presented as mean values ± SE (standard error of the mean).

Results

Seed water uptake

The speed of water uptake is calculated according to the formula:

$$v_{\text{water uptake}} = \frac{m_{\text{imbided seed}} - m_{\text{dry seed}}}{t}$$

where

$v_{\text{water uptake}}$: speed of water uptake [mg $seed^{-1}$ h^{-1}],

$m_{\text{imbibed seed}}$: average weight of imbibed seed [mg $seed^{-1}$]

$m_{\text{dry seed}}$: average initial seed weight [mg $seed^{-1}$] before the experiment,

t: time duration of imbibition [h].

The highest speed of water uptake is found in soybean seeds, followed by common bean and maize (Fig. 1). In soybean, most rapid imbibition is detected in the control variant (Fig. 1), while seeds imbibed between layers of moist paper show the slowest rate of water uptake. Similarly for the variant imbibing between layers of moist paper, the application of 100 and 1000 mg L^{-1} MWCNTs significantly slowed down the seed water uptake by 12 % as compared to the control. Also in maize, seed imbibition between layers of moist filter paper and MWCNTs treatments reduced the speed of the water uptake. However, for MWCNT treatments, this reduction is not significant. A similar but not significant trend is observed for common bean.

Germination test

Germination percentage (GP_i) for each observation is calculated according to the formula[15]:

$$GP_i = 100\frac{n_i}{N}$$

where

GP_i: germination percentage at the i^{th} observation [%],

n_i: number of seeds, germinated from the beginning of the experiment to the i^{th} observation and

N: total number of seeds.

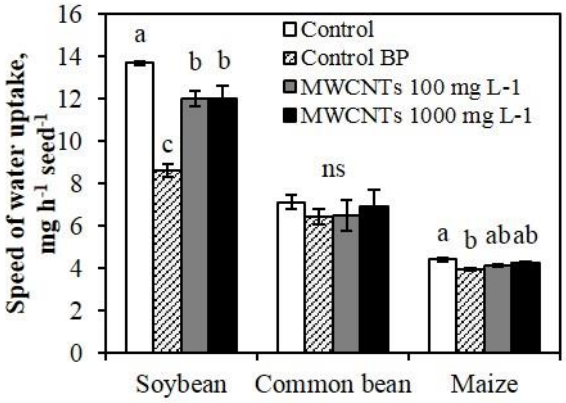

Figure 1. Speed of water uptake by soybean, common bean and maize seeds during 12 h of imbibition in Petri dishes (Control (DI water), MWCNTs 100 and 1000 mg L^{-1}) and in between filter paper (Control BP). Values represent mean values ± SEM of four replicates. Different letters (a, b, c) indicate significant difference between treatments (one-way ANOVA, Tukey test, $P \leq 0.05$). ns−not significant, MWCNTs−multi-walled carbon nanotubes, DI water−deionized water.

The mean germination time (*MGT*), days for germination of 50 % of all germinated seeds, is calculated as described by formula[15]:

$$MGT = \frac{\sum_{i=1}^{k} n_i t_i}{\sum_{i=1}^{k} n_i}$$

where

t_i: time from the beginning of the experiment to the i^{th} observation [days],

n_i: number of seeds germinated on the i^{th} day and

k: last day of germination.

Stimulation of germination percentage (*GP*, %) by MWCNT application is detectable only in soybean but not in common bean and maize (Fig. 2). Enhanced *GP* of soybean is first detectable on the second day of the experiment and remains elevated till the day of the final count (Fig. 2A). The application of MWCNTs with a concentration of 1000 mg L^{-1} significantly increased the final *GP* of soybean seeds by 28% as compared to the control experiment. The treatment with a concentration of 100 mg L^{-1} of MWCNT the *GP* increased by 25%, although this effect is not significant.

In common bean (Fig. 2B) and maize (Fig. 2C) the *GP* does not significantly differ. The mean germination time (*MGT*) of all the studied plant species is not affected by MWCNT application (data not shown).

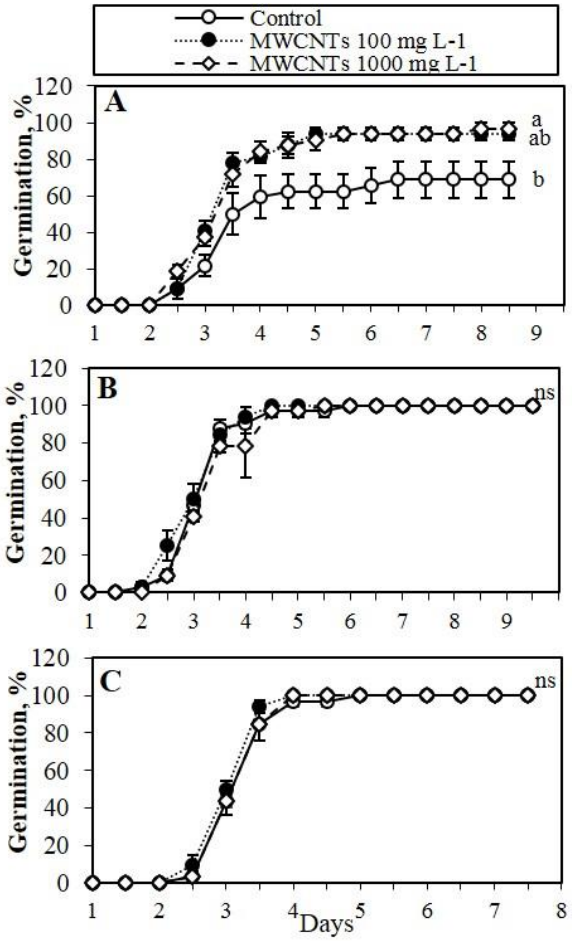

Figure 2. Germination percentage (*GP*, %) of (A) soybean, (B) common bean and (C) maize seeds in DI water (Control) and in MWCNTs (100 and 1000 mg L^{-1}) suspensions. Values represent mean values ± SEM of four replicates. Different letters (a, b) indicate significant difference between treatments (one-way ANOVA, Tukey test, $P \leq 0.005$), ns−not significant. MWCNTs−multi-walled carbon nanotubes, DI water−deionized water.

In all cases, the percentage of abnormal seedlings, according to the ISTA rules,[13] positively correlates with the speed of seed water uptake by soybean (R^2=0.92, P=0.08), common bean (R^2=0.99, P=0.01) and maize seeds (R^2=0.73, P=0.27) measured during the first 12 h of the seed imbibition (Fig. 3). For all tested plant species, the highest percentage of abnormal seedlings was observed in the control variants imbibed in Petri dishes in a film of free water, while the seeds imbibing between filter paper with the slowest rate of water uptake developed the smallest number of abnormal seedlings.

Seedling development

Abnormal seedlings were discarded at final harvest (10 DAS) and the measured growth characteristics refer to normal developed seedlings according to the ISTA rules.[13]

In soybean, the short-term (36 h) seed treatment with 100 and 1000 mg L^{-1} of MWCNTs did not affect shoot length, shoot and root dry weight of seedlings. However, the total root length was significantly reduced, while average root diameter increased in both MWCNT treatments (Table 2). In the control between layers of moist paper the dry root weight of soybean seedlings decreased as compared to theother treatments and the total root length was shorter than in the control, but longer as compared to MWCNTs treatments.

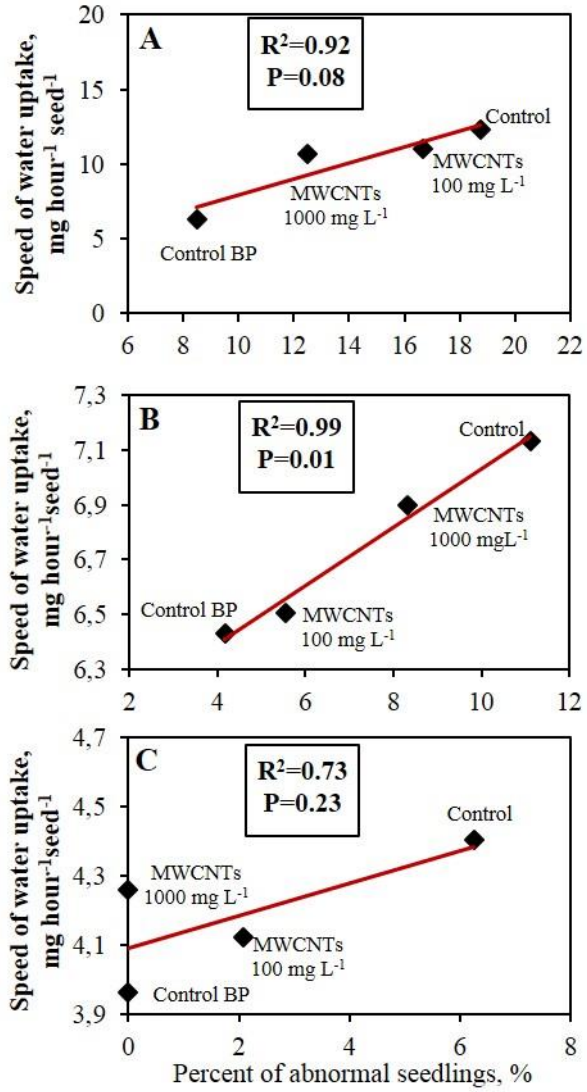

Figure 3. Correlation between speed of water uptake by seeds during the first 12 h of imbibition and formation of abnormal seedlings (%) at 10 days after sowing (DAS). Soybean (A), common bean (B) and maize (C) seeds were treated in Petri dishes for 36 h by 100 and 1000 mg L^{-1} MWCNTs or DI water (Control) and by DI water between moist filter paper (control BP) and subsequently grown in filter paper rolls moistened with DI water. MWCNTs−multi-walled carbon nanotubes, DI water−deionized water.

The application of 1000 mg L^{-1} MWCNTs reduced the root dry weight of common bean and increased the shoot dry weight of maize seedlings as compared to the untreated control. There is also a trend for declining total root length of common bean and maize seedlings induced by 1000 mg L^{-1} MWCNTs as compared to the control, although not significant (Table 2).

The analysis of root diameter distribution reveals a reduction of fine root length (diameter: 0.0−0.2 and 0.2−0.4 mm) of soybean in both applied MWCNT concentrations, while the length of roots with a diameter of 0.4−0.6 mm decreased only by the application of 1000 mg L^{-1} MWCNTs (Table 3). Similarly, in maize the length of fine roots (0.0−0.2 mm) decreased in the 1000 mg L^{-1} MWCNT variant (Table 3).

Assessment of root activity

As indicators for root activity, nitrate uptake of the seedlings was measured by nitrate depletion of a nutrient solution. Additionally, vitality staining of the root tissue with 2, 3, 5-triphenyl tetrazolium chloride (TTC) was performed, followed by extraction and photometric quantification of the red triphenylformazan formed by the metabolic activity of the roots.

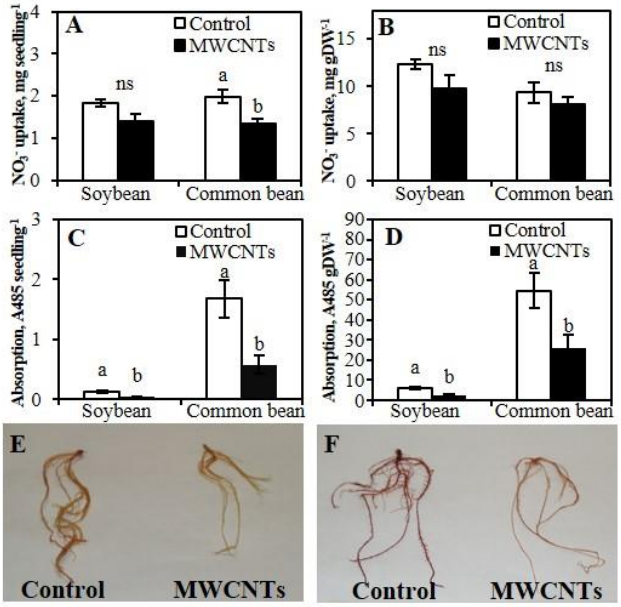

Figure 4. Assessment of root activity of soybean and common bean seedlings. (A) Nitrate uptake per plant [mg $seedling^{-1}$] and (B) per unit root dry weight [mg g_{DW}^{-1}] by 10-days old soybean and common bean seedlings cultivated in nutrient solution during 24 h. (C) Absorption of a triphenylformazan (TF) at 485 nm per seedling [A485 $seedling^{-1}$] and (D) per unit root dry weight [A485 g_{DW}^{-1}] as a product of 2, 3, 5-triphenyl tetrazolium chloride (TTC) reduction by the roots of 10-days old soybean and common bean seedlings immersed for 24 h in 0.08% TTC solution followed by ethanol extraction. (E) Roots of soybean and (F) common bean seedlings after staining with 0.08% TTC. The seedlings (A−F) were developed from seeds treated in Petri dishes for 36 h with 1000 mg L^{-1} MWCNTs or DI water (Control) and subsequently grown in filter paper rolls moistened with DI water. Values represent mean values ± SEM of five replicates. Different letters (a, b) indicate significant differences between treatments (*t*-Student test, $P \leq 0.005$), ns−not significant. MWCNTs−multi-walled carbon nanotubes, DI water−deionised water.

Table 2. Growth characteristics of 10-days old soybean, common bean and maize seedlings, developed from seeds exposed to MWCNTs for 36 h and subsequently grown in filter paper rolls. The seeds were treated in Petri dishes either with DI water (Control) or MWCNTs suspensions (100 and 1000 mg L^{-1}) or imbibed slowly between filter paper with DI water (control BP).

Treatment	Shoot length, cm $plant^{-1}$	Shoot dry matter, mg $plant^{-1}$	Root dry matter, mg $plant^{-1}$	Total root length,cm $plant^{-1}$	Average root diameter, mm
Soybean *(Glycine max* (L.) Merr)					
Control	17.6 ± 0.7 a	95.56 ± 3.69 a	16.70 ± 1.26 a	981.1 ± 23.0 a	0.25 ± 0.00 b
Control BP	12.6 ± 0.4 b	94.35 ± 6.07 a	15.50 ± 1.18 b	820.2 ± 14.5 b	0.26 ± 0.00 b
MWCNTs 100 mg L^{-1}	18.8 ± 0.5 a	101.05 ± 4.21 a	21.17 ± 1.38 a	523.2 ± 18.4 c	0.33 ± 0.01 a
MWCNTs 1000 mg L^{-1}	18.8 ± 0.7 a	93.51 ± 2.85 a	17.90 ± 0.75a	458.5 ± 5.8 d	0.33 ± 0.00 a
Common bean (*Phaseolus vulgaris* L.)					
Control	17.2 ± 0.3 a	161.20 ± 5.04 a	37.26 ± 0.96 a	137.7 ± 22.3 a	0.39 ± 0.02 a
Control BP	17.2 ± 0.3 a	154.61 ± 6.19 a	34.35 ± 1.53 a	86.3 ± 9.2 a	0.33 ± 0.02 a
MWCNTs 100 mg L^{-1}	16.7 ± 0.2 a	143.45 ± 12.92 a	31.81 ± 2.69 a	91.7 ± 16.7 a	0.30 ± 0.03 a
MWCNTs 1000 mg L^{-1}	16.5 ± 0.4 a	143.42 ± 13.16 a	28.41 ± 3.12 b	91.2 ± 8.6 a	0.31 ± 0.02 a
Maize (*Zea maize* L.)					
Control	10.9 ± 0.5 a	28.10 ± 0.76 b	42.23 ± 1.93 a	93.5 ± 5.5 a	0.77 ± 0.02 a
Control BP	11.0 ± 0.4 a	25.88 ± 1.49 b	41.00 ± 2.27 a	92.1 ± 5.1 a	0.76 ± 0.02 a
MWCNTs 100 mg L^{-1}	11.3 ± 0.4 a	29.29 ± 2.25 b	44.06 ± 2.04 a	91.3 ± 6.8 a	0.76 ± 0.01 a
MWCNTs 1000 mg L^{-1}	10.7 ± 0.4 a	38.13 ± 2.09 a	39.27 ± 1.86 a	77.1 ± 7.1 a	0.75 ± 0.03 a

Note: Results represent mean values ± SEM of 6 replicates. Different letters (a, b, c, d) indicate significant differences between treatments (one-way ANOVA, Tukey test, $P \leq 0.05$). Control BP−control between paper, MWCNTs−multi walled carbon nanotubes, DI water−deionized water.

Table 3. Length of fine root fractions of 10-days old soybean, common bean and maize seedlings, developed from seeds exposed to MWCNTs for 36 h and subsequently grown in filter paper rolls. The seeds were treated in Petri dishes either with DI water (Control) or MWCNT suspensions (100 and 1000 mg L^{-1}) or imbibed slowly between filter paper with DI water (control BP).

Treatment	Fine root length (0 ≤ 0.2 mm), cm $plant^{-1}$	Fine root length (0.2 ≤ 0.4 mm), cm $plant^{-1}$	Fine root length (0.4 ≤ 0.6 mm), cm $plant^{-1}$
Soybean (*Glycine max* (L.) Merr)			
Control	679.2 ± 42.7 a	72.2 ± 6.3 a	51.7 ± 3.6 a
Control BP	586.2 ± 14.4 b	65.2 ± 1.7 a	53.9 ± 4.6 a
MWCNTs 100 mg L^{-1}	327.1 ± 18.3 c	33.7 ± 2.5 b	43.3 ± 3.5 ab
MWCNTs 1000 mg L^{-1}	287.4 ± 10.2 c	26.8 ± 1.7 b	36.4 ± 2.7 b
Common bean (*Phaseolus vulgaris* L.)			
Control	0.5 ± 0.1 a	14.5 ± 1.3 a	79.8 ± 7.8 a
Control BP	0.4 ± 0.0 a	10.8 ± 1.8 a	79.2 ± 3.5 a
MWCNTs 100 mg L^{-1}	0.5 ± 0.0 a	14.4 ± 2.3 a	69.9 ± 6.8 a
MWCNTs 1000 mg L^{-1}	0.5 ± 0.1 a	13.3 ± 2.2 a	93.0 ± 10.4 a
Maize (*Zea maize* L.)			
Control	24.2 ± 2.6 a	14.1 ± 2.7 a	3.4 ± 0.3 a
Control BP	24.6 ± 0.8 a	10.5 ± 1.4 a	4.6 ± 0.8 a
MWCNTs 100 mg L^{-1}	20.6 ± 1.1 ab	16.0 ± 1.9 a	3.7 ± 0.2 a
MWCNTs 1000 mg L^{-1}	15.7 ± 2.0 b	17.3 ± 2.6 a	4.1 ± 0.4 a

Note: Results represent mean values ± SEM of 6 replicates. Different letters (a, b, c) indicate significant differences between treatments (one-way ANOVA, Tukey test, $P \leq 0.05$). Control BP−control between paper, MWCNTs−multi-walled carbon nanotubes, DI water−deionized water.

Nitrate uptake of common bean seedlings developed from seeds treated with MWCNTs (36 h, 1000 mg L^{-1}) was significantly reduced as compared to the untreated control (Fig. 4A) and a similar but not significant trend was also recorded for soybean. This was associated with a significant reduction in root length in the MWCNT variants of soybean and common bean (Appendix B). However, analysis of specific nitrate uptake per unit of dry root weight revealed no inhibition related with the application of MWCNTs (Fig. 4B).

The TTC reduction assay revealed significantly inhibited dehydrogenase activity in the seedlings roots exposed to MWCNT treatments. The visual evaluation of stained root samples showed less intensive red coloration of the soybean and common bean roots developed from the MWCNT-treated seeds (Fig. 4E, F). The amount of produced TF was approximately 50% less in MWCNT treatments compared to the corresponding controls (Fig 4C, D).

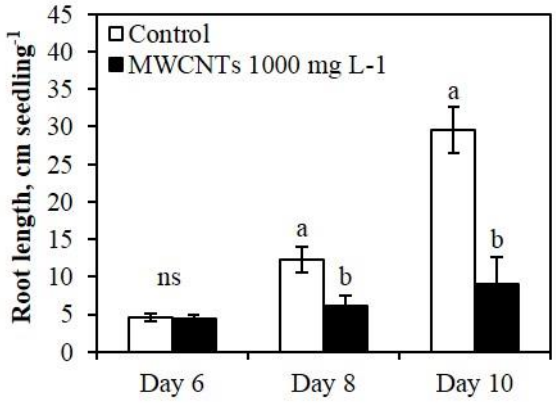

Figure 5. Total root length of 6, 8 and 10-days old soybean seedlings, developed from seeds treated in Petri dishes with and without MWCNTs (1000 mg L^{-1} for 36 h) and grown in filter paper rolls moistened with DI water. Different letters (a, b) indicate significant differences between treatments (Student t-test, $P \leq 0.05$), ns−not significant. MWCNTs−multi-walled carbon nanotubes, DI water−deionised water.

Table 4. Total root length [cm $plant^{-1}$] of 10-days old soybean seedlings, developed from seeds treated in Petri dishes for 6, 12, 24, 30 and 36 h with MWCNTs (1000 mg L^{-1}) or DI water (Control) and subsequently grown in filter paper rolls.

Seed treatment duration, h	Total root length, cm $plant^{-1}$	
	Control	MWCNTs 1000 mg L^{-1}
6	91.2 ± 10.3 a	87.7 ± 3.5 a
12	89.3 ± 6.8 a	82.2 ± 8.7 a
24	77.2 ± 5.4 a	72.7 ± 3.6 a
30	73.4 ± 5.8 a	65.9 ± 4.4 a
36	70.8 ± 4.6 a	60.6 ± 1.6 b

Note: Results represent mean values ± SEM of 4 replicates. Different letters (a, b) in the same line indicate significant difference between treatments (Student t-test, $P \leq 0.05$). MWCNTs−multi-walled carbon nanotubes, DI water−deionised water.

MWCNT exposure time

To determine the minimum time period for seed exposure required for induction of plant damage induced by MWCNTs in soybean seedlings developed from seeds treated with MWCNTs (1000 mg L^{-1}) were investigated after exposure times of 6, 12, 24 and 36 h. Significantly reduced total root length as compared to the control variant were first recorded after 36 h of seed exposure to MWCNTs (Table 4) and is detectable earliest at 8 DAS (Fig. 5).

Discussion

The present study reveals differences in responses to short-term MWCNT seed exposure in three different plant species (*Glycine max* (L.) Merr), *Phaseolus vulgaris* L., *Zea mays* L.) in a standard germination test according to the ISTA rules,[13] showing both positive and negative effects on plant development. MWCNT suspensions were applied for 36 h prior to radicle emergence in Petri dishes on filter paper in two concentrations (100 and 1000 mg L^{-1}), as used in previous studies investigating CNT effects on plant growth[1-9] (reviewed by O. Zaytseva and G. Neumann[11]). The selected concentrations translated into a CNT dosage of 50 and 500 µg MWCNTs $seed^{-1}$. However, a closer look at the culture system shows that only traces of the applied MWCNTs had direct seed contact, while by far the majority of the MWCNTs remained sticking to the germination paper.

The most striking positive MWCNT effect on plant development is a 30% stimulation in germination, reflected in germination percentage (Fig. 2) and development of abnormal seedlings according to the ISTA classification (Fig. 3) recorded in soybean with a germination rate of approximately 65% in the untreated control. This effect is not detectable in common bean or maize, with untreated control variants, reaching almost 100 % germination. The variability in MWCNT-induced stimulation of germination may reflect interspecific differences. On the other hand, seed lot effects related with differences in seed quality and seed aging[19] indicated by different germination rates of the untreated controls, may offer an alternative explanation. A clear distinction would require a comparison of seed lots with a comparable vitality for all tested plant species.

Similar to this study, positive effects of MWCNTs exposure at concentrations between 10 and 200 mg L^{-1} on seed germination and seedling growth have been reported for barley, wheat, maize, peanut (*Arachis hypogaea* L.), soybean and tomato.[1-4] Increased germination has been related with improved seed water uptake during imbibition as a putative consequence of a MWCNT-induced seed coat and cell wall perforation and increased expression of water channel proteins (aquaporins)[3] involved in water uptake, germination, root elongation and also in many stress responses.[20] Additionally, the beneficial impact on plant growth, frequently observed at lower doses of MWCNT has been attributed to hormesis effects[9,21] (reviewed by O. Zaytseva and G. Neumann[11]). However in the current study, the treatment with increasing MWCNT concentration, promoted the positive effects on seed germination in soybean (Fig. 2A), associated with a reduction in the speed of seed water uptake during imbibition (Fig. 1). Moreover, the speed of water uptake in all investigated plant species during seed imbibition is positively correlated with the formation of abnormal seedlings according to the ISTA classification[13] and the lowest rate is recorded for seeds imbibed very slowly between layers of moist filter paper (Fig. 3). Imbibition damages, such as disturbed reconstitution of cell membranes, resulting in reduced

germination[22,23] often occur as a result of a rapid seed water uptake in large-seeded leguminous plants, exposed e.g. to excessive soil moisture levels. A large amount of hydrophobic proteins on the seed coat surface of soybean[24] may allow preferential adsorption of the hydrophobic MWCNTs similar to seed dressing agents. Seed dressings can slow down the speed of water uptake, thereby reducing the risk of imbibition damage,[25] and obviously the MWCNT treatments had a similar function in our experiments. Moreover, seeds with impaired seed vitality (induced e.g. by seed aging) are particularly sensitive to additional stress factors, such as imbibition damage. The low germination rate recorded for the untreated soybean seed lot (65%) used in this study (Fig. 2) may indicate a similar seed vitality problem, associated with a high responsiveness to protective seed dressing treatments and therefore, also to MWCNT application.

However, despite the beneficial effects of short-term MWCNT seed treatments on germination, a negative impact on further seedling development is detected in all tested plant species. The development of root growth and fine root production was inhibited at 10 DAS (Tables 2, 3 and 4) which is particularly important for spatial nutrient acquisition. Accordingly, nitrate uptake measured as nitrate depletion in a hydroponic growth medium is significantly reduced in common bean seedlings with a similar trend also in soybean (10 DAS) exposed to 36 h of MWCNT seed treatments (Fig 4). However, only nitrate uptake per plant is reduced by the MWCNT treatments, while the specific uptake rate per unit root dry weight remains unaffected. This finding suggests that the reduction in nitrate uptake is mainly a consequence of inhibited root growth and not of a limitation in the specific uptake activity. By contrast, vitality staining of the root tissue with TTC (2, 3, 5-triphenyl tetrazolium choride) revealed reduced triphenylformazan (TF) formation per unit root dry biomass of the MWCNT-treated common bean and soybean seedlings. This findings indicate lower metabolic activity and lower vitality of the root tissue, which is potentially responsible for the limitation of root growth.

Apart from plant growth stimulation,[1,3,4] negative growth effects have been similarly reported in the literature for a range of plant species including red spinach, rice, lettuce and cucumber particularly at higher dosages of MWCNT application. Growth restrictions have been related with MWCNT-induced indication of oxidative stress, membrane damage, electrolyte leakage, mitochondrial dysfunctions and DNA aberrations.[7,8,26,27]

Conclusion

The present study demonstrates that MWCNT effects on plant growth are highly variable depending on plant species, but also on the physiological status and the developmental stage of individual plants. The different plant responses to MWCNT treatments are observed under strictly controlled experimental conditions, largely excluding environmental factors and effects induced by carbon nanomaterials of different origin or agglomeration status.[28,29] Apart from the well-documented stimulation of germination by increased water uptake during imbibition associated with seed coat perforation and upregulation of aquaporin genes,[1,3,29,30] the results demonstrates that MWCNT seed treatments can also exert protective effects by reducing the speed of water uptake thereby minimizing the detrimental effects of imbibition damage,[31] particularly in seeds with limited vitality (Figs. 2 and 3). In soybean, the protective effect seems to be restricted mainly to the first 24 h of seedling development as approximate time period required for complete seed imbibition. A significant reduction in water uptake in MWCNT-treated seeds is already detectable after 12 h of imbibition (Fig. 1), although the promoting effect on germination rate started to appear at 3 DAS (Fig. 2).

By contrast, inhibitory effects on plant growth induced by MWCNT treatments are first detectable at 8 DAS (Fig. 5) and in all investigated plant species root growth is primarily affected (Table 2). In soybean, MWCNT exposure for at least 36 h prior to radicle emergence is required (Table 4) to induce root growth inhibition at 8 DAS (Fig. 5), associated with reduced metabolic activity of the roots (Fig. 4). The molecular and physiological events determining the inhibition of root growth during later seedling development already within 36 h after sowing, remain to be elucidated. A reduced establishment of a functional root system can act as a cause of inhibitory effects on further plant development with pleiotropic patterns, particularly under conditions of limited nutrient and water availability, requiring adaptive responses in root growth for adequate nutrient acquisition. This holds true for soil culture in general with additional impact of abiotic and biotic stress factors. This situation may further contribute to the reported variability of plant responses due to exposure to carbon nanomaterials.

Acknowledgment

The author (OZ) is grateful to the Ministry of Science, Research and the Arts of Baden-Württemberg (Germany) and the Education, Audiovisual and Culture Executive Agency of the European Union for financial support. Furthermore, the authors would like to thank Dr. S. Bopper for methodological consulting and A. Walton for proof reading of the article.

The authors declare that they have no conflict of interest.

References

[1]Khodakovskaya, M., Dervishi, E., Mahmood, M., Xu, Y., Li, Z., Watanabe, F. and Biris, A. S., *ACS Nano*, **2009**, 3*(10)*, 3221–3227.

[2]Morla, S., Rao, C. Ramachandra S. V. and Chakrapani, R., *J. Chem., Biol. Phys. Sci*., **2011**, 1*(2)*, 328–334.

[3]Lahiani, M. H., Dervishi, E., Chen, J., Nima, Z., Gaume, A., Biris, A. S. and Khodakovskaya, M. V., *ACS Appl. Mater. Interfaces*, **2013**, 5*(16)*, 7965–7973.

[4]Srivastava A., Rao D. P., *Eur. Chem. Bull*., **2014**, 3*(5)*, 502–504.

[5]Lin, D. and Xing, B., *Environ. Pollut*., **2007**, 150*(2)*, 243–250.

[6]Stampoulis, D., Sinha, S. K. and White, *J. C., Environ. Sci. Technol.*, **2009**, 43*(24)*, 9473–9479.

[7]Begum, P. and Fugetsu, B., *J. Hazard. Mater*., **2012**, 243, 212–222.

[8]Begum, P., Ikhtiari, R., Fugetsu, B., Matsuoka, M., Akasaka, T. and Watari, F., *Appl. Surf. Sci*., **2012**, 262, 120–124.

[9]Ghodake, G., Seo, Y. Deuk, Park, D. and Lee, D. Sung, *J. Nanoelectron. Optoelectron*., **2010**, 5*(2)*, 157–160.

[10]Larue, C., Pinault, M., Czarny, B., Georgin, D., Jaillard, D., Bendiab, N., Mayne-L'Hermite, M., Taran, F., Dive, V. and Carrière, M., *J. Hazard. Mater*., **2012**, 227-228, 155–163.

[11]Zaytseva, O., Neumann, G., *Chemical and Biological Technologies in Agriculture*, **2016** (in press).

[12]Miralles, P., Johnson, E., Church, T. L. and Harris, A. T., *J. R. Soc. Interface*, **2012**, 9*(77)*, 3514–3527.

[13]The International Seed Testing Association (ISTA), *ISTA Rules Full Issue*, **2015**.

[14]Mavi, K., Demir, I. and Matthews, S., *Seed Sci. Technol.*, **2010**, 38*(1)*, 14–25.

[15]Ranal, M. A., de Santana, D. G., Ferreira, W. R., Mendes-Rodrigues, C., *Rev. Bras. Bot*., **2009**, 32*(4)*, 849–855.

[16]Ren, C., Bilyeu, D., Roberts, C. A. and Beuselinck, P. R., *Seed Sci. Technol*., **2007**, 35*(2)*, 303–317.

[17]Ritchie S W, Hanway J. J, Thompson H. E, Benson G. O., *How a soybean plant develops, Iowa State University*, **1994**.

[18]Chen, C.-W., Yang, Y.-W., Lur, H.-S., Tsai, Y.-G. and Chang, M.-C., *Plant Cell Physiol*., **2006**, 47*(1)*, 1–13.

[19]Rastegar, Z., Sedghi, M., Khomari, S., *Notulae Sci. Biol*., **2011**, 3*(3)*, 126–129.

[20]Afzal, Z., Howton, T., Sun, Y. and Mukhtar, M., *J. Dev. Biol.*, **2016**, 4*(1)*, 9.

[21]Tiwari, D. K., Dasgupta-Schubert, N., Villaseñor Cendejas, L. M., Villegas, J., Carreto Montoya, L. and Borjas García, S. E., *Appl. Nanosci*, **2014**, 4*(5)*, 577–591.

[22]Chachalis, D. and Smith, M. L., *J. New Seeds*, **2001**, 2*(3)*, 27–36.

[23]Powell, A. A., Oliveira, M. de A. and Matthews, S., *J. Exp. Bot.*, **1986**, 37*(5)*, 716–722.

[24]Gijzen, M., Miller, S. S., Kuflu, K., Buzzell, R. I. and Miki, B. L., *Plant Physiol*., **1999**, 120*(4)*, 951–959.

[25]Khan A. A. (ed.), *The physiology and biochemistry of seed development, dormancy and germination, Elsevier Biomedical Press*, **1977**.

[26]Ghosh, M., Chakraborty, A., Bandyopadhyay, M. and Mukherjee, A., *J. Hazard. Mater*., **2011**, 197, 327–336.

[27]Ghosh, M., Bhadra, S., Adegoke, A., Bandyopadhyay, M. and Mukherjee, A., *Mutat. Res., Fundam. Mol. Mech. Mutagen.*, **2015**, 774, 49–58.

[28]Lin, C., Fugetsu, B., Su, Y. and Watari, F., *J. Hazard. Mater*., **2009**, 170*(2-3)*, 578–583.

[29]Villagarcia, H., Dervishi, E., Silva, K. de, Biris, A. S. and Khodakovskaya, M. V., *Small*, **2012**, 8*(15)*, 2328–2334.

[30]Khodakovskaya M., Silva, K. de, Biris, A. S., Dervishi, E. and Villagarcia, H., *ACS Nano*, **2012**, 6*(3)*, 2128–2135.

[31]Duke, S. H., Kakefuda, G., Henson, C. A., Loeffler, N. L. and Hulle, N. M., *Physiol. Plant*, **1986**, 68*(4)*, 625–631.

Received: 12.06.2016.
Accepted: 28.07.2016.